Capturing Forest Dynamics in Hydrological Modeling

by

Henrique Haas

A thesis submitted to the Graduate Faculty of
Auburn University
in partial fulfillment of the
requirements for the Degree of
Master of Science

Auburn, Alabama
August 7, 2020

Approved by

Latif Kalin, Chair, Professor of Hydrology, School of Forestry & Wildlife Sciences
Puneet Srivastava, Co-chair, Professor and Associate Dean, College of Agriculture & Natural Resources, University of Maryland
Lana Narine, Assistant Professor of Geospatial Analytics, School of Forestry & Wildlife Sciences
Sanjiv Kumar, Assistant Professor of Earth System, School of Forestry & Wildlife Sciences

ABSTRACT

Forests can cover a significant portion of watersheds and affect rainfall interception, water losses through evapotranspiration (ET), surface runoff, and aquifer recharge. Despite their critical role in the hydrologic cycle, tree growth and dynamics are typically ignored or superficially considered in watershed modeling studies. This study aims to improve the plant database of the Soil and Water Assessment Tool (SWAT) model for the two dominant pine species in the Southeastern U.S., loblolly pine (*Pinus Taeda* L.) and slash pine (*Pinus Elliotti*). Tree growth-related parameters in SWAT were calibrated at field level for four pine plantations across Alabama, Georgia, and Florida. Improved parameter estimates were transferred from the field plots to two nearby forested watersheds with observed streamflow data. Comparison between improved and default parameterizations showed that the improved SWAT outperformed the default model in simulating leaf area index (LAI), biomass accumulation, and ET at all study sites. At the watershed-scale, models considering the improved representation of forest dynamics showed superior performance and reduced uncertainties in predicting daily streamflow, with *NSE* values ranging from 0.52 to 0.8. Our findings reveal the importance of accurately representing forest dynamics in hydrological models.

Contents

List of Tables

Chapter 2

Chapter 3

List of Figures

Chapter 2

Chapter 3

CHAPTER 1: GENERAL INTRODUCTION

Forest and Water Relationships and its Importance for Hydrologic Modeling Studies

Forests provide important ecosystem services such as improved soil water infiltration, soil loss mitigation, water quality purification, and provision of biomass (Mwangi et al., 2016). Forests also interact with incoming water from the atmosphere and feed back to affect watershed water balance (Ma et al., 2019). For example, a portion of rainfall is immediately intercepted by the plant canopy and becomes readily available for evaporation. The remaining water volume is redistributed into surface runoff, infiltration, soil percolation, subsurface flow, and eventually groundwater recharge. Evapotranspiration (ET) usually represents the largest component of the water balance (Marek et al., 2016). In the southeastern U.S., roughly 70% of the precipitation is lost to ET (McLaughlin et al., 2013). The plant root system can alter the soil configuration and enhance soil infiltration capacity (J. K. Kim et al., 2014). Some deep-rooted trees can extract water from the groundwater to meet their water demands (J. K. Kim et al., 2014; Li et al., 2018; Zhang et al., 2017). As a consequence, water extraction by deep-rooted trees can lower the groundwater table and reduce the amount of groundwater released to streams as baseflow (Mwangi et al., 2016). In the long-term, precipitation, ET and streamflow are the main drivers of the water budget in a watershed (Liu et al., 2018). Thus, the long-term watershed streamflow depends on the relationship between precipitation and ET. Since ET typically dominates watershed water losses, deforestation and/or conversion of vegetation to other land-uses can have significant impacts on the watershed water yield. In fact, several studies have demonstrated that afforestation, deforestation, and basal area and leaf area control can severely change the watershed's water regime (e.g., Caro Camargo and Velandia Tarazona, 2019; Dalzell and Mulla, 2018; Khanal and Parajuli, 2013; Shope et al., 2014). However, there is no clear consensus on the magnitude and direction of these changes.

Some studies suggest that enhanced water yield as a result of deforestation (Ellison et al., 2012; Filoso et al., 2017; Sun et al., 2005), other studies demonstrate the contrary (Jackson et al., 2005; Liang et al., 2015). Evaristo and McDonnell (2019) addressed this issue in their study on 440,000 catchments worldwide. Their results showed that vegetation removal schemes (such as deforestation or thinning) are more likely to increase water yield in areas where potential water storage (the amount of water that can be held between the soil surface and the unweathered bedrock) is high. Conversely, little or no increases in annual water yield are likely to occur when vegetation removal takes place in areas of low potential water storage. They further demonstrated that ET is the most important factor in predicting the response of runoff to forestation.

It is obvious that understanding the interplays between vegetation and hydrology is critical for better watershed management and planning. Hydrological response to forest management has traditionally been assessed by paired watershed studies (Evaristo and McDonnell, 2019). However, such landscape experiments usually provide only local and short-term insights and can be expensive, laborious, and time-consuming. As an alternative, hydrological models are commonly used to describe and understand the interactions between vegetation and hydrology. Due to their efficiency and cost-effectiveness, models have been increasingly applied to watersheds for decision making (Taylor et al., 2016). In simple terms, a model is a simplified representation of reality through a set of mathematical relationships. Models can aid managers and decision-makers to estimate risks, understand uncertainties, assess multiple management scenarios, and predict future environmental conditions at local, regional, national, or continental scales. Over the last decades, modelers benefited from advances in numerical approaches, computing capacities, development of calibration software, and availability of observed data for model calibration and validation (Shifley et al., 2017). Consequently, the number of modelling studies linking hydrology

and vegetation became more abundant. For example, Kelly et al. (2016) used a nonlinear time series regression model to investigate potential interactions between climate and forest management in altering streamflow. Their results suggested that vegetation might be managed to compensate for streamflow response due to climate change effects such as extreme changes in precipitation. Liu et al. (2018) analyzed 30 catchments using the Budyko's theoretical framework to study the effects of climate and land cover change on streamflow. Their results showed a coequal role of climate and vegetation on streamflow response, highlighting the importance of forest management on future water production.

Although useful, empirical models highly depend on the statistical relationships obtained through regression analysis of observed data and are usually only suitable for the conditions under which the relationships have been developed. On the other hand, physically-based models (also referred to as process-based models) represent a category of models based on physical principles such as conservation of mass and momentum. These types of models usually require a large number of input parameters, which can often be obtained through field measurements. Some models are classified as hybrids, because they are developed to bridge the gap between conventional empirical models based on statistical relationships and process-based models. One example of such a model is the Physiological Processes Predicting Growth (3-PG) (Landsberg and Waring, 1997). The 3-PG model is a stand-level simulator to predict the growth of mono-specific trees. Although robust at the stand-level scale, these types of models are not applicable at larger scales where several stand species spread across the landscape. Linking stand-level models to hydrological models provides a more solid mechanism to evaluate how different forest management operations affect water yield at regional scales. In such cases, a watershed-scale approach is necessary.

Many watershed models have been developed and selecting the most suitable model to be employed in a research project can be a challenging task. Among the most widely used watershed-scale models are the Agricultural Non-Point Source (AGNPS) (Young et al., 1989), Hydrologic Modeling System (HEC-HMS) (Feldman, 2000), Hydrological Simulation Program Fortran (HSPF) (Bicknell et al., 1997), Kinematic Runoff and Erosion Model (KINEROS) (Woolhiser et al., 1990), and the Soil and Water Assessment Tool (SWAT) (Arnold et al., 1998) model. These physically-based watershed models are usually calibrated by comparing in-stream simulated fluxes with observed data at the watershed outlet, without paying much attention to the ability of the model in simulating processes that occur within the watershed, between streams and upland areas (Yen et al., 2014). Intra-watershed processes such as leaf area index (LAI) development, biomass production, ET, and soil moisture dynamics are often neglected or overlooked in watershed modelling studies. Given the intrinsic relationship between vegetation and hydrology, neglecting such interior watershed behaviors during model calibration may reduce model reliability and potentially lead to flawed conclusions.

As a popular physically-based watershed model, the Soil and Water Assessment Tool (SWAT) has found wide applications for various purposes worldwide. For instance, it has been used in estimating water yield (Abou Rafee et al., 2019; Adla et al., 2019; Kaur et al., 2019; Qi et al., 2019; Visakh et al., 2019; Zang and Mao, 2019), sediment loss (Brighenti et al., 2019; Himanshu et al., 2019; Mishra et al., 2007; Mukundan et al., 2010; Singh et al., 2014; Vigiak et al., 2015; Wellen et al., 2014), nutrient loading (Akhavan et al., 2010; Chu et al., 2004; Haas et al., 2016; Ikenberry et al., 2017; Kemanian et al., 2011; Kiani et al., 2018; Pohlert et al., 2007; Risal and Parajuli, 2019), and assessing impacts of climate change (Ahn et al., 2016; Anjum et al., 2019; Awan and Ismaeel, 2014; Bhatta et al., 2019; Jianzhong Lu et al., 2017; Zhu et al., 2016),

and land use/cover change (Anand et al., 2018; Jodar-Abellan et al., 2018; Li et al., 2014; Romanowicz et al., 2005; Teklay et al., 2019; Wang et al., 2018). SWAT has also been applied to predict crop yield at the field scale (Cibin et al., 2016; Mittelstet, 2015; Nair et al., 2011; R. Srinivasan et al., 2010; Trybula et al., 2015; Wang et al., 2015) and to assess the benefits of perennial vegetation on water quality (Dalzell and Mulla, 2018). Despite being used for a wide range of applications, SWAT has not been sufficiently tested in forested ecosystems (Amatya and Jha, 2011; Yang et al., 2019). More than a decade ago, an invited SWAT review paper (Gassman et al., 2007) highlighted that expansion of SWAT's plant database was needed to support a larger variety of plant species that could be simulated in the model.

SWAT incorporates a simplified version of the Environmental Policy Integrated Climate (EPIC) model (Williams, 1990) to simulate plant growth. The initialization of the growth cycle in SWAT is based on the Heat Unit Theory: plants require a certain amount of heat to reach maturity, which is only reached when a plant-specific total heat unit is attained. Once the plant reaches maturity, it stops transpiring and uptake of water and nutrients. The growth cycle is restarted every year based on a latitude-dependent dormancy routine. At the beginning of each growth cycle, the accumulated heat units drop to zero, and the LAI is set to a plant-specific minimum value (Neitsch et al., 2011). The actual plant growth is based on solar radiation and light conversion efficiency. This type of model is sometimes referred to as a "radiation-crop model" since it depends on the efficiency of converting photosynthetically active radiation into biomass (Jiang et al., 2017). Although simple, robust, and straightforward for simulating crop biomass, SWAT's plant growth model presents some shortcomings, especially when it comes to tree growth modeling. For example, SWAT assumes that radiation use efficiency of a plant (efficiency in converting radiation into biomass) is constant when it is well known that it can vary during the year (Clifton-brown et

al., 2004). More importantly, SWAT uses the same set of variables to simulate all types of plants, meaning that in SWAT, crop and tree growth are only distinguished by the use of different parameter values. The default parameter values representing tree growth in SWAT were defined, in most of the cases, based on personal communication (Arnold et al., 2012). This clearly warrants the necessity of improving the model's plant database to simulate tree growth based on specific species and environmental conditions.

Only a handful of studies have reported the parameterization of SWAT's plant database for trees. Amatya and Jha (2011) applied a SWAT model to simulate streamflow in a forested watershed (Pine and mixed hardwood forest) in South Carolina. To that end, they changed the model's default LAI value from 3 m^2/m^2 to 5 m^2/m^2, and the canopy storage capacity to 0.5 mm. However, the authors expressed the need for further investigation of forested systems to reduce uncertainties in flow predictions. Similarly, Mwangi et al. (2016) increased SWAT's minimum LAI from 0.75 m^2/m^2 to 3 m^2/m^2, which is a typical value for the studied region (Mau Forest in Kenya). This region is mainly dominated by a variety of broad leaved species (Kinyanjui et al., 2014). Their results showed an improved model's performance in predicting ET and tree water use after LAI parameterization. Shope et al. (2014) conducted a comprehensive calibration of 15 vegetation related parameters to improve SWAT's skills in simulating LAI of deciduous forests in South Korea. Khanal and Parajuli (2014) assessed the sensitivity of seven SWAT plant database parameters to simulate forest (Longleaf pine and mixed hardwood) biomass in east-central Mississippi. Their results showed that only three parameters are sensitive to forest biomass production: (i) the fraction of growing season at which senescence becomes the dominant growth process, (ii) radiation use efficiency, and (iii) potential maximum LAI. Other studies have applied SWAT to investigate the effects of forest management on streamflow response without reporting

any tree growth calibration (e.g. Khanal and Parajuli, 2013; Y. Kim et al., 2014; Kushwaha and Jain, 2013; Zhang et al., 2019).

Another tier of studies has changed the SWAT's internal structure through code modification to improve SWAT's capabilities in simulating tree growth. Yang and Zhang (2016) identified unrealistic parameters and processes for modelling evergreen, deciduous, and mixed forests in SWAT. Based on carbon biomass, net primary productivity (NPP), net ecosystem exchange (NEE) and evapotranspiration data collected across ten Ameriflux sites covering different regions of the U.S., the authors demonstrated that default SWAT model (i) overestimates tree maximum leaf area index, overestimates optimum and base temperature, and overestimates the amount of leaf biomass converted to soil residue; and (ii) underestimates tree radiation use efficiency. As a result of this unrealistic default model parameterization, model estimates of forest biomass, ET, and NPP were significantly underestimated in comparison to benchmark data. They also modified SWAT to include a new phosphorus supply routine from parental material weathering. After model modification and parameterization, tree biomass production and NPP were significantly improved in SWAT. However, the authors did not calibrate the model's LAI dynamics. Since SWAT uses the daily LAI to compute daily biomass accumulation, and ET, ignoring leaf phenology certainly affects the model's performance. Yang et al. (2018) built upon this site level improved SWAT parameterization to test the model in a forested watershed located across the border between Wisconsin and Minnesota. Their results showed the important role of forest ecosystems in the watershed scale water budget and the connections between terrestrial and riverine processes. Once again, the authors did not incorporate LAI into the model calibration processes. Moreover, they lumped deciduous and evergreen forests together to analyze model outputs and did not report which model parameters were sensitive to tree biomass, ET, and NPP.

As an addition to that study, Yang et al. (2019) further examined how those improved five forest parameters affected simulated streamflow, sediment, and nitrogen export under future climate conditions at the same watershed. Their results showed that the improved SWAT model reduced estimates of water, sediment, and nitrogen fluxes when compared to the default model configuration. Although they transferred the improved model parameters from previous studies, simulated processes related to tree growth (such as LAI and biomass) were not compared to any benchmark data. Guo et al. (2018) included a new LAI parameter, a new LAI algorithm, and a new leaf biomass algorithm in SWAT to predict *Populus* tree growth. The new LAI parameter was added to the plant database to describe how LAI increases to the maximum potential value, considering varying tree densities. Their results showed that 10 out of 35 SWAT plant database parameters were sensitive to *Populus* biomass yield and that modeled aboveground biomass and LAI from the modified SWAT model were satisfactory based on observed annual data. That is the only study found in the literature that performed both LAI and biomass calibration of trees based on measured data with SWAT. However, the proposed model parameterization and modification were meant to improve biomass estimates of *Populus* only, not evergreen or deciduous trees.

Modeling tree growth with SWAT in tropical and subtropical regions is especially challenging because, unlike temperate regions, plants in the tropics do not undergo dormancy over the year. Some research has been done to overcome this shortcoming. For example, Wagner et al. (2011), when applying SWAT in India, modified the dormancy subroutine by shifting it to the dry season (from April to May). The authors also increased the maximum leaf area index to 6 m^2/m^2, based on remote sensing derived data, to better describe the phenology of the local semi-evergreen species. Strauch and Volk (2013) presented an alternative modeling approach to initiate the annual growing cycle based on changes in soil moisture, instead of dormancy. The authors tested the

methodology in Brazil by calibrating LAI and ET of evergreen trees and perennials against remote sensing data. Their results showed that the modified model can reasonably represent the seasonal dynamics of the tropical species. Similarly, Alemayehu et al. (2017) presented a modified SWAT model, referred to as SWAT-T, that uses a quotient of rainfall and reference evapotranspiration to dynamically initiate a new growth cycle. The alternative model was tested in Kenya and Tanzania and results showed that simulated LAI and ET exhibit a good agreement with remote sensing data. Ma et al. (2019) integrated spatially and temporally continuous LAI products from Moderate Resolution Imaging Spectroradiometer (MODIS) into SWAT to replace the original model's LAI routine. The model was tested in China and results showed a more accurate relation between simulated LAI and precipitation data. Watson et al. (2008) developed an alternative SWAT model ($SWAT_{BF}$), which is based on several modifications made to the original model to better represent processes occurring within forested watersheds on the Boreal Plain in Canada. One of the added features is a litter layer on the forest floor, which was meant to work as an additional interception storage compartment. Their results showed overall good model performance in simulating daily and monthly runoff. Watson et al. (2005) integrated the forest growth model 3-PG with SWAT to improve simulation of LAI for evergreen trees in Australia. The coupled model was called SWAT/3-PG and results showed more realistic and accurate simulations of LAI of eucalypts and pines compared to the original version of SWAT. SWAT/3-PG's plausibility in simulating LAI was assessed based on data derived from Landsat satellite imagery.

Given the importance that vegetation plays on simulated in-stream processes in SWAT and the limitations of the default model's plant database in regards to trees, it is fair to say that it needs to be revised and improved before conducting hydrological and water quality assessments. To that end, it is important to develop a reliable SWAT plant database, with parameter values derived from

field measurements and literature review. Moreover, the true nexus between vegetation and hydrology can only be evaluated in SWAT if the full tree growth cycle is captured. Consequently, LAI dynamics, tree biomass production, and evapotranspiration are processes that must be considered simultaneously in SWAT applications, even if the focus is forecasting streamflow. This issue becomes even more crucial for regions where forests cover a large portion of the landscape, such as the southeastern U.S. Almost one-third of the forested lands in the contiguous U.S. are in the southeastern U.S., comprising of approximately 99 million hectares (Bracho et al., 2018). This region is the number one producer of timber in the U.S., with planted pine covering over 15 million hectares of land (Gavazzi et al., 2016). Loblolly pine (*Pinus taeda* L.) is the most widely planted species, representing approximately 69% of the total planted pine (Bracho et al., 2018). Slash pine (*Pinus elliottii*) is the second most cultivated pine specifies in the southeastern U.S., covering an area of approximately 4.2 million hectares (Gonzalez-Benecke et al., 2014) Consequently, any hydrological study conducted with the SWAT model in this region should give special attention to model parameters related to tree growth prediction.

OBJECTIVES AND HYPOTHESIS

The three overreaching goals of this research are:

1. Construct a SWAT plant database parameterization for loblolly and slash pine based on data derived from literature, field observations and remote sensing products;
2. Calibrate and validate the model at the field scale basis for multiple sites across the southeastern U.S. for biomass production, LAI dynamics, and ET;
3. Transfer the calibrated model parameters to watersheds located near each of the sites to investigate the impact of vegetation growth calibration on watershed-scale water balance.

It is hypothesized that improved prediction of LAI, biomass, and evapotranspiration will alter the watershed water balance because of the implications of improved canopy water storage on water evaporation and redistribution over the land and through the soil profile. It is also hypothesized that model parameters calibrated at the field scale level can be transferred to watershed-scale models for improved tree growth and streamflow prediction.

THESIS OUTLINE

The thesis is divided into two major topics: (I) model parameterization and calibration of key forest processes at the field-scale level in the Southeastern U.S., and (II) validation of the proposed forest parameterization at the watershed-scale and assessment of its implications on watershed hydrological predictions. Each of these topics is developed as a single chapter and formatted as a standalone journal paper.

Chapter two presents an improved parameterization of SWAT's plant database for loblolly pine and slash pine, the two dominant pine species in the Southeastern U.S. The proposed parameterization aimed at enhancing SWAT's skills in forested ecosystems. Parameter values representing key forest processes in the model were derived via species-specific field-measured data, remotely-sensed derived LAI and ET, published literature, and expert knowledge. To assess the quality of this parameterization, simulated LAI, total biomass, and ET were compared against field observations and MODIS derived data. Four pine plantation fields spread across Alabama, Georgia, and Florida were selected as test beds. The study sites differ in terms of planted species (i.e., loblolly pine or slash pine), area, management (e.g., fertilizer application, site preparation, planting age), soil, and climate conditions.

Chapter three explores the impacts of the forest parameterization developed in chapter two on watershed hydrology. To that end, the previously calibrated parameter values regulating LAI,

total biomass, and ET were transferred to two nearby forested watersheds. The selected watersheds are predominately covered by either loblolly pine or slash pine trees and located in Georgia and Florida. A series of modeling experiments were designed to progressively constrain more model variables with additional observed data. These experiments helped to isolate the impacts of LAI, biomass, and ET on streamflow prediction and water budget computation at each watershed. The implications of improved forest processes on automated streamflow calibration were analyzed by comparing two different model calibration strategies: first, streamflow was calibrated without adjusting simulated LAI, biomass, and ET in the models. Next, previously calibrated parameter values describing LAI, biomass, and ET were incorporated into the model, and then streamflow-related parameters were optimized. The interplays between terrestrial processes and in-stream processes were further scrutinized in the models by comparing fifty eco-hydrological parameters against observations derived from gauged streamflow.

The fourth chapter closes the thesis by summarizing the main findings obtained throughout this study, highlighting some shortcomings, and pointing out future research directions.

REFERENCES

Abou Rafee, S.A., Uvo, C.B., Martins, J.A., Domingues, L.M., Rudke, A.P., Fujita, T., Freitas, E.D., 2019. Large-Scale Hydrological Modelling of the Upper Paraná River Basin. Water 11, 882. https://doi.org/10.3390/w11050882

Adla, S., Tripathi, S., Disse, M., 2019. Can We Calibrate a Daily Time-Step Hydrological Model Using Monthly Time-Step Discharge Data? Water 11, 1750. https://doi.org/10.3390/w11091750

Ahn, S.R., Jeong, J.H., Kim, S.J., 2016. Assessing drought threats to agricultural water supplies under climate change by combining the SWAT and MODSIM models for the Geum River basin, South Korea. Hydrological Sciences Journal/Journal des Sciences Hydrologiques 61, 2740–2753. https://doi.org/10.1080/02626667.2015.1112905

Akhavan, S., Abedi-Koupai, J., Mousavi, S.-F., Afyuni, M., Eslamian, S.-S., Abbaspour, K.C., 2010. Application of SWAT model to investigate nitrate leaching in Hamadan–Bahar Watershed, Iran. Agriculture, Ecosystems & Environment 139, 675–688. https://doi.org/10.1016/j.agee.2010.10.015

Alemayehu, T., Griensven, A. van, Woldegiorgis, B.T., Bauwens, W., 2017. An improved SWAT vegetation growth module and its evaluation for four tropical ecosystems. Hydrology and Earth System Sciences 21, 4449–4467. https://doi.org/10.5194/hess-21-4449-2017

Amatya, D.M., Jha, M.K., 2011. Evaluating the SWAT model for a low-gradient forested watershed in coastal South Carolina. American Society of Agricultural and Biological Engineers (ASABE) 54(6):2151-2163 54, 2151–2163.

Anand, J., Gosain, A. k., Khosa, R., 2018. Prediction of land use changes based on Land Change Modeler and attribution of changes in the water balance of Ganga basin to land use change using the SWAT model. Science of the Total Environment 644, 503–519. https://doi.org/10.1016/j.scitotenv.2018.07.017

Anjum, M.N., Ding, Y., Shangguan, D., 2019. Simulation of the projected climate change impacts on the river flow regimes under CMIP5 RCP scenarios in the westerlies dominated belt, northern Pakistan. Atmospheric Research 227, 233–248. https://doi.org/10.1016/j.atmosres.2019.05.017

Arnold, J.G., Srinivasan, R., Muttiah, R.S., Williams, J.R., 1998. Large Area Hydrologic Modeling and Assessment Part I: Model Development1. JAWRA Journal of the American Water Resources Association 34, 73–89. https://doi.org/10.1111/j.1752-1688.1998.tb05961.x

Awan, U.K., Ismaeel, A., 2014. A new technique to map groundwater recharge in irrigated areas using a SWAT model under changing climate. Journal of Hydrology 519, 1368–1382. https://doi.org/10.1016/j.jhydrol.2014.08.049

Bhatta, B., Shrestha, S., Shrestha, P.K., Talchabhadel, R., 2019. Evaluation and application of a SWAT model to assess the climate change impact on the hydrology of the Himalayan River Basin. CATENA 181, 104082–104082. https://doi.org/10.1016/j.catena.2019.104082

Bicknell, B.R., Imhoff, J.C., Kittle, J.L., Donigian, A.S., Johanson, R.C., n.d. Hydrological Simulation Program--FORTRAN User's Manual for Version 11 2.

Bracho, R., Vogel, J.G., Will, R.E., Noormets, A., Samuelson, L.J., Jokela, E.J., Gonzalez-Benecke, C.A., Gezan, S.A., Markewitz, D., Seiler, J.R., Strahm, B.D., Teskey, R.O., Fox, T.R., Kane, M.B., Laviner, M.A., McElligot, K.M., Yang, J., Lin, W., Meek, C.R., Cucinella, J., Akers, M.K., Martin, T.A., 2018. Carbon accumulation in loblolly pine plantations is increased by fertilization across a soil moisture availability gradient. Forest Ecology and Management 424, 39–52. https://doi.org/10.1016/j.foreco.2018.04.029

Brighenti, T.M., Bonumá, N.B., Grison, F., Mota, A. de A., Kobiyama, M., Chaffe, P.L.B., 2019. Two calibration methods for modeling streamflow and suspended sediment with the swat model. Ecological Engineering 127, 103–113. https://doi.org/10.1016/j.ecoleng.2018.11.007

Caro Camargo, C.A., Velandia Tarazona, J.E., 2019. The effect of changes in vegetation cover on the hydrological response of the sub-basin Los Pozos. DYNA 86, 182–191. https://doi.org/10.15446/dyna.v86n208.74115

Chu, T.W., Shirmohammadi, A., Montas, H., Sadeghi, A., 2004. Evaluation of the Swat Model's Sediment and Nutrient Components in the Piedmont Physiographic Region of Maryland. Transactions of the ASAE 47, 1523–1538. https://doi.org/10.13031/2013.17632

Cibin, R., Trybula, E., Chaubey, I., Brouder, S.M., Volenec, J.J., 2016. Watershed-scale impacts of bioenergy crops on hydrology and water quality using improved SWAT model. GCB Bioenergy 8, 837–848. https://doi.org/10.1111/gcbb.12307

Clifton-brown, J.C., Stampfl, P.F., Jones, M.B., 2004. Miscanthus biomass production for energy in Europe and its potential contribution to decreasing fossil fuel carbon emissions. Global Change Biology 10, 509–518. https://doi.org/10.1111/j.1529-8817.2003.00749.x

Dalzell, B.J., Mulla, D.J., 2018. Perennial vegetation impacts on stream discharge and channel sources of sediment in the Minnesota River Basin. Journal of Soil and Water Conservation 73, 120–132. https://doi.org/10.2489/jswc.73.2.120

Ellison, D., N Futter, M., Bishop, K., 2012. On the forest cover–water yield debate: from demand- to supply-side thinking. Glob Chang Biol 18, 806–820. https://doi.org/10.1111/j.1365-2486.2011.02589.x

Evaristo, J., McDonnell, J.J., 2019. Global analysis of streamflow response to forest management. Nature 570, 455–461. https://doi.org/10.1038/s41586-019-1306-0

Filoso, S., Bezerra, M.O., Weiss, K.C.B., Palmer, M.A., 2017. Impacts of forest restoration on water yield: A systematic review. PLoS One 12. https://doi.org/10.1371/journal.pone.0183210

Gavazzi, M.J., Sun, G., McNulty, S.G., Treasure, E.A., Wightman, M.G., 2016. Canopy Rainfall Interception Measured over Ten Years in a Coastal Plain Loblolly Pine (Pinus taeda L.) Plantation. Trans. ASABE 59, 601–610. https://doi.org/10.13031/trans.59.11101

Gonzalez-Benecke, C.A., Jokela, E.J., Cropper, W.P., Bracho, R., Leduc, D.J., 2014. Parameterization of the 3-PG model for Pinus elliottii stands using alternative methods to estimate fertility rating, biomass partitioning and canopy closure. Forest Ecology and Management 327, 55–75. https://doi.org/10.1016/j.foreco.2014.04.030

Guo, T., Engel, B.A., Shao, G., Arnold, J.G., Srinivasan, R., Kiniry, J.R., 2018. Development and improvement of the simulation of woody bioenergy crops in the Soil and Water Assessment Tool (SWAT). Environmental Modelling & Software. https://doi.org/10.1016/j.envsoft.2018.08.030

Haas, M.B., Guse, B., Pfannerstill, M., Fohrer, N., 2016. A joined multi-metric calibration of river discharge and nitrate loads with different performance measures. Journal of Hydrology 536, 534–545. https://doi.org/10.1016/j.jhydrol.2016.03.001

Himanshu, S.K., Pandey, A., Yadav, B., Gupta, A., 2019. Evaluation of best management practices for sediment and nutrient loss control using SWAT model. Soil & Tillage Research 192, 42–58. https://doi.org/10.1016/j.still.2019.04.016

Ikenberry, C.D., Crumpton, W.G., Arnold, J.G., Soupir, M.L., Gassman, P.W., 2017. Evaluation of Existing and Modified Wetland Equations in the SWAT Model. Journal of the American Water Resources Association 53, 1267–1280. https://doi.org/10.1111/1752-1688.12570

Jackson, R.B., Jobbagy, E.G., Avissar, R., Roy, S.B., Barrett, D.J., Cook, C.W., Farley, K.A., McCarl, B.A., Murray, B.C., 2005. Trading Water for Carbon with Biological Carbon Sequestration 310, 5.

Jiang, R., Wang, T., Shao, J., Guo, S., Zhu, W., Yu, Y., Chen, S., Hatano, R., 2017. Modeling the biomass of energy crops: Descriptions, strengths and prospective | Elsevier Enhanced Reader [WWW Document]. Journal of Integrative Agriculture. https://doi.org/10.1016/S2095-3119(16)61592-7

Jianzhong Lu, Xiaolin Cui, Xiaoling Chen, Sauvage, S., Perez, J.-M.S., 2017. Evaluation of hydrological response to extreme climate variability using SWAT model: application to the Fuhe basin of Poyang Lake watershed, China. Hydrology Research 48, 1730–1744. https://doi.org/10.2166/nh.2016.115

Jodar-Abellan, A., Valdes-Abellan, J., Pla, C., Gomariz-Castillo, F., 2018. Impact of land use changes on flash flood prediction using a sub-daily SWAT model in five Mediterranean ungauged watersheds (SE Spain) | Elsevier Enhanced Reader [WWW Document]. https://doi.org/10.1016/j.scitotenv.2018.12.034

Kaur, B., Shrestha, N.K., Daggupati, P., Rudra, R.P., Goel, P.K., Shukla, R., Allataifeh, N., 2019. Water Security Assessment of the Grand River Watershed in Southwestern Ontario, Canada. Sustainability 11, 1883. https://doi.org/10.3390/su11071883

Kelly, C.N., McGuire, K.J., Miniat, C.F., Vose, J.M., 2016. Streamflow response to increasing precipitation extremes altered by forest management: Forest Management, Streamflow, and Extreme Precipitation. Geophys. Res. Lett. 43, 3727–3736. https://doi.org/10.1002/2016GL068058

Kemanian, A.R., Julich, S., Manoranjan, V.S., Arnold, J.R., 2011. Integrating soil carbon cycling with that of nitrogen and phosphorus in the watershed model SWAT: Theory and model testing. Ecological Modelling 222, 1913–1921. https://doi.org/10.1016/j.ecolmodel.2011.03.017

Khanal, S., Parajuli, P.B., 2014. Sensitivity Analysis and Evaluation of Forest Biomass Production Potential Using SWAT Model. JSBS 04, 136–147. https://doi.org/10.4236/jsbs.2014.42013

Khanal, S., Parajuli, P.B., 2013. Evaluating the Impacts of Forest Clear Cutting on Water and Sediment Yields Using SWAT in Mississippi. Journal of Water Resource and Protection 5, 720–726. https://doi.org/10.4236/jwarp.2013.54047

Kiani, F., Behtarinejad, B., Najafinejad, A., Kaboli, R., 2018. Simulation of Nitrogen and Phosphorus Losses in Loess Landforms of Northern Iran. Eurasian Soil Science 51, 176–182. https://doi.org/10.1134/S1064229318020035

Kim, J.K., Onda, Y., Kim, M.S., Yang, D.Y., 2014. Plot-scale study of surface runoff on well-covered forest floors under different canopy species | Elsevier Enhanced Reader [WWW Document]. URL https://reader.elsevier.com/reader/sd/pii/S1040618214004996?token=A32619D1C00AFCEB542AF13D66834EFF99BD5C182F1BA2C60523A3C8691343F34FB5DB3FFBAD6065CB7626D082C50A6F (accessed 9.24.19).

Kim, Y., Band, L.E., Song, C., 2014. The Influence of Forest Regrowth on the Stream Discharge in the North Carolina Piedmont Watersheds. JAWRA Journal of the American Water Resources Association 50, 57–73. https://doi.org/10.1111/jawr.12115

Kinyanjui, M.J., Shisanya, C.A., Nyabuti, O.K., Waqo, W.P., Ojwala, M.A., 2014. Assessing Tree Species Dominance along an Agro Ecological Gradient in the Mau Forest Complex, Kenya. http://dx.doi.org/10.4236/oje.2014.411056

Kushwaha, A., Jain, M.K., 2013. Hydrological Simulation in a Forest Dominated Watershed in Himalayan Region using SWAT Model. Water Resour Manage 27, 3005–3023. https://doi.org/10.1007/s11269-013-0329-9

Landsberg, J.J., Waring, R.H., 1997. A generalised model of forest productivity using simplified concepts of radiation-use efficiency, carbon balance and partitioning. Forest Ecology and Management 95, 209–228. https://doi.org/10.1016/S0378-1127(97)00026-1

Li, C., Sun, F., Xu, Y., Chen, T., Liu, M., Hu, Y., 2014. Combining CLUE-S and SWAT models to forecast land use change and non-point source pollution impact at a watershed scale in Liaoning Province, China. Chinese Geographical Science 24, 540–550. https://doi.org/10.1007/s11769-014-0661-x

Li, H., Si, B., Li, M., 2018. Rooting depth controls potential groundwater recharge on hillslopes: EBSCOhost [WWW Document]. URL http://eds.b.ebscohost.com/ehost/detail/detail?vid=0&sid=55bccc04-ce30-470d-98b9-cc4bf6acfd90%40sessionmgr101&bdata=JnNpdGU9ZWhvc3QtbGl2ZQ%3d%3d#AN=131543337&db=aph (accessed 9.24.19).

Liang, W., Bai, D., Wang, F., Fu, B., Yan, J., Wang, S., Yang, Y., Long, D., Feng, M., 2015. Quantifying the impacts of climate change and ecological restoration on streamflow changes based on a Budyko hydrological model in China's Loess Plateau. Water Resources Research 51, 6500–6519. https://doi.org/10.1002/2014WR016589

Liu, N., Harper, R.J., Smettem, K.R.J., Dell, B., Liu, S., 2018. Responses of streamflow to vegetation and climate change in southwestern Australia | Elsevier Enhanced Reader [WWW Document]. https://doi.org/10.1016/j.jhydrol.2019.03.005

Ma, T., Duan, Z., Li, R., Song, X., 2019. Enhancing SWAT with remotely sensed LAI for improved modelling of ecohydrological process in subtropics. Journal of Hydrology 570, 802–815. https://doi.org/10.1016/j.jhydrol.2019.01.024

Marek, G.W., Gowda, P.H., Evett, S.R., Baumhardt, R.L., Brauer, D.A., Howell, T., Marek, T.H., Srinivasan, R., 2016. Calibration and Validation of the SWAT Model for Predicting Daily ET over Irrigated Crops in the Texas High Plains Using Lysimetric Data. https://doi.org/10.13031/trans.59.10926

McLaughlin, D.L., Kaplan, D.A., Cohen, M.J., 2013. Managing Forests for Increased Regional Water Yield in the Southeastern U.S. Coastal Plain. JAWRA Journal of the American Water Resources Association 49, 953–965. https://doi.org/10.1111/jawr.12073

Mishra, A., Froebrich, J., Gassman, P.W., 2007. Evaluation of the Swat Model for Assessing Sediment Control Structures in a Small Watershed in India. Transactions of the ASABE 50, 469–477. https://doi.org/10.13031/2013.22637

Mittelstet, A.R., 2015. Using SWAT to simulate crop yields and salinity levels in the North Fork River Basin, USA. International Journal of Agricultural and Biological Engineering 8, 16.

Mukundan, R., Radcliffe, D.E., Risse, L.M., 2010. Spatial resolution of soil data and channel erosion effects on SWAT model predictions of flow and sediment. Journal of Soil & Water Conservation 65, 92–104. https://doi.org/10.2489/jSWC.65.2.92

Mwangi, H.M., Julich, S., Patil, S.D., McDonald, M.A., Feger, K.-H., 2016. Modelling the impact of agroforestry on hydrology of Mara River Basin in East Africa - Mwangi - 2016 - Hydrological Processes - Wiley Online Library [WWW Document]. Hydrological Processes. URL https://onlinelibrary.wiley.com/doi/full/10.1002/hyp.10852 (accessed 9.24.19).

Nair, S.S., King, K.W., Witter, J.D., Sohngen, B.L., Fausey, N.R., 2011. Importance of Crop Yield in Calibrating Watershed Water Quality Simulation Tools1. JAWRA Journal of the American Water Resources Association 47, 1285–1297. https://doi.org/10.1111/j.1752-1688.2011.00570.x

P. D. Wagner, S. Kumar, P. Fiener, K. Schneider, 2011. Technical Note: Hydrological Modeling with SWAT in a Monsoon-Driven Environment: Experience from the Western Ghats, India. Transactions of the ASABE 54, 1783–1790. https://doi.org/10.13031/2013.39846

P. W. Gassman, M. R. Reyes, C. H. Green, J. G. Arnold, 2007. The Soil and Water Assessment Tool: Historical Development, Applications, and Future Research Directions. Transactions of the ASABE 50, 1211–1250. https://doi.org/10.13031/2013.23637

Pohlert, T., Huisman, J. a., Breuer, L., Frede, H.-G., 2007. Integration of a detailed biogeochemical model into SWAT for improved nitrogen predictions—Model development, sensitivity, and GLUE analysis. Ecological Modelling 203, 215–228. https://doi.org/10.1016/j.ecolmodel.2006.11.019

Qi, J., Wang, Q., Zhang, X., 2019. On the Use of NLDAS2 Weather Data for Hydrologic Modeling in the Upper Mississippi River Basin. Water 11, 960. https://doi.org/10.3390/w11050960

R. Srinivasan, X. Zhang, J. Arnold, 2010. SWAT Ungauged: Hydrological Budget and Crop Yield Predictions in the Upper Mississippi River Basin. Transactions of the ASABE 53, 1533–1546. https://doi.org/10.13031/2013.34903

Risal, A., Parajuli, P.B., 2019. Quantification and simulation of nutrient sources at watershed scale in Mississippi. Science of the Total Environment 670, 633–643. https://doi.org/10.1016/j.scitotenv.2019.03.233

Romanowicz, A. a., Vanclooster, M., Rounsevell, M., La Junesse, I., 2005. Sensitivity of the SWAT model to the soil and land use data parametrisation: a case study in the Thyle catchment, Belgium. Ecological Modelling 187, 27–39. https://doi.org/10.1016/j.ecolmodel.2005.01.025

Shifley, S.R., He, H.S., Lischke, H., Wang, W.J., Jin, W., Gustafson, E.J., Thompson, J.R., Thompson, F.R., Dijak, W.D., Yang, J., 2017. The past and future of modeling forest dynamics: from growth and yield curves to forest landscape models. Landscape Ecol 32, 1307–1325. https://doi.org/10.1007/s10980-017-0540-9

Shope, C.L., Maharjan, G.R., Tenhunen, J., Seo, B., Kim, K., Riley, J., Arnhold, S., Koellner, T., Ok, Y.S., Peiffer, S., Kim, B., Park, J.-H., Huwe, B., 2014. Using the SWAT model to improve process descriptions and define hydrologic partitioning in South Korea. Hydrol. Earth Syst. Sci. 18, 539–557. https://doi.org/10.5194/hess-18-539-2014

Singh, A., Imtiyaz, Mohd., Isaac, R. k., Denis, D. m., 2014. Assessing the performance and uncertainty analysis of the SWAT and RBNN models for simulation of sediment yield in the Nagwa watershed, India. Hydrological Sciences Journal/Journal des Sciences Hydrologiques 59, 351–364. https://doi.org/10.1080/02626667.2013.872787

Strauch, M., Volk, M., 2013. SWAT plant growth modification for improved modeling of perennial vegetation in the tropics. Ecological Modelling 269, 98–112. https://doi.org/10.1016/j.ecolmodel.2013.08.013

Sun, G., McNulty, S.G., Lu, J., Amatya, D.M., Liang, Y., Kolka, R.K., 2005. Regional annual water yield from forest lands and its response to potential deforestation across the southeastern United States. Journal of Hydrology 308, 258–268. https://doi.org/10.1016/j.jhydrol.2004.11.021

Taylor, S.D., He, Y., Hiscock, K.M., 2016. Modelling the impacts of agricultural management practices on river water quality in Eastern England | Elsevier Enhanced Reader [WWW Document]. URL https://reader.elsevier.com/reader/sd/pii/S0301479716302316?token=DC3DF796543B01A969B98F89FD2595B97C503525ABC4F8CB13E82B44A871A6884FB60533F01B7C8EC2DE4FEF14C85A74 (accessed 9.25.19).

Teklay, A., Dile, Y.T., Setegn, S.G., Demissie, S.S., Asfaw, D.H., 2019. Evaluation of static and dynamic land use data for watershed hydrologic process simulation: A case study in Gummara watershed, Ethiopia. CATENA 172, 65–75. https://doi.org/10.1016/j.catena.2018.08.013

Trybula, E.M., Cibin, R., Burks, J.L., Chaubey, I., Brouder, S.M., Volenec, J.J., 2015. Perennial rhizomatous grasses as bioenergy feedstock in SWAT: parameter development and model improvement. GCB Bioenergy 7, 1185–1202. https://doi.org/10.1111/gcbb.12210

Vigiak, O., Malagó, A., Bouraoui, F., Vanmaercke, M., Poesen, J., 2015. Adapting SWAT hillslope erosion model to predict sediment concentrations and yields in large Basins. Science of the Total Environment 538, 855–875. https://doi.org/10.1016/j.scitotenv.2015.08.095

Visakh, S., Raju, P.V., Kulkarni, S.S., Diwakar, P.G., 2019. Inter-comparison of water balance components of river basins draining into selected delta districts of Eastern India. Science of The Total Environment 654, 1258–1269. https://doi.org/10.1016/j.scitotenv.2018.11.162

Wang, Q., Liu, R., Men, C., Guo, L., Miao, Y., 2018. Effects of dynamic land use inputs on improvement of SWAT model performance and uncertainty analysis of outputs. Journal of Hydrology 563, 874–886. https://doi.org/10.1016/j.jhydrol.2018.06.063

Wang, R., Bowling, L.C., Cherkauer, K.A., 2015. Estimation of the effects of climate variability on crop yield in the Midwest USA | Elsevier Enhanced Reader [WWW Document]. Agricultural and Forest Meteorology. https://doi.org/10.1016/j.agrformet.2015.10.001

Watson, B., Coops, N., Selvalingam, S., Ghafouri, M., 2005. Integration of 3-PG into SWAT to simulate the growth of evergreen forests. SWAT 2005 : 3rd International SWAT Conference 142–152.

Watson, B.M., McKeown, R.A., Putz, G., MacDonald, J.D., 2008. Modification of SWAT for modelling streamflow from forested watersheds on the Canadian Boreal Plain. Journal of Environmental Engineering and Science 7, 145–159. https://doi.org/10.1139/S09-003

Wellen, C., Arhonditsis, G.B., Long, T., Boyd, D., 2014. Quantifying the uncertainty of nonpoint source attribution in distributed water quality models: A Bayesian assessment of SWAT's sediment export predictions. Journal of Hydrology 519, 3353–3368. https://doi.org/10.1016/j.jhydrol.2014.10.007

Williams, J.R., 1990. The erosion-productivity impact calculator (EPIC) model: a case history. Phil. Trans. R. Soc. Lond. B 329, 421–428. https://doi.org/10.1098/rstb.1990.0184

Yang, Q., Almendinger, J.E., Zhang, X., Huang, M., Chen, X., Leng, G., Zhou, Y., Zhao, K., Asrar, G.R., Srinivasan, R., Li, X., 2018. Enhancing SWAT simulation of forest ecosystems for water resource assessment: A case study in the St. Croix River basin. Ecological Engineering 120, 422–431. https://doi.org/10.1016/j.ecoleng.2018.06.020

Yang, Q., Zhang, X., 2016. Improving SWAT for simulating water and carbon fluxes of forest ecosystems. Science of The Total Environment 569–570, 1478–1488. https://doi.org/10.1016/j.scitotenv.2016.06.238

Yang, Q., Zhang, X., Almendinger, J.E., Huang, M., Leng, G., Zhou, Y., Zhao, K., Asrar, G.R., Li, X., Qiu, J., 2019. Improving the SWAT forest module for enhancing water resource

projections: A case study in the St. Croix River basin. Hydrological Processes 33, 864–875. https://doi.org/10.1002/hyp.13370

Yen, H., Bailey, R.T., Arabi, M., Ahmadi, M., White, M.J., Arnold, J.G., 2014. The Role of Interior Watershed Processes in Improving Parameter Estimation and Performance of Watershed Models. Journal of Environment Quality 43, 1601. https://doi.org/10.2134/jeq2013.03.0110

Young, R.A., Onstad, C.A., Bosch, D.D., Anderson, W.P., 1989. AGNPS: A nonpoint-source pollution model for evaluating agricultural watersheds. Journal of Soil and Water Conservation 44, 168–173.

Zang, C., Mao, G., 2019. A Spatial and Temporal Study of the Green and Blue Water Flow Distribution in Typical Ecosystems and its Ecosystem Services Function in an Arid Basin. Water 11, 97. https://doi.org/10.3390/w11010097

Zhang, S., Li, Z., Hou, X., Yi, Y., 2019. Impacts on watershed-scale runoff and sediment yield resulting from synergetic changes in climate and vegetation. CATENA 179, 129–138. https://doi.org/10.1016/j.catena.2019.04.007

Zhang, Z., Li, M., Si, B., Feng, H., 2017. Deep rooted apple trees decrease groundwater recharge in the highland regio...: EBSCOhost [WWW Document]. URL http://eds.b.ebscohost.com/ehost/detail/detail?vid=0&sid=6343cce6-9722-455a-af40-56bcd440c015%40pdc-v-sessmgr05&bdata=JnNpdGU9ZWhvc3QtbGl2ZQ%3d%3d#AN=127920571&db=aph (accessed 9.24.19).

Zhu, Q., Zhang, X., Ma, C., Gao, C., Xu, Y.-P., 2016. Investigating the uncertainty and transferability of parameters in SWAT model under climate change. Hydrological Sciences Journal/Journal des Sciences Hydrologiques 61, 914–930. https://doi.org/10.1080/02626667.2014.1000915

CHAPTER 2: The Role of Forests in Improving Biophysical Parameter Estimation and Plant Growth Representation in Hydrological Models: A field-scale approach in the Southeastern United States

ABSTRACT

This study aims to improve the plant database of the Soil and Water Assessment Tool (SWAT) model for two dominant pine species in the Southeastern U.S. (SE-US). To accomplish this goal, we parameterized SWAT with species-specific parameter values describing the growth and dynamics of loblolly pine (*Pinus Taeda* L.) and slash pine (*Pinus Elliotti*), the two dominant tree species in the SE-US. We derived physically-meaningful parameter values from publicly available remote-sensing products, field measurements, published literature, and expert knowledge. We identified unrealistic parameter values related to tree growth prediction in SWAT and model limitations to simulate juvenile trees. In this paper, we articulate on these shortcomings and propose an improved model parameterization that allows reasonable simulation of young trees. We applied SWAT under its default settings and parameterized version to four pine plantation fields to simulate leaf area index (LAI), biomass accumulation, and evapotranspiration (ET) under varying management, soil, and climate conditions. Tree growth-related parameters were calibrated within a physically-meaningful range at the field-scale in Alabama, Georgia, and Florida. Model skills in predicting these processes were tested using MODIS LAI and ET derived data, as well as field observations of total biomass. The results show that the improved SWAT outperformed the default model in simulating LAI, biomass accumulation, and ET at all sites. Under the improved parameterization, SWAT was able to explain up to 52% of the variation in seasonal LAI, 47% of the variation in monthly ET, and 99% of the variation in annual biomass. Furthermore, the updated forest parameterization significantly affected the mean annual water budget across all sites. The proposed changes did not alter the model's structure and are flexible and ready to go, which should benefit future modeling studies conducted in the SE-US

Keywords:

Leaf area index, Biomass, Evapotranspiration, SWAT, MODIS, Forest modeling

INTRODUCTION

Southern pines are one of the important tree species in the Southeastern United States (SE-US) covering about 28 million hectares (ha) of the 83 million ha of timberland in the region. The region, as a result, is responsible for producing approximately 60% of the total U.S. timber and about 18% of the global supply of industrial wood (Gonzalez-Benecke et al., 2014a). In this context, loblolly pine (*Pinus taeda*) is the nation's leading timber species, covering about 13 million ha and is considered to be the most important commercial tree species in the world (Will et al., 2015). As the most commonly planted tree species in the U.S., loblolly pine accounts for 84% of all seedlings planted in the SE-US (Wightman et al., 2016). The second most cultivated tree species in this region is the slash pine (*Pinus elliottii*), which has been planted on more than 4.2 million ha (Gonzalez-Benecke et al., 2014a).

Forests play a critical role in the land phase of hydrological water balance and greatly impact blue water (streamflow, subsurface flow, baseflow) and green water (evapotranspiration and soil water storage). Green water is defined as the water stored in unsaturated soil layers and plant canopy (Falkenmark M. and Rockström J., 2006; Veettil and Mishra, 2016). Blue water is the water flowing through the surface (e.g., lakes) and subsurface (e.g., aquifers) media that can be directly used for human needs (Falkenmark M. and Rockström J., 2006; Naderi, 2020; Veettil and Mishra, 2016). In the SE-US, evapotranspiration (ET) accounts for 70% of rainfall losses (McLaughlin et al., 2013). Ford et al. (2004) reported the average water use of slash pine and loblolly pine as being 99.3 L/day and 138 L/day, respectively. Gonzalez-Benecke et al. (2011) found daily transpiration in slash pine to be 39 L/tree, while a value of 20.35 L/day was reported for loblolly pine by another study (Martin, 1999). Wightman et al. (2016) found annual transpiration in a loblolly pine plantation in northern Florida corresponding to 35.2% (535 mm) of

annual rainfall. Recent research also showed that loblolly pine forests intercept between 14% and 28% of total rainfall through canopy storage (Gavazzi et al., 2016). Clearly, forests play a central role in the region's hydrological cycle and are likely to continue influencing the hydrology of the SE-US.

Investigating the interplays between forest and hydrology is a complex task and usually requires a combination of field studies and modeling approaches (Golden et al., 2016). A hydrological model capable of representing forest dynamics accurately can be a useful tool to supplement field measurements (e.g., predict long-term rainfall loss to ET). Likewise, field measurements can provide valuable information to enhance a hydrological model's representation of fundamental forest dynamics (e.g., leaf area index (LAI) dynamics). Process-based hydrological models have been applied in many studies to represent forest hydrological processes in the SE-US. Saleh et al. (2004) modified the process-based Agricultural Policy/Environmental eXtender (APEX) model (Williams et al., 2008) to improve estimations of flow, sediment, and nutrient losses from silvicultural lands in Texas. Iiames et al. (2018) applied the United States Department of Agriculture (USDA) Environmental Policy Integrated Climate (EPIC) model (Williams, 1990) to estimate LAI at four mixed-forest stands in Virginia and North Carolina. Amatya and Skaggs (2001) applied the field scale DRAINMOD (Skaggs, 1978) model to predict daily water table height in experimental watersheds located on a loblolly pine plantation in North Carolina. Although based on physical principles and equations, models such as APEX, EPIC, and DRAINMOD are appropriate only at plot or stand scale. Watershed-scale models are necessary for regional-scale evaluations to account for the spatial variability in stand species, soil, and climate.

As a popular process-based watershed model, the Soil and Water Assessment Tool (SWAT) (Arnold et al., 1998) has been used for a wide range of applications worldwide (Gassman et al., 2004). SWAT is capable of simulating varying land-management practices such as fertilizer application, irrigation, biomass harvest, and plant rotation. This makes SWAT suitable for forestry applications on managed plantations. However, SWAT has not been sufficiently tested in forested ecosystems (Amatya and Jha, 2011; Yang et al., 2019). SWAT incorporates a simplified version of EPIC to simulate plant growth based on the amount of heat required by a plant to reach its maturity. In SWAT, tree growth and dynamics are modeled based on the same set of parameters used to model crops. In other words, the main difference between a crop and a tree in SWAT is the value assigned to each parameter. Default parameter values representing tree growth in SWAT were defined, in most of the cases, based on personal communication (Arnold et al., 2012). Yang and Zhang (2016) identified unrealistic parameter values for modeling evergreen, deciduous, and mixed forests in SWAT's default plant parameterization. Guo et al. (2018) highlighted that LAI estimates in SWAT are not applicable for tree growth prior to maturity since LAI of young trees is not allowed to reach stand maximum LAI before canopy closure. The latter becomes an issue in regions such as the SE-US, where seedlings are planted all over the landscape.

Although SWAT has been extensively applied for improving and evaluating crop yield simulation (Cibin et al., 2016a; Karki et al., 2019; Mittelstet, 2015; Nair et al., 2011; Srinivasan et al., 2010; Trybula et al., 2015; Wang et al., 2015), there is no study, to the best of the author's knowledge, that evaluated SWAT's capabilities in predicting loblolly and slash pine dynamics. Since field studies in forestry are usually expensive and time-consuming, there is a scarcity of field observations and measurements spatially distributed across large areas (watersheds). The availability of published data and long-term field-measured data from forestry studies managed by

the Plantation Management Research Cooperative (PMRC) in Alabama, the Forest Biology Research Cooperative (FBRC) in Florida, and the Forest Modelling Research Cooperative (FMRC) in Georgia presented a great opportunity for us to derive realistic parameter values for pine trees simulation in SWAT as well as assess the model's capabilities in simulating key forest processes in operational pine plantations covering a wide range of age, management conditions, physical characteristics, and geographical distribution across the SE-US. In this paper, we take advantage of these shared datasets, combined with high temporal and spatial resolution remote-sensed data, expert knowledge, and published information to conduct a detailed parameterization of SWAT's plant database and calibrate modeled LAI dynamics, biomass accumulation, and ET rates for the two dominant tree species in the SE-US. The true nexus between vegetation and hydrology can only be evaluated in SWAT if the full tree growth cycle is captured. Consequently, LAI dynamics, tree biomass production, and evapotranspiration are processes that must be considered simultaneously in SWAT applications.

The overreaching goal of this study is to parameterize the SWAT model for loblolly pine and slash pine trees in the SE-US. The specific objectives are (1) assess SWAT's capabilities in simulating LAI, biomass accumulation, and ET at individual pine plantation fields under different soil, climate, and management conditions; (2) demonstrate a simple approach allowing simulation of young trees in SWAT; (3) show the impacts of phenological calibration on water resources. To the best of our knowledge, this is the first study to calibrate and evaluate the coupled interactions between tree LAI, biomass, and ET in SWAT, and thus, should have significant contribution to future hydrological modeling efforts in the SE-US.

MATERIALS AND METHODS

Study sites

Field measured data from four pine plantations across the SE-US were used for this study. Three of the sites had loblolly pine plantations and were located in Georgia, Alabama, and Florida (Fig. 1). The fourth and the only field with slash pine plantation was located in Florida and was about 4 km away from the loblolly pine site (Fig. 1). Characteristics of each site are summarized and presented in Table 1.

The IMP–GA site consists of a 6 hectare intensively managed loblolly pine plantation (IMP) located in Stewart County, in west Georgia. The plot is representative of contemporary silviculture of loblolly pine plantations and includes management strategies such as site preparation and controlled competition (Russell et al., 2010). The site was established in 1999 in 6-year-old stands and continued to be monitored every 2 years until 2005. From 2008 to 2010, measurements of total tree biomass were annual. The plot is part of a long-term productivity study administered by the Forest Modeling Research Cooperative at Virginia Tech University.

The SAGCD–AL site consists of a 10-hectare installation designed to represent two levels of management intensity: operational and intensive culture (Zhao et al., 2012). The site is located in St. Clair County, north-central Alabama and was established by the Plantation Management Research Cooperatives as part of 23 site installations of the loblolly pine culture/density study in 1997-1998 across the SE-US.

There are two sites in Florida, one loblolly pine plantation (IMPAC – FL) and one slash pine plantation (MIZE–FL). The IMPAC–FL site consists of a 9-hectare loblolly pine plantation located approximately 10 km north of Gainesville in Alachua County. The site was established in 1981 by the Forest Biology Research Cooperative when 1-year old loblolly pine seedlings were

planted at a 1.8 X 3.6 m spacing (Jokela and Martin, 2000). Fertilization occurred annually from 1983 to 1993 at the following Nitrogen (N) and Phosphorus (P) rates: 360 Kg of N/ha, and 143 kg of P/ha. The MIZE–FL site consists of a 28-hectare slash pine plantation, located approximately 15 km northeast of Gainesville in Alachua County. This site was established in December 1998 – January 1999. The plantation was fertilized with 40 Kg of N/ha and 45 Kg of P/ha in 2002 (Bracho et al., 2012).

SWAT model

Model description

SWAT (Arnold et al., 1998) is a process-based, semi-distributed watershed-scale eco-hydrological model developed by the USDA Agricultural Research Service (ARS). Major model components include weather, hydrology, plant growth, water quality, and land management. SWAT was originally developed for the prediction of the long-term impact of rural and agricultural management practices on water, sediment, and nutrients in large, complex watersheds with varying soils, land use, and management conditions. SWAT is commonly integrated into GIS interfaces (e.g. ArcSWAT; QSWAT) that allow for the use of spatial information such as land use/land cover, topography, and soils. What makes SWAT especially different from lumped watershed models is how spatial heterogeneity is represented in the model. SWAT delineates a watershed into multiple subbasins based on drainage areas of tributaries. Within each subbasin, unique combinations of land use, soil, and topography called Hydrologic Response Units (HRUs) are created and summed for each subbasin (Neitsch et al., 2011). HRU's are the smallest computational unit in SWAT and provide an efficient way to discretize large watersheds. Most of the land phase processes in SWAT, including water flow, nutrient transformation and transport, and vegetation growth are simulated at the HRU level. At the sub-basin level, SWAT integrates land phase and channel processes.

SWAT provides three methods for estimating evapotranspiration: Penman-Monteith (Monteith, 1965), Priestley-Taylor (Priestley and Taylor, 1972), and Hargraves (Hargreaves and Samani, 1985). In this study, we use Penman-Monteith, since MODIS ET estimates are also based on the physical principles underlying by the Penman-Monteith method. Equation (1) describes the Penman-Monteith method:

$$\lambda E = \frac{\Delta.(H_{net}-G)+\rho_{air}.c_p.[e_z^o-e_z]/r_a}{\Delta+\Upsilon.(1+\frac{r_c}{r_a})} \qquad (1)$$

where, λE is the evaporative latent heat flux density (MJ/m^2.d), Δ is the slope of saturation vapor pressure-temperature curve (KPa/ °C), H_{net} is the net radiation (MJ/m^2.d), G is the heat flux density to the ground (MJ/m^2.d), ρ_{air} is the air density (kg/m^3), c_p is the specific heat at constant pressure (MJ/kg. °C), e_z^o is the saturation vapor pressure of air at height z (kPa), e_z is the water vapor pressure of air at height z (kPa), Υ is the psychrometric constant (kPa/°C), r_c is the plant canopy resistance (s/m), and r_a is the diffusion resistance of the air layer (aerodynamic resistance) (s/m). SWAT calculates r_c using the following relationship:

$$r_c = \frac{r_l}{0.5\ .LAI} \qquad (2)$$

where, r_l is the minimum effective stomatal resistance for a single leaf (s/m), and *LAI* is the one sided green leaf per unit of ground area (m^2/m^2). *LAI* is an important variable linking water and energy fluxes. In SWAT, *LAI* is a key parameter associated with plant growth and development, as described next.

Forest dynamics modeling in SWAT

In SWAT, the potential plant phenological development is simulated based on daily accumulated heat units under optimal conditions (Neitsch et al., 2011). SWAT assumes, based on

the Heat Unit Theory, that each plant has its base, optimum, and maximum temperature for growth. Plant growth in SWAT is only triggered when the mean daily temperature is equal or higher than a plant specified base temperature (*T_BASE*). The total number of heat units required to bring a plant to maturity is a user-defined parameter (*PHU*). SWAT then calculates the total potential heat units for the plant as a summation of the number of heat units accumulated on a given day. The fraction of potential heat units accumulated on a given day is calculated as:

$$fr_{PHU} = \frac{\sum_{i=1}^{d} HU_i}{PHU} \quad (3)$$

where, fr_{PHU} is the fraction of potential heat unit accumulated for the plant on a given day, HU_i is the heat unit accumulated by plant on day *i*, and *PHU* is the total heat unit necessary to bring the plant to maturity. Initially, LAI development in SWAT is defined by the optimal leaf area development curve:

$$fr_{LAImx} = \frac{fr_{PHU}}{fr_{PHU} + e^{(l_1 - l_2 . fr_{PHU})}} \quad (4)$$

where, fr_{LAImx} is the fraction of the plant's maximum *LAI* corresponding to a given fraction of potential heat units, l_1 and l_2 are shape coefficients calculated based on user-defined input parameters.

Once triggered by accumulated heat units, potential plant growth is modeled by simulating leaf area development, light interception, and conversion of intercepted light into biomass. The *LAI* on day *i* is calculated as

$$LAI_i = LAI_{i-1} + \left(fr_{LAImx,i} - fr_{LAImx,i-1}\right).\left(\frac{yr_{cur}}{yr_{fulldev}}\right).LAI_{mx}.(1 - exp\left(5.\left(LAI_{i-1} - \left(\frac{yr_{cur}}{yr_{fulldev}}\right).LAI_{mx}\right)\right)) \quad (5)$$

where, LAI_{i-1} is the leaf area index of the previous day, $fr_{LAImx,i}$ and $fr_{LAImx,i-1}$ are the fraction of plant's maximum *LAI* for day *i* and *i*-1, LAI_{mx} is the maximum *LAI*, yr_{cur} is the age of the tree (years), and $yr_{fulldev}$ is the number of years for tree species to reach full development.

Potential biomass accumulation is estimated based on the plant's efficiency in converting radiation into biomass. The amount of daily solar radiation intercepted by the leaf area of the plant is calculated using Beer's law (Monsi and Saeki, 1953).

$$H_{phosyn} = 0.5.H_{day}.(1 - \exp(-k_l.LAI)) \quad (6)$$

where. H_{phosyn} is the amount of intercepted photosynthetically active radiation on a given day (MJ/m^2), H_{day} is the incident total solar radiation (MJ/m^2), $0.5.H_{day}$ is the incident photosynthetically active radiation (MJ/m^2), and k_l is the light extinction coefficient.

The maximum biomass at the end of day *i* resulting from the intercepted photosynthetically active radiation is estimated as:

$$bio_i = bio_{i-1} + RUE\ .H_{phosyn} \quad (7)$$

where, bio_{i-1} is the biomass on day *i*-1 (kg/ha), and *RUE* is the radiation use efficiency of the plant (g/MJ).

Tree biomass accumulation within a single year is limited to a fixed amount determined by the age of the tree relative to the number of years for the tree to reach full development. Until the trees in an HRU reach full development, the amount of biomass they can accumulate in a single year is limited to:

$$bio_{annual} = 1000.\left(\frac{yr_{cur}}{yr_{fulldev}}\right).bio_{fulldev} \quad (8)$$

where, bio_{annual} is the amount of biomass a tree can accumulate in a single year (kg/ha), yr_{cur} is the current age of the tree (years), $yr_{fulldev}$ is the number of years for the tree to reach full development, $bio_{fulldev}$ is the biomass of a fully developed tree stand for the specific tree species (tons/ha). Once the total growth in biomass in a year is reached, no more growth occurs until the following year when a new annual limit is calculated. Moreover, once a tree stand has reached its biomass limit for a year, the increase in plant biomass for a day is set to zero.

SWAT limitations for simulating tree growth before maturity

The equations and parameters described in the previous section represent the annual growth of a fully-developed tree in SWAT. SWAT allows the simulation of young trees through a planting operation in the model's management file (*.mgt*). When a seedling is planted, the user has to define the age of the seedling, which is represented in the model by the parameter *CURYR_MAT*. The number of years required for the planted tree to transition from seedling to a fully-developed tree is defined in the model's plant database by the parameter *MAT_YRS*. SWAT then limits the annual amount of biomass that the planted tree can accumulate until it reaches maturity (Eq.8). *MAT_YRS* is set to 30 years in the model's plant database for evergreen forests (FRSE). This value is reasonable for pine trees, as the literature suggests (United States Department of Agriculture Forest Service, 1990). However, a limitation arises from the fact that the maximum *LAI* is adjusted in SWAT by considering the ratio between the current age of the tree (*CURYR_MAT*) and the number of years needed for the tree to reach full development (*MAT_YRS*) (Eq. 5). For instance, let us consider a pine seedling planted in the first year of simulation (*CURYR_MAT*=1) and requiring 30 years to become a fully-developed tree (*MAT_YRS*=30), with maximum stand biomass of 200 tons/ha (*BMX_TREES*=200). Under optimum conditions, there will be approximately 7 tons/ha of biomass accumulation each year at stand level, according to Eq. 8. This rate of growth can be

considered realistic for a pine tree, for example, as indicated by studies such as Samuelson et al. (2014). However, since the maximum *LAI* is reduced to $LAI_{mx}/30$ (Eq. 5), the accumulated *LAI* on a given day (Eq. 5) becomes excessively small, which consequently delays the LAI development in SWAT. Fig 2 illustrates this for two cases. Case I shows annual biomass and *LAI* simulated in SWAT without a planting operation. In this case, *LAI* development and biomass accumulation are representative of a fully-developed tree. Consequently, model calibration against field observations of LAI and biomass of juvenile trees becomes a challenge under this scenario. Alternatively, case II exemplifies the situation described earlier, where trees are planted as seedlings in SWAT. It can be seen that stand-level biomass accumulation rate is reasonable with recently planted trees. However, *LAI* development is affected such that there is no *LAI* accumulation for the first 8 years, which can be mathematically understood through Eq. 5. In case II, *LAI* stays constant at the minimum *LAI* value, which is defined in SWAT's plant database (*ALAI_MIN*) for mature trees. SWAT never allows *LAI* to drop below *ALAI_MIN*. Hence, SWAT's ability to simultaneously simulate tree biomass accumulation and *LAI* development before maturity is limited. Calibrating *LAI* and biomass of young trees together in SWAT is, therefore, problematic. Annual maximum *LAI* could be calibrated individually by assigning *MAT_YRS* a value lower than 30 so that *LAI* development begins from the first year of simulation. However, if biomass was to be calibrated next, the simulated values would be excessively high for juvenile trees, since the ratio between *CURYR_MAT* and *MAT_YRS* would become larger in Eq. 8. This shortcoming in SWAT's plant growth module challenges the model application in areas where trees are widely planted, such as the SE-US.

Model setup and data collection

SWAT requires spatially distributed data of topography, soil types, and land use/cover. Additionally, daily climate data is required to run the model. The complete set of climate variables required to drive the hydrological processes in SWAT is comprised of precipitation, maximum and minimum temperature, solar radiation, wind speed, and relative humidity. Table 2 shows the data used as input in the model as well as the data used to perform model calibration.

As we had access to observed data from measurement plots, we were able to perform model calibration for annual maximum *LAI* and total annual biomass at each site. The datasets from long-term productivity studies of loblolly pine (Gonzalez-Benecke et al., 2016) and slash pine (Gonzalez-Benecke et al., 2014b) were shared with us via personal communication and are listed in Table 2. At some sites, field observations represented experiments such as thinning and varied planting density. For such cases, we used data measurements referring to the control scenario only. The period covered by available measured-data slightly varied from site to site (Table 1).

This study uses remotely sensed *LAI* estimates to derive model parameters controlling the optimal *LAI* development curve in SWAT and evaluate SWAT's plausibility in simulating seasonal LAI. NASA's MOD15A2H Version 6 Moderate Resolution Imaging Spectroradiometer (MODIS) combined Leaf Area Index (*LAI*) and Fraction of Photosynthetically Active Radiation (*FPAR*) product (Myneni, 2015) is used as reference data. This product is a 4-day composite dataset with 500 meters pixel resolution. The algorithm automatically chooses the best pixel available from all the acquisitions of the Terra and Aqua sensors in a 4-days period.

Similarly, remote-sensing estimates of ET were used to calibrate modeled ET on a monthly basis in SWAT. We use MOD16A2 Version 6 Evapotranspiration/Latent Heat Flux product (Running, 2017), which is based on the Penman-Monteith framework. This dataset is an 8-day

composite produced at 500 meters of cell resolution. The 8-days ET estimates were aggregated into monthly time-step to be used as a benchmark during the model calibration process.

We used MODIS estimates of LAI and ET from 2002 to 2018 at the sites SAGCD – AL and IMP – GA. At the sites IMPAC – FL and MIZE – FL, silvicultural rotations were implemented in 2009 and 2013, respectively. Because of the land cover change stemming from these rotations, we did not derive remote-sensed data after 2008 and 2012 at IMPAC – FL, and MIZE – FL, respectively. At all sites, remote-sensing time-series were derived from the Google Earth Engine platform (Gorelick et al., 2017) through a series of automated routines.

The dataset listed in Table 2 was used to develop and setup four field-scale SWAT models using SWAT2012 (revision 664). Since the standard SWAT HRU definition provides no means for representing realistic field-scale management strategies (e.g., forest plots might spread across several HRUs), we employed the approach described by Marek et al. (2016) to delineate meaningful field-boundaries based on an area of interest (AOI). First, the AOI representing each loblolly pine plantation was delineated and later used as mask during the watershed delineation process within ArcSWAT. After artificial subbasins and tributaries were created based on the landscape topography, the longest reach was identified by using the field "shape_length" in the attribute table of the feature. The subbasin having the longest reach was then selected to be representative of the field area and the HRU's were eventually created by assigning a single HRU to the subbasin. It is worth mentioning that ArcSWAT offers the user two options to determine the HRU distribution across the watershed area: assign a single HRU to each subbasin, or assign multiple HRU's to each subbasin. When a single HRU per subbasin is assigned, the HRU is created based on the dominant land use class, soil type, and slope within each subbasin. When multiple HRU's are assigned, they are created based on user-defined thresholds for land use, soil, and slope

classes. To delineate field-scale models, this research selected the dominant HRU option. The final product was a "watershed" having one subbasin and one HRU. To make sure that the area of the single subbasin and HRU matched exactly the area of the pine plantation fields, the following files had to be adjusted in the ArcSWAT project database ("ProjectName".mdb file): "Basins", "hrus" and "Watershed". Last, a test run of each model was performed to verify if the area in the model output files *.sub* and *.hru* were representative of the real field areas.

Model parameterization

Here we propose to implement an improved forest parameterization for loblolly and slash pine trees in SWAT. To that end, we included two new plant types in SWAT's plant database: loblolly pine (LBPN) and slash pine (SLPN). Initially, we parameterized the new plant types with the default values representing the annual growth of evergreen forests in SWAT (FRSE). Next, we revised default parameter values in SWAT's plant database and when necessary, modified them based on published literature, field observations, remote-sensing information, and expert judgment. The parameters included in the parameterization presented in this study were selected based on expert knowledge and the model's functionalities (Neitsch et al., 2011). We selected key parameters representing tree growth and development in the model's .hru, .dat, and .mgt files. A brief description of each plant-parameter included in the current study is given in Table S1 in the supplementary materials.

The importance of the selected plant-related parameters in simulating LAI, biomass, and ET in SWAT was assessed through global sensitivity analysis and quantified based on *p-values* (*p-value* < 0.05 was assumed to indicate a parameter having a significant effect on a modeled process). We use the automated calibration software SWAT Calibration and Uncertainty Program (SWAT-CUP) (Abbaspour, 2015) to carry out the global sensitivity analysis and model calibration.

Model calibration

The Sequential Uncertainty Fitting – SUFI-2 (Abbaspour et al., 2004) algorithm in SWAT-CUP was used to perform automated model calibration within the range of values derived for each parameter during the parameterization phase. First, annual maximum LAI and total annual biomass were calibrated simultaneously against field measured data at each site. LAI and biomass were calibrated at the same time to avoid the model's drawbacks described in section 2.2.3. We used King-Gupta Efficiency (*KGE*) (Gupta et al., 2009) as the objective function and assigned equal weights to each variable, which allowed us to equally emphasize LAI and biomass so that the model performance with respect to LAI did not degrade its performance relative to biomass. The period used to perform LAI and biomass calibration varied across the study sites. At SAGCD – AL, model calibration was performed from 2002-2010. At IMP – GA from 1999-2010, at IMPAC – FL from 1987-2008, and at MIZE – FL from 2001-2012. For each model, a 3 years warm-up period was used to accurately initialize conditions such as antecedent soil moisture in the model and the trees were planted as seedlings during this period to avoid bare soil conditions.

Next, ET calibration was carried out separately at each site by running iterations of 500 simulations. As described earlier, we used MODIS 8-days ET estimates to calibrate ET in SWAT. For ET calibration, we used the percentage bias (PBIAS) as the objective function in SUFI-2 to avoid excessive over or underestimation of simulated ET. We did not opt for objective functions such as NSE and KGE since they are sensitive to peaks and MODIS ET estimates are very noisy, often showing multiple peaks during the year. As a result, a good match between simulated and observed ET based on NSE and/or KGE would be unlikely and could yield unrealistic parameter values. The calibration periods were 2002-2018 at SAGCD – AL and IMP –GA, 2002-2008 at IMPAC – FL, and 2002-2012 at MIZE – FL.

Model performances were assessed by graphical analyses of simulated versus observed plots, and the statistical metrics coefficient of determination (R^2), *PBIAS*, and the Root Mean Square Error (*RMSE*). These statistical metrics are commonly used to evaluate model performance in simulating variables such as LAI, biomass, and ET (Alemayehu et al., 2017; Strauch and Volk, 2013; Yang et al., 2018; Yang and Zhang, 2016).

Impacts of improved forest dynamics on water fluxes

The changes promoted by the improved forest parameterization on SWAT's water balance computations were assessed by comparing the mean annual water budget simulated with the default and improved models. Model outputs from the HRU (*.hru*) and the standard output summary (*output.std*) files were used to analyze the differences in simulated green and blue water fluxes under the default and improved parameterization scenarios. We follow the approach described by Naderi (2020) to quantify blue waters in SWAT. Total blue water is the sum of surface runoff (*SURQ*), lateral flow (*LATQ*), and baseflow (*GW_Q*). Subsurface blue water (or aquifer storage) is defined as total aquifer recharge minus baseflow (*GW_RCHG*) - (*GW_Q*).

RESULTS

Model parameterization

The first step in improving SWAT's skills in simulating plant growth and dynamics involved deriving physically-meaningful parameter values. Parameters representing processes in process-based models can often be measured through field experiments or derived via physically-based equations. Table 3 shows the parameters modified by our parameterization and the approaches used.

Some parameters do not explicitly describe a physically-based process in SWAT, but rather a mathematical process-level understanding. For such cases, we found relationships between

observed data and SWAT's equations to derive realistic values for these parameters. Fig. 3 illustrates such a case for the parameterization of the LAI curve in SWAT. Based on MODIS 4-days LAI estimates, we parameterized the seasonal LAI dynamics in SWAT by tweaking parameters controlling the length of the growing season (*HEAT_UNITS*), the first and second points in the optimum LAI development curve (*FRGRW1- LAIMX1, FRGRW2- LAIMX2*), and the fraction of the growing season when LAI starts to decline (*DLAI*). Another similar example is EPCO, which regulates the soil depth used to meet the plant's water uptake demand in SWAT. The default value for EPCO is 0.95 in SWAT, which means 50% of the water uptake occurs in the upper 6% of the root zone (Neitsch et al., 2011), based on the relationship that assumes that root density is greatest near the soil surface and decreases with depth. We used field-measured values of rooting depth and root mass for loblolly and slash pine to develop a relationship and fit it to SWAT's water uptake equation. This allowed us to derive more realistic and species-specific values for *EPCO* (Table 3). *EPCO*'s absolute range goes from 0.01 to 1, and as it approaches to one the model allows more of the water uptake demand to be met by deep soil layers (Arnold et al., 2011). Since the climate within the natural range of slash pine is wet with an average rainfall of 1270 mm/year (Lohrey and Kossuth, 1990), the rooting depth of slash pine is usually shallower compared to loblolly pine. The latter can help to interpret the smaller value of *EPCO* derived for slash pine in comparison to loblolly pine.

The parameters listed under expert knowledge in Table 3 had their values derived through personal communication or based on the authors' judgment. For the parameters revised based on published literature, we derived a range of values, since we usually found multiple sources for each parameter. One special case is *BIO_LEAF* (the amount of plant biomass converted to residue during dormancy), for which we calculated the fraction of leaf biomass corresponding to

aboveground biomass using field measurements. This fraction varied across the analyzed sites and ranged from 8 to 12%. Although this did not tell us the value of *BIO_LEAF*, it indicated that its value should not be higher than 12%, since loblolly and slash pine are evergreen trees and consequently do not lose all of their leaves during the year. We then further refined this range through literature review (Table 3). The only parameter that had its value directly derived from field measurements was *BMX_TREES* (the maximum biomass of a mature forest stand). Based on the available field-measured data, we verified that trees stopped accumulating significant amounts of biomass once a total biomass value of approximately 180 tons/ha was reached. Finally, we derived values for the maximum potential leaf area index (*BLAI*) and minimum leaf area index (*ALAI_MIN*) using remote-sensed LAI data across all sites. For each year of retrieved data, we were able to record the maximum and minimum LAI for loblolly and slash pine at each study site. This allowed us to define a range of maximum and minimum LAI for loblolly and slash pine in SWAT (Table 3).

The importance of each parameter listed in Table 3 in modeling forest growth in SWAT was assessed through global sensitivity analysis using the calibration software SWAT-CUP. The *p-values* are shown in Tables S1-S4 in the supplementary materials. It can be noticed in Table 3 that several parameters in SWAT's plant database did not accurately represent loblolly pine and slash pine processes with the default model settings. We can highlight parameters such as *BLAI*, *ALAI_MIN*, *BIO_E*, *BIO_LEAF*, and *GSI*, all of which showed significant impacts on processes such as LAI development, biomass accumulation, and evapotranspiration (Tables S1-S4 in the supplementary materials).

Modeling young trees in SWAT

The current study simulates the growth of young trees, with ages ranging from 3 to 6 years old at the beginning of the simulation period. To realistically model juvenile trees in SWAT, we planted trees as a seedling in SWAT's management file. Whenever a planting operation is initialized in the model, the user is forced to insert a value for the parameter *CURYR_MAT*, which is defined as the age of seedling in SWAT's input/output documentation (Arnold et al., 2010). As described in section 2.2.3., the parameters in SWAT's plant database represent the annual growth of a fully-developed tree. The model's limitation in simulating the growth of young trees challenges multivariable calibration of LAI and biomass. Since biomass accumulation in SWAT is a function of the radiant energy absorbed by the plant canopy and its efficiency in converting radiation into biomass (Equations (7)), tree biomass depends on LAI simulation (Arnold et al., 2011). Here, we used an alternative approach to find a balance between calibrated LAI and biomass for planted trees. The parameter *CURYR_MAT* was assigned a fixed value of 1 year for all study sites, while the number of years required for the tree to reach full development (MAT_YRS) was calibrated within a defined range of 3-5 years old (Table 3). Based upon personal communication with professionals of the tree nursery industry, 3 to 5 years was defined as a reasonable time needed for loblolly and slash pine trees to transition from seedling to a sapling. In other words, instead of assigning to *MAT_YRS* a value portraying the annual growth of a fully-develop tree, we forced SWAT to transition the planted trees from seedling to a sapling.

SWAT calibration of annual maximum LAI and annual total biomass

After SWAT parameterization, iterations of 1,000 model runs were performed in the software SWAT-CUP to match simulated annual maximum LAI ($LAI_{max,yr}$) and annual total biomass ($BIO_{tot,yr}$) with the respective field observations at each site.

The temporal variability of observed and simulated $LAI_{max,yr}$ as well as the models' performances are shown in Fig.4. The improved parameterization yielded better model performance for all rating metrics at the IMPAC–FL site only. For all other sites, the improved model parameterization performed poorer than the default parameterization for at least one of the selected statistical metrics. Overall, it is possible to notice that the improved parameterization reduced the model overestimation of $LAI_{max,yr}$ for loblolly pine trees and the underestimation for slash pine (see P_{BIAS} values in Table at the bottom of Fig. 4). The only exception was the SAGCD–AL site, where the improved parameterization further increased the overestimation of $LAI_{max,yr}$ for loblolly pine. However, the temporal pattern of observed $LAI_{max,yr}$ was better explained with the improved parameterization at SAGCD-AL, as evidenced by the increase in R^2 from 0.03 to 0.51.

Clearly, with the improved parameterization, the modeled $BIO_{tot,yr}$ better matched the observations across all sites (Fig. 5). With the default models, $BIO_{tot,yr}$ was underestimated more than 70% at all sites, with the highest underestimation found at IMPAC–FL, where SWAT underestimated the observed total biomass by 85%. In the simulations with the improved models, $BIO_{tot,yr}$ underestimation decreased to values as low as 3.7% at MIZE – FL and turned to 22% of overestimation at SAGCD–AL. At SAGCD–AL, the improved model failed to capture the observed total biomass at the beginning of the simulation period. During the first year of simulation, SWAT predicted 34 tons/ha of biomass accumulation, which is 90% higher than the observed value for this year. This can be attributed to the tree's fast transition from seedling to a sapling in the model since the parameter *MAT_YRS* received a calibrated value of 3.3 years at SAGCD–AL (Table 4). This issue could be fixed by increasing the value of *MAT_YRS* to slow down biomass accumulation during the initial growth stages. However, this solution would delay LAI development, which would lead to a significant underestimation of LAI at this site.

The new parameterization also led to significant improvements in temporal estimates at all sites (Fig. 5). In the simulations with the improved parameterization, the simulated $BIO_{tot,yr}$ better fitted the observations, as demonstrated by R^2 values higher than 0.95 at all sites. With the default parameterization, SWAT was not able to achieve R^2 values higher than 0.51. The smaller *RMSE* values achieved under the improved parameterization further denote SWAT's enhancement in replicating observed total annual biomass across all study sites. Considering the fact that the average observed $BIO_{tot,yr}$ ranged from 56 to 133 tons/ha across the study sites, the *RMSE* values ranging from 62 to 127 tons/ha obtained with the default models indicate serious shortcomings. On the contrary, the improved models lowered *RMSE* to the 8.6-23 tons/ha range.

It can be noticed in Fig. 5 that the simulated biomass with the improved model parameterization stayed constant once it reached 200 tons/ha at the IMPAC–FL site. This happened because SWAT reached the maximum allowed biomass for a mature tree at this site. This behavior was managed in the model by calibrating the parameter *BMX_TREES* (Table 4). In reality, the biomass accumulation does not stay perfectly constant once a tree reaches its maturity. Rather, the growing process slows down and biomass accumulation diminishes. However, there is no mechanism capable of altering the growth rate over the simulation period in SWAT. Alternatively, we constrained *BMX_TREES* to match the biomass observations as close as possible.

Model performance in simulating monthly LAI

Fig. 6 shows simulated monthly LAI at each site compared to MODIS LAI. Since the MODIS product used by the current study does not have data availability before July of 2002, the period displayed in Fig. 6 does not exactly reflect the period shown in Fig. 4. Particularly, the

initial growth stages after planting could not be captured by remotely sensed LAI across the study sites.

Overall, it can be seen that monthly LAI estimates with the new model parameterization matched MODIS LAI better than the default parameterization (Fig. 6). The improved model parameterization increased R^2 values from near zero to values as high as 0.52, with the highest improvement found at IMP–GA. With the default plant database, SWAT systematically overestimated LAI for loblolly pine. In the simulation with the new model parameterization, the overestimation of LAI decreased from 73% to 4% at the IMPAC–FL site. At the SAGCD – AL, and IMP – GA sites, LAI overestimations of 7.5% and 48% turned to 27% and 19% of underestimation, respectively, under the improved model parameterization. The underestimation at IMP–GA with the improved model parameterization comes from SWAT's inability to capture MODIS peaks in 2004, 2008, and 2017. At SAGCD–AL, SWAT failed to capture the LAI dynamics in the beginning of the growing season several times over the simulation period, leading to a substantial underestimation of monthly LAI under the improved parameterization. MODIS estimated LAI began to increase around February, whilst SWAT simulated LAI under the improved parameterization stayed constant until April at SAGCD-AL. The former may be related to the understory greening captured by MODIS derived data. It might also indicate that the parameterization presented here can be further improved. At the slash pine site MIZE–FL, SWAT underestimated LAI by 17% with default parameterization. With the improved parameterization, SWAT overestimated LAI by only 8%. This is mainly due to the adjustment of the parameter controlling the maximum LAI in SWAT, which was increased from 5 m^2/m^2 to 7 m^2/m^2. Oddly, the LAI curves simulated under the default parameterization showed an unrealistic shape at all sites (Fig. 6). In some cases, LAI appeared to decline to a random value at which it stayed constant

before declining to its minimum. In other cases, LAI declined to a certain value and suddenly went back to the growing cycle without dropping to the minimum value. This can be considered a structural limitation of the default models and may also be related to the poorly defined LAI shape parameters after a planting operation in SWAT.

In order to enhance SWAT's performance in simulating LAI, several parameters were modified in the model's plant database (*crop.dat*) and management file (*.mgt*). Initially, parameters responsible for the shape of the LAI curve had their values derived from MODIS, as discussed in section 2.4 and illustrated by Fig. 3. The calibrated values of parameters describing LAI development are shown in Table 4 and can help to understand the different LAI dynamics across the study sites. It can be noticed from Figures 6 and S1 that the maximum LAI value reached at SAGCD–AL is higher compared to the other loblolly pine sites. The latter is due to a larger calibrated value for the parameter BLAI (Table 4). SWAT predicted LAI starts declining around early September at IMP–GA and SAGCD–AL sites, and early October at the IMPAC–FL site (Fig. S1). As shown in Table 4, the calibrated value of *DLAI* is higher at IMPAC–FL compared to IMP–GA and SAGCD–AL, which explains the late LAI decline in Florida. For the slash pine site MIZE–FL, predicted LAI development was significantly different compared to the loblolly pine sites (Fig. S1). The simulated growth of slash pine trees was faster, with LAI beginning to increase in February and reaching its maximum value in April. The late LAI decline (November) predicted for slash pine at the MIZE–FL site is due to a high value of *DLAI* (Table 4).

ET calibration

SWAT was able to capture the interannual and seasonal variability of ET reasonably well at all sites with the default and improved parameterizations (Fig. 7). However, in the simulations with the default parameterization, SWAT significantly underestimated ET compared to MODIS

estimates. At the SAGCD–AL site, we compared SWAT daily ET estimates against 8-days MODIS ET from 2001 to 2018. The seasonal trend could not be accurately analyzed at this site because approximately 20% of the retrieved MODIS data was missing (162 data points). As a consequence, a continuous monthly time series for the period 2001-2018 could not be obtained at SAGCD – AL. Based on the assumption that the 8-days MODIS ET estimates are evenly distributed over the 8-days period, we derived daily ET estimates from the 8-days MODIS ET algorithm and compared these data against the respective daily values predicted by SWAT. The average daily ET simulated by the default model was 1.52 ± 1 mm in the period 2001-2018. Compared to MODIS estimates, it represented 13% underestimation. The average daily ET estimated by MODIS in this period was 1.76 ± 1.17 mm. With the improved model parameterization, simulated daily ET increased to 1.80 ± 1.35 mm. Compared to MODIS, the improved parameterization overestimated ET by only 3% in the period 2001-2018 at SAGCD – AL.

At the IMP–GA site, the default model parameterization underestimated monthly ET by 15.5% compared to MODIS in the period 2001-2018. The average monthly ET estimated by the default model was 50 ± 27 mm, while the average monthly ET estimated by MODIS was 60 ± 30 mm. The improved model parameterization increased monthly ET estimates of 60 ± 44 mm, or 0.48% higher than MODIS estimates. It is possible to notice from Fig. 7 that SWAT simulated some ET peaks that were not observed by MODIS estimates at this site, especially in 2008 and 2011. Rainfall in 2008 was 15% higher (1,476 mm) than the average for the period 2001-2018, which combined to 17% of missing data from MODIS during 2008 could explain the absence of a higher MODIS peak for this year. As for 2011, rainfall was below average and MODIS missing data accounted for only 10%. However, most of the MODIS missing data in 2011 occurred in July,

which may explain the surprisingly low ET estimated by MODIS during the summer. It is worth mentioning that there are uncertainties related to the MODIS ET algorithm. Mu et al. (2013) reported 24% mean absolute error between MODIS ET values and observations across 46 eddy flux towers.

At the IMPAC – FL site, the default parameterization led to substantial underestimation of ET from 2001-2008, especially in 2005, when the default model dramatically underestimated ET during summer months. The average monthly ET estimated under the default parameterization was 53.6 ± 25.5 mm during 2001-2008, or 18.5% lower than MODIS estimates of 65.86 ± 27.66 mm. Under the improved parameterization, ET predicted by SWAT increased to 60 ± 31.8 mm, which lowered ET underestimation to 8.7% (Table 7). Likewise, at the MIZE – FL site, monthly ET simulated by the default model was significantly underestimated compared to MODIS. With the default parameterization, SWAT underestimated ET by 43%. The average monthly ET estimated with the default plant database was 53 ± 25.2 mm from 2001 to 2012, which largely differed from the MODIS estimates of 93 ± 38.3 mm. With the improved parameterization, average monthly ET estimates raised to 75.3 ± 31.8 mm, which decreased SWAT's underestimation of ET to 19.2% in comparison to MODIS estimates (Table 7). Although 19.2% of underestimation might seem high, the average annual ET simulated by the improved model (893 ± 56 mm) was in good accordance with the values reported by McLaughlin et al. (2013). The authors compiled a wide range of studies investigating ET in the Southeastern Coastal Plain and revealed an ET range of 754-1168 mm/year at slash pine plantations in Florida.

Impacts of improved forest dynamics on water fluxes

Fig. 8 summarizes the mean annual water balance at each study site, under default and improved model parameterizations. Overall, it can be seen that ET not only dominated the water

budget at all sites but also was the component that changed the most under the new model parameterization. Unfortunately, we did not have observations of surface runoff, lateral flow, or baseflow at any site to assess if the improved forest parameterization changed SWAT's hydrological predictions in the right or wrong direction. However, the enhanced model's performance in simulating ET under the improved parameterization might indicate that other water balance components improved as well. Foremost, largely different water budgets predicted with the two parameterization schemes (Fig. 8 and Tables 5) depicted a major role played by forests in SWAT's hydrological computations.

At SAGCD–AL, ET corresponded to 43% of the water balance in the default model (616 mm), followed by 31% of baseflow (446 mm) and 26% of surface runoff (385 mm). ET increased 18% in the improved model scenario, which altered the water balance configuration to 51% of ET (748 mm), 26% of baseflow (375 mm), and 23% of surface runoff (329 mm) (Fig. 8 and Table 5). The high surface runoff rates simulated at SAGCD–AL can be explained by the hydrological soil group (HSG) at this site, which is D. At IMP–GA, as a result of 15% increase in ET with the improved parameterization, baseflow was reduced from 368 mm (or 30% of the water balance) to 295 mm (or 24% of the water balance), while surface runoff rates decreased from 200 mm/year (16% of the water balance) to 170 mm/year (14% of the water balance) (Fig 8 and Table 5). Similar trends were found at IMPAC–FL, but with the main difference observed in subsurface fluxes. With default SWAT forest parameterization, ET represented 55.5% of the water budget (670 mm), while baseflow and lateral flow represented 43% (516 mm) and 0.2% (12 mm), respectively. Under the improved forest parameterization, ET/P increased to 61% (ET=744 mm), while the ratio of baseflow to precipitation dropped to 37% (448 mm) and lateral flow remained unchanged. Surface runoff was insignificant at this site. The negligible surface runoff at IMPAC–FL is likely due the

site's HSG being A. At IMPAC–FL, the soil texture consists of 95% of sand. The most dramatic effect of improved forest parameterization on water resources was found at the slash pine site MIZE–FL. In the simulation with the default SWAT forest parameterization, 54% of the annual precipitation was lost as ET (637 mm), 39% contributed to baseflow (456 mm), 7% contributed to surface flow (74 mm), and 1% contributed to subsurface flow (13 mm). The improved model parameterization altered this budget such that 75% of the annual rainfall was lost to ET (894 mm), 19% contributed to baseflow (231 mm), 5% contributed to surface flow (56.61 mm), and 1% contributed to subsurface flow (11 mm) (Fig. 8 and Table 5). Baseflow was impacted more than any other water balance component with a reduction of 50%.

Table 5 shows in more detail the effect of improved forest parameterization on water fluxes. Overall, increases in ET from 10 to 30% across all sites reduced surface water (SURQ) in 6-33% and groundwater storage (GW_RCHG minus GW_Q) in 7-26%.

Fig. 9 illustrates the difference in groundwater recharge simulated with the default and improved models. The sites SAGCD–AL, IMP–GA, and IMPAC–FL showed similar trends, with recharge reductions of 75 mm (15%), 76 mm (18%), and 71 mm (13%), respectively, in the simulations with the improved model (Table 5). IMPAC – FL exhibited the highest groundwater recharge rate across all sites (496 mm/year). Considering the site's HSG A, this result is not surprising. The lowest groundwater recharge rate occurred at MIZE – FL, as expected since slash pine trees showed the highest water loss via ET amongst all sites.

DISCUSSION

Modeling forest dynamics in SWAT

Many of the parameters in SWAT's plant database were originally parameterized based on observations from annual crops. However, the differences in growth rate, size, water and nutrient

demands, biomass accumulation, and energy exchange, for example, highly differ from crops to trees. Thus, our improved parameterization aimed to enable SWAT to reasonably simulate the growth and dynamics of two widely cultivated tree species in the SE-US and serve as a starting point for future modeling studies in this region. We acknowledge that some of the parameters calibrated here are highly site-specific (e.g., BMX_TREES) and may not be directly incorporated into other modeling studies. However, given the wide geographical and climatological range of sites considered in this study, the parameterization presented here should be useful for large parts of the modeling community.

Although SWAT presented a poor performance in simulating $LAI_{max,yr}$ even with an improved parameterization, it can be seen as a necessary tradeoff to ensure accurate simulation of biomass (section 2.2.3). In the simulations with the improved model parameterization, the parameter values assigned to *MAT_YRS* and *CURYR_MAT* described tree growth from seedling to a sapling. As shown in Table 4, the calibrated values of *MAT_YRS* ranged from 2 to 4. Consequently, the transition from seedling to a fully-developed tree (in this case a sapling) was quite fast, which explains the model overestimation of $LAI_{max,yr}$ for all loblolly pine sites (Table 4). The default models overestimated $LAI_{max,yr}$ because of an excessively high value assigned to the parameter controlling the maximum potential leaf area index (*BLAI*). By default, *BLAI* has a value of 5 m^2/m^2 in SWAT, which is too high for loblolly pine trees, as supported by the field observations (Fig. 4). Iiames et al. (2018) also reported 5 m^2/m^2 as an unrealistically large value to represent maximum LAI for loblolly pine trees. In contrast, observed $LAI_{max,yr}$ for slash pine reached values up to 8 m^2/m^2, which lead to bigger underestimation in the default forest parameterization compared to the improved parameterization. With the new parameterization, the

calibrated *BLAI* value for MIZE–FL increased from 5 m^2/m^2 to 7 m^2/m^2, which approximated the simulated $LAI_{max,yr}$ to the observations and consequently reduced model underestimation.

The main reason behind SWAT's poor performance in simulating tree biomass with the default model parameterization is an unrealistically high value for the parameter *BIO_LEAF*. This parameter controls the fraction of the tree's total biomass converted to residue during dormancy. By default, SWAT assigns 30% of the plant's biomass as residue to the ground every year. Yang and Zhang (2016) also noticed this issue in their study. Fig. 5 illustrates this shortcoming. It is possible to see that the default models could not develop a growing trend over the simulation period at all sites. This is because 30% of the total tree biomass was assigned as residue to the forest floor every year, impeding reasonable biomass accumulation.

Based on field measurements of aboveground biomass and foliage biomass, we could determine a more realistic fraction of biomass annually converted to residue across all sites (Tables 3 and 4). An unrealistically high fraction of biomass converted to residue every year can also threaten SWAT's water quality applications in highly forested ecosystems. For instance, SWAT considers three organic nitrogen pools to model the nitrogen cycle in the soil (Neitsch et al., 2011). The fresh nitrogen pool is associated with plant residue and is a direct source of nitrate (NO_3) through mineralization. As a consequence, the higher the amount of residue on the ground the higher the NO_3 available to be transported to water bodies. In our study, the amount of residue on the forest floor was higher under the default model parameterization compared to the improved parameterization at all sites (Tables S6-S9 under supplementary materials). More importantly, the simulated annual mineralization of fresh organic nitrogen was indeed higher in the simulations with the default models. At SAGCD–AL, the mineralization of fresh organic residue was 4.58 kg/ha.yr under the default forest parameterization and 2.28 kg/ha.yr with the improved

parameterization. At IMPAC–FL, IMP–GA, and MIZE–FL the reductions from default to improved models were 9.37 to 3.96 kg/ha.yr, 7.84 to 2.5 kg/ha.yr, and 9.61 to 1.77 kg/ha.yr, respectively. Unfortunately, we did not have observations to calibrate parameters related to mineralization and nitrification rates in SWAT. Although this is beyond the scope of this study and must be addressed in a future effort, it is interesting to notice how the characterization of forest dynamics can affect the soil nutrient cycling in hydrological models. Similarly, the amount of residue on soil surface also affects the sediment yield in SWAT under the Universal Soil Loss Equation (USLE) (Williams, 1995) since the USLE's cover and management factor is computed as a function of plant residue (Neitsch et al., 2011).

Besides interfering with the nutrient cycling in SWAT, biomass also affects the soil evaporation in the model. The soil evaporation is calculated in SWAT as

$$E_s = E_0'.e^{-5X10^{-5}.CV} \quad (10)$$

where E_0 is the potential ET adjusted for canopy interception, and CV is the aboveground biomass and residue (Neitsch et al., 2011). Hence, biomass is not only an important variable describing tree growth in SWAT but also a player in the model's nitrogen cycling and soil water evaporation. With potential impacts on hydrology and water quality, biomass should not be overlooked in hydrological modeling applications, especially in forested ecosystems. Our findings point to the necessity of revising model parameters related to forest growth and dynamics when applying SWAT in forestlands and highlight the benefits of our improved model parameterization.

Monthly LAI

In SWAT, LAI affects the simulation of processes such as canopy storage, canopy resistance in the Penman-Monteith equation, biomass accumulation, and management operations

(Neitsch et al., 2011). Therefore, accurate simulation of LAI dynamics is key to realistically simulate other hydrological processes in SWAT and increase the model's reliability. Despite the uncertainties inherent to the MODIS LAI algorithm, remotely sensed LAI proved to be a useful source of data to derive species-specific phenological information and stand characteristics. A combined set of field measurements and remote sensing data helped us to improve SWAT's capabilities in simulating LAI across the SE-US. The results achieved in this study consistently demonstrate SWAT's skills in predicting LAI dynamics under the improved model parameterization.

The LAI seasonality predicted by all models showed good agreement with MODIS estimates and findings from forestry studies. For instance, Wightman et al. (2016) found peaks of LAI occurring at the end of July in Northern Florida. The authors also reported peak values of LAI ranging from 2-3.6 m^2/m^2 in the period 2012-2013. The magnitude of maximum LAI reported by the authors is similar to the values predicted in the current study (Fig. 6), although the simulated maximum LAI is usually attained at the end of August. The divergent timing of maximum LAI may be due to natural variability, site's management conditions, or annual variation associated with climatic variability between our study site and that of Wightman et al. (2016). Another reason could be the uncertainties associated with MODIS LAI estimates, which might have delayed the LAI peak during the parameterization stage. Samuelson et al. (2017) reported peak LAI in late August or early September for loblolly pine fields in GA. The authors also found peaks of LAI ranging from 2 to 3.2 m^2/m^2. Both the timing of LAI peaks and the magnitude are in good agreement with the results found by the present study in Georgia (Figure 6).

The maximum predicted LAI for slash pine ranged from 4.2 to 5.5 m^2/m^2. Bracho et al. (2012) reported LAI peak of 7 m^2/m^2 for slash pine in Florida, seven years after planting. Although

the calibrated *BLAI* value for slash pine was 7 m^2/m^2 (Table 4), this value was never reached over the simulation period. This is because LAI growth stops once the number of needed heat units is achieved in SWAT. Since slash pine trees accumulated the required number of heat units before reaching the maximum LAI, the value assigned to *BLAI* was not reached. In case a larger *PHU* value was inserted, the beginning of the growing season would be delayed and consequently, the agreement between simulated monthly LAI and MODIS estimates would deteriorate. It is possible to see in Fig 6. that the seasonal variability in MODIS LAI is especially high for slash pine (MIZE – FL). This raises uncertainties concerning our model calibration for slash pine, particularly regarding to the length of the growing season.

Modeling ET

The model parameterization presented in this study remarkably increased the precipitation lost as ET at all study sites. As a result, the consistent model underestimation of ET produced by the default parameterization was mitigated and better matched MODIS ET estimates under the improved model parameterization. Studies such as Yang et al. (2018) also found the default SWAT model to significantly underestimate ET in forested ecosystems. Although LAI and biomass affect ET estimates in SWAT (Eq. 2 and 10), we had to further calibrate some ET related parameters to account for variation among tree species and climate conditions (Table 4).

Overall, the maximum stomatal conductance (*GSI*) revealed to be the most sensitive parameter for ET across all sites (Tables S1-S4 in the supplementary materials). The calibrated values of *GSI* ranged from 0.006 to 0.011 m/s, significantly higher than the default value of 0.002 m/s. The extremely low default value for *GSI* could be one major reason behind SWAT's poor performance in capturing the magnitude of ET estimates with the default plant database.

Not surprisingly, the average annual ET at MIZE–FL (893 ± 56 mm) exceeded all other sites. This was expected given that the simulated LAI at MIZE–FL was substantially larger compared to the other sites. IMP–GA and IMPAC–FL exhibited similar average annual ET values, 734 ± 77 mm and 744 ± 68 mm, respectively, likely because of the similarities in annual rainfalls (Table 1). Despite receiving the highest amount of annual precipitation across all sites, SAGCD–AL did not show the highest ET losses. At this site, the simulated average annual ET from 2001-2018 was 737 ± 67 mm. This could be related to the soil type at SAGCD – AL, which is prone to generate high surface runoff rates and produce a quick response to rainfall. Another reason could be the low soil evaporation at this site. As discussed earlier, biomass was overestimated by 22% at SAGCD – AL. Because more aboveground biomass means less soil evaporation (Eq. 10), the evaporation demand at SAGCD – AL was essentially met by canopy storage. It could explain the high calibrated value for maximum canopy storage (CANMX) at this site (Table 4), as well as the high sensitivity of ET to this parameter (Table S3).

Impacts of improved forest dynamics on hydrology

Water fluxes such as surface runoff (SURQ), percolation (PERC), groundwater recharge (GW_RCHG), and baseflow (GW_Q) significantly decreased under the improved model parameterization (Table 5). In general, the most significant changes occurred at the MIZE–FL site. This is not surprising, considering that simulated LAI and ET losses for slash pine were higher compared to the other study sites. The reductions in water yield achieved with the improved forest parameterization across all sites should not come as surprise given that ET/P significantly increased. The higher amounts of water lost to the atmosphere as vapor under the improved parameterization scenario decreased the outflow from the study sites compared to the default forest parameterization.

Our results consistently showed the effects of forests on SWAT's water budget and hydrological fluxes. ET is usually the main component of the water budget, with fractions as high as 90% of the rainfall in forested ecosystems (McLaughlin et al., 2013). Consequently, small changes in ET can lead to major impacts on other water balance components. If forest dynamics are not considered in hydrological modeling studies conducted in highly forested areas, the results could be flawed. Land use/land cover change studies considering the impacts of afforestation and/or deforestation on water resources, for example, should accurately simulate forest dynamics before drawing scenarios. In this context, our study holds the promise to contribute to future hydrological modeling studies in forestlands.

CONCLUSIONS

Given the extent of planted loblolly pine and slash pine in the SE-US, it is fundamental to consider the forest growth and dynamics in hydrological modeling studies in this region. Here we examined SWAT's capabilities in simulating key forest processes at four pine plantations in the SE-US. Our results showed that under the default forest parameterization, SWAT cannot accurately represent forest dynamics due to unrealistic parameter values in the model's plant database. Furthermore, SWAT showed limitations to simulate juvenile trees. Under the default scenario, annual and seasonal LAI of loblolly pine trees were highly overestimated by SWAT. In contrast, SWAT underestimated LAI for slash pine trees. Additionally, the default model parameterization of forests largely underestimated annual biomass and seasonal ET across all study sites regardless of the tree species.

Our improved parameterization of SWAT's plant database proved to significantly enhance forest modeling processes such as LAI, biomass, and ET. By revising SWAT's default plant database parameters and altering them to accurately represent loblolly and slash pine, we were

able to initialize the model under the right conditions. This led to a satisfactory calibration of LAI and biomass for planted trees, although tradeoffs were unavoidable given the model's current structure. By using remote-sensing MODIS LAI estimates we were able to verify that our parameterization reasonably described LAI seasonality in the SE-US. Likewise, by further refining ET related parameters, we achieved good agreements between SWAT simulated ET and MODIS ET estimates. Simulated biomass improved tremendously with the improved model parameterization and closely matched field observations at all sites.

Our parameterization translated into changes in the simulated water budget, with high impacts on soil water content, surface, and subsurface fluxes. Overall, the new parameterization decreased simulated surface runoff and baseflow at all sites. The extent to which the improved forest parameterization affected hydrological processes in SWAT suggested that forest dynamics should be considered before conducting any model application in forested ecosystems.

Remote-sensed data, such as MODIS, revealed to be a useful reference to derive species-specific parameter values and test the model's plausibility in simulating LAI and ET processes. Besides being freely and readily available, MODIS data has global spatial coverage and high temporal resolutions. Since phenological observations and stand's characteristics are rarely available at high spatial resolutions, remote-sensing data can be a good alternative to test our proposed parameterization in larger areas, such as watersheds.

Our study can help to improve hydrological modeling efforts in forested watersheds. In a subsequent study, we intend to extend our field-scale effort to the watershed-scale and test our parameterization with long-term streamflow records. We expect that by demonstrating SWAT's capabilities in simulating slash and loblolly pine and its impacts on hydrology, this study opens precedents to other researchers to account for forest dynamics in hydrological modeling studies.

We acknowledge that the results reached here might have been different if we were using another process-based watershed model. However, most of the process-based watershed models require similar input data and are based on almost the same physical principles. With this in mind, the results should be similar to what was found in this study and our findings should be applicable to a wide range of models.

FIGURES

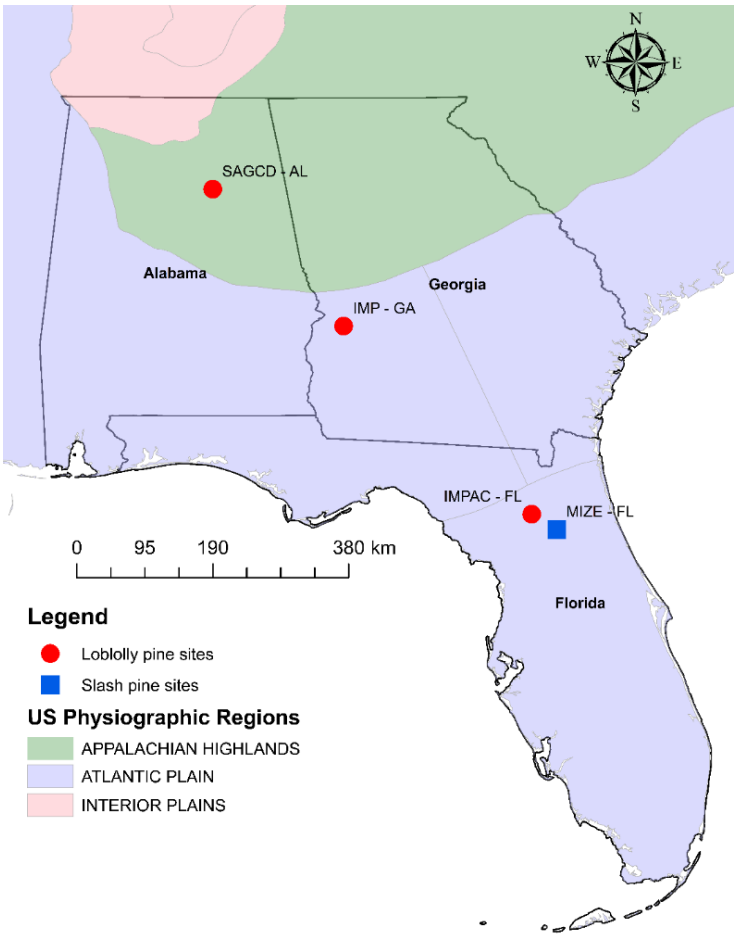

Figure 1. Spatial distribution and location of the study-sites comprised of four pine plantation fields located in Alabama, Georgia, and Florida. Red circles represent loblolly pine sites while the blue square represents the slash pine site.

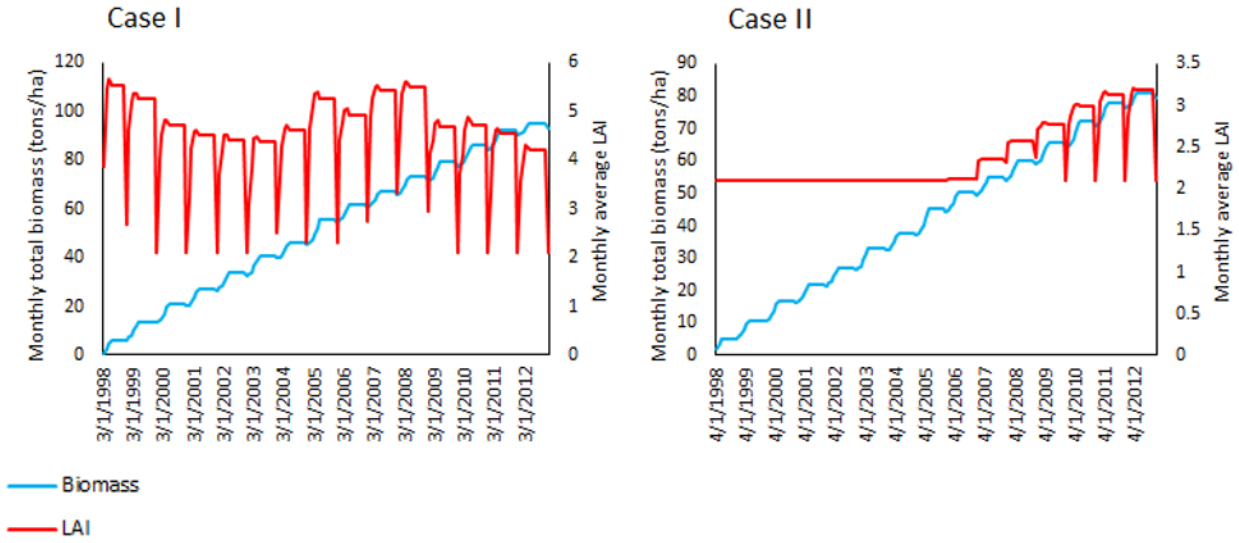

Figure 2. SWAT limitations in simulating tree growth before maturity. Case I: Monthly LAI and monthly total biomass simulated as fully developed trees. Case II: Monthly LAI and monthly total biomass simulated through a planting operation. Note that in case II LAI takes several years to start growing beyond the pre-defined minimum leaf area index value.

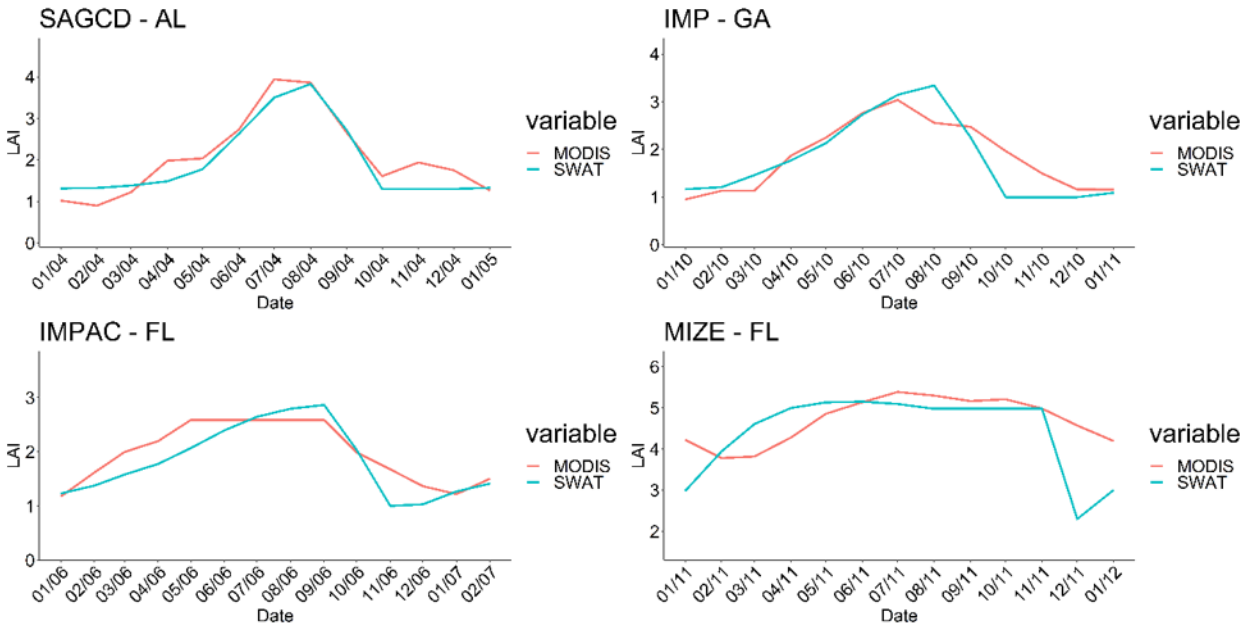

Figure 3. Parameterization of LAI development shape in SWAT. Model parameters regulating the shape of the optimal leaf area index development curve were derived based on remotely sensed LAI derived from MODIS.

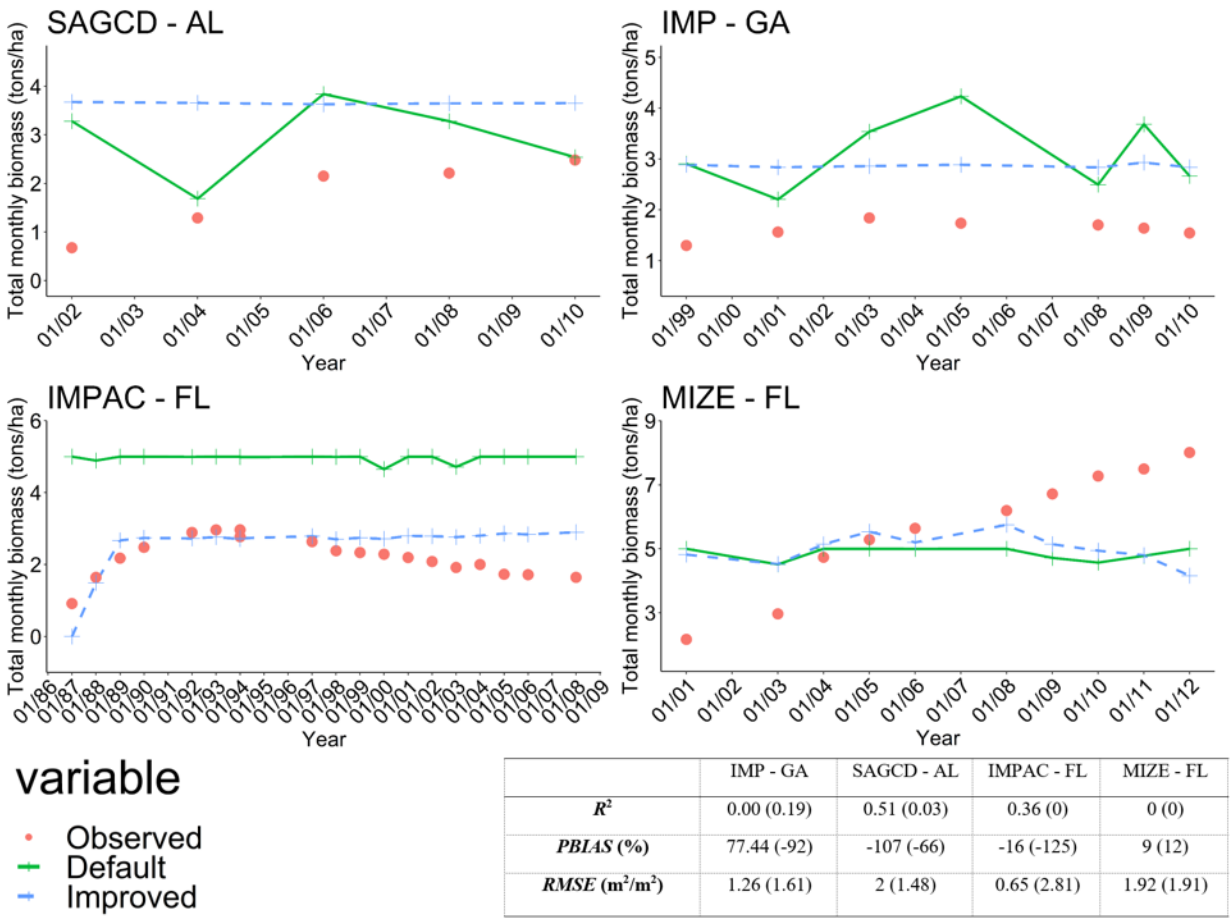

	IMP - GA	SAGCD - AL	IMPAC - FL	MIZE - FL
R^2	0.00 (0.19)	0.51 (0.03)	0.36 (0)	0 (0)
***PBIAS* (%)**	77.44 (-92)	-107 (-66)	-16 (-125)	9 (12)
***RMSE* (m^2/m^2)**	1.26 (1.61)	2 (1.48)	0.65 (2.81)	1.92 (1.91)

Figure 4. Simulated versus field-measured annual maximum LAI under default and improved model parameterizations. The bottom table shows the model performance for predicting annual maximum LAI under default and improved parameterizations. Values in parenthesis refer to the default model performance.

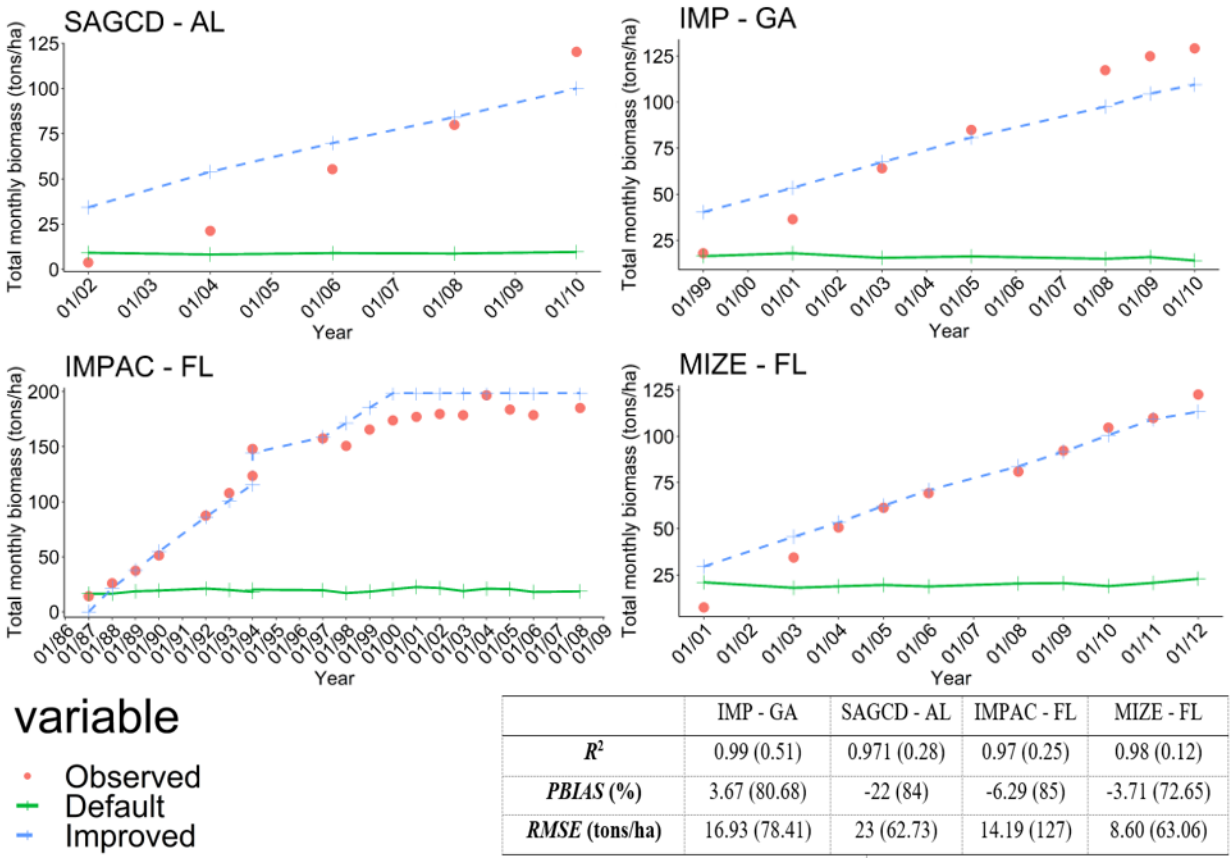

	IMP - GA	SAGCD - AL	IMPAC - FL	MIZE - FL
R^2	0.99 (0.51)	0.971 (0.28)	0.97 (0.25)	0.98 (0.12)
***PBIAS* (%)**	3.67 (80.68)	-22 (84)	-6.29 (85)	-3.71 (72.65)
***RMSE* (tons/ha)**	16.93 (78.41)	23 (62.73)	14.19 (127)	8.60 (63.06)

Figure 5. Simulated versus field measured total annual biomass under default and improved model parameterizations. The bottom table shows the model performance for predicting annual biomass under default and improved parameterizations. Values in parenthesis refer to the default model performance.

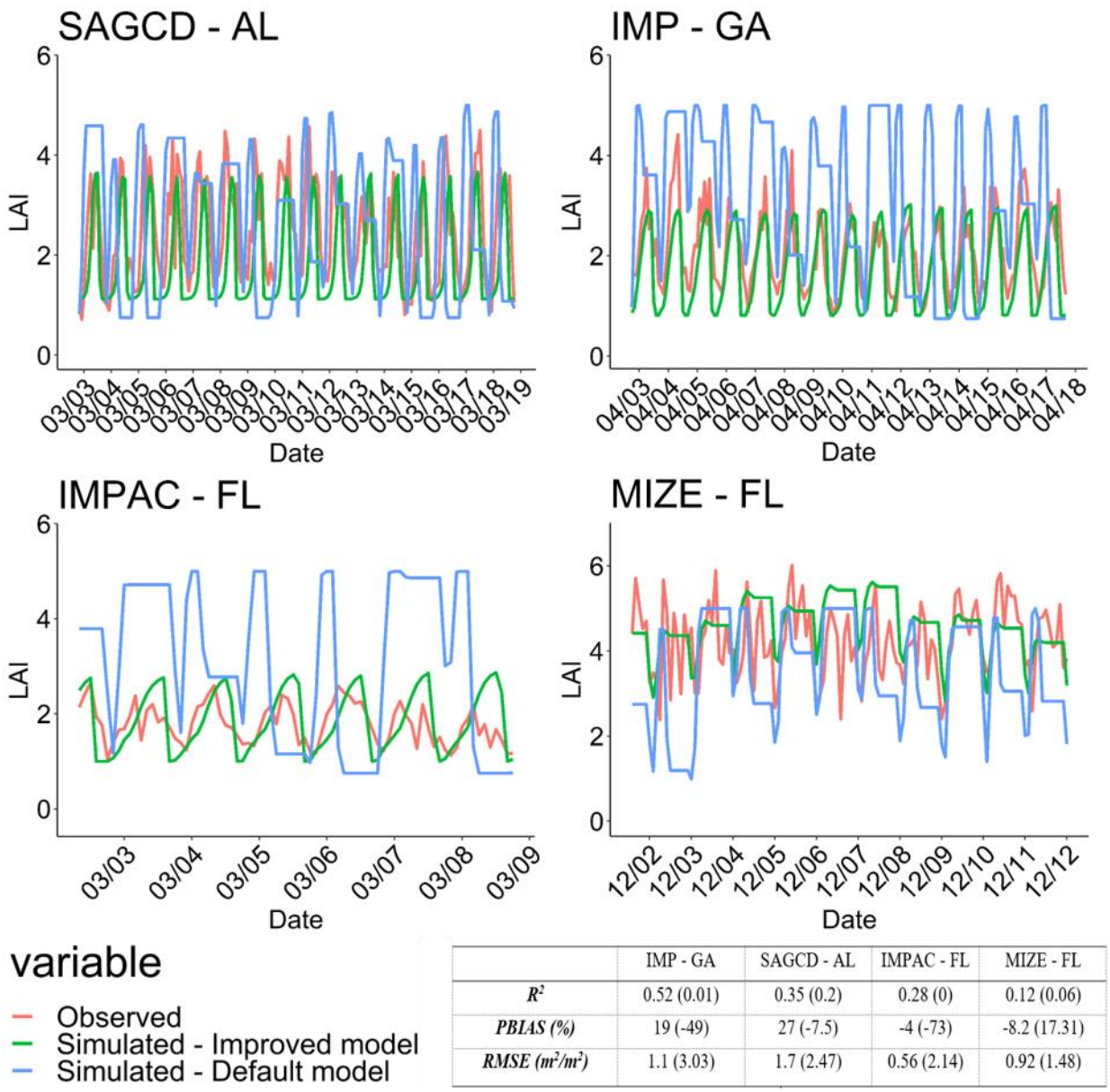

	IMP - GA	SAGCD - AL	IMPAC - FL	MIZE - FL
R^2	0.52 (0.01)	0.35 (0.2)	0.28 (0)	0.12 (0.06)
PBIAS (%)	19 (-49)	27 (-7.5)	-4 (-73)	-8.2 (17.31)
RMSE (m^2/m^2)	1.1 (3.03)	1.7 (2.47)	0.56 (2.14)	0.92 (1.48)

Figure 6. Simulated versus MODIS LAI under default and improved model parameterizations. The bottom table shows the model performance for predicting monthly LAI under default and improved parameterizations. Values in parenthesis refer to the default model performance.

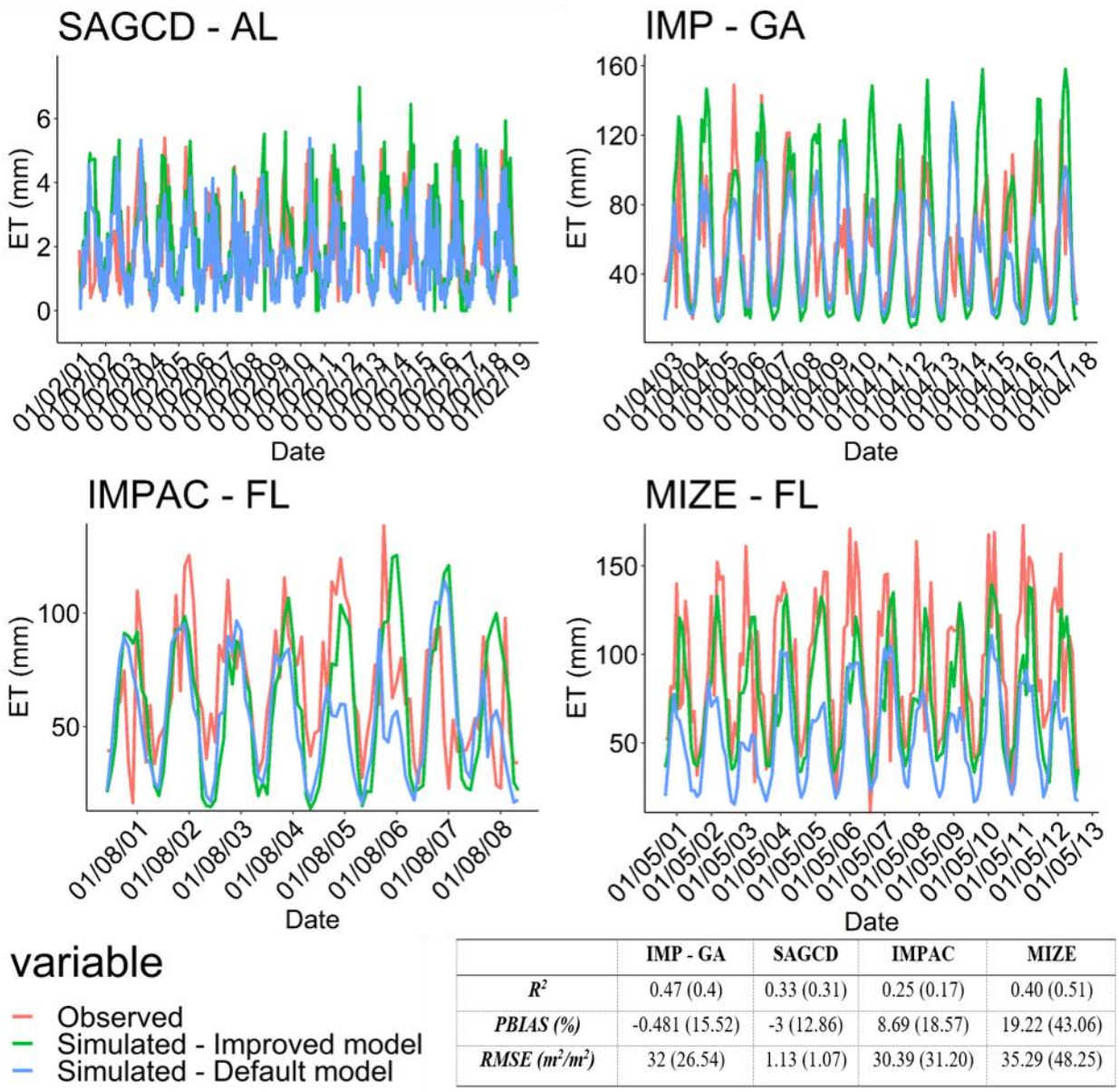

	IMP - GA	SAGCD	IMPAC	MIZE
R^2	0.47 (0.4)	0.33 (0.31)	0.25 (0.17)	0.40 (0.51)
PBIAS (%)	-0.481 (15.52)	-3 (12.86)	8.69 (18.57)	19.22 (43.06)
RMSE (m^2/m^2)	32 (26.54)	1.13 (1.07)	30.39 (31.20)	35.29 (48.25)

Figure 7. Simulated versus MODIS ET under default and improved model parameterizations. The bottom table shows the SWAT model performance for predicting monthly ET under default and improved parameterizations. Values in parenthesis refer to the default model performance.

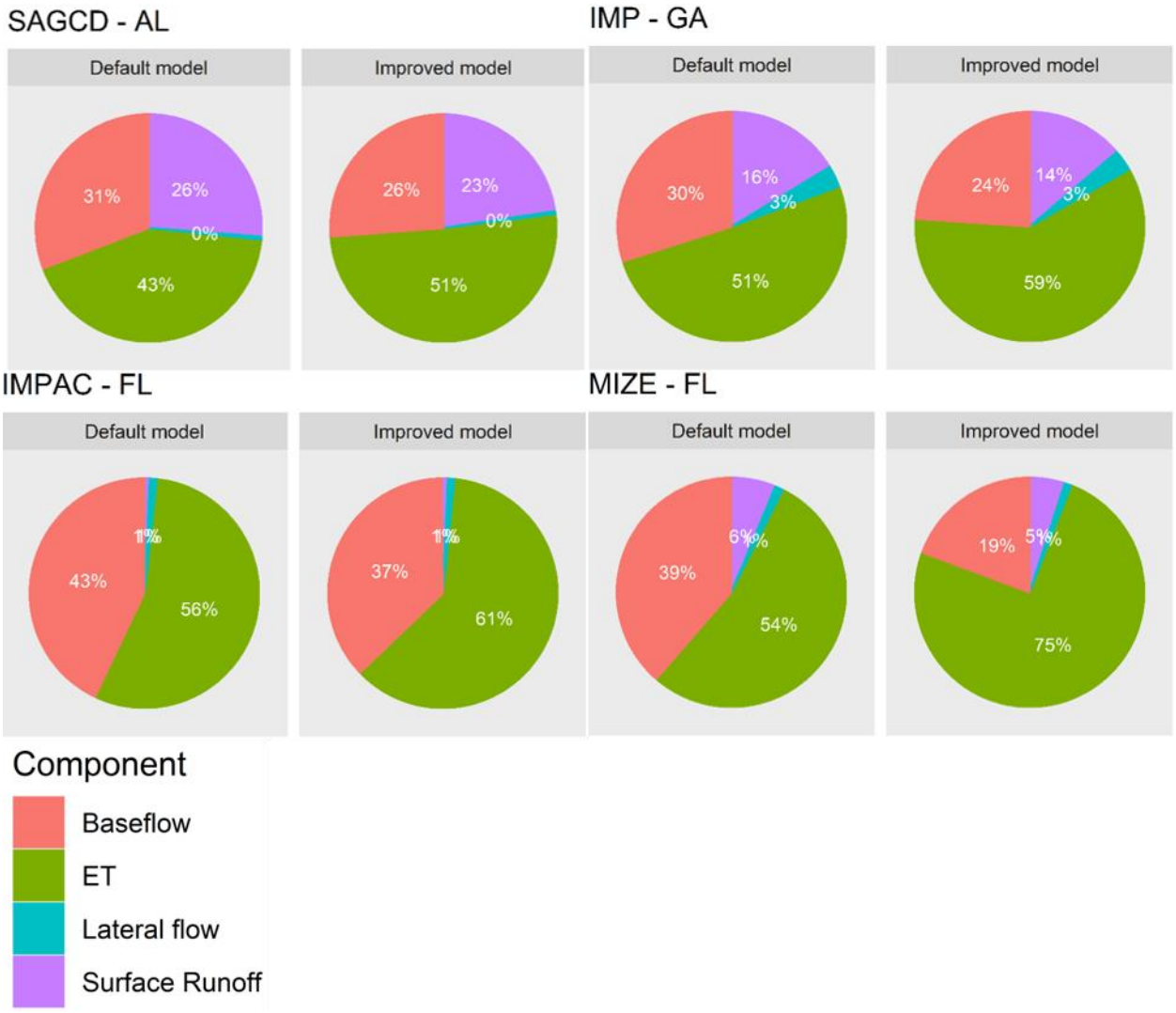

Figure 8. Mean annual water budget under default and improved model parameterization across all sites.

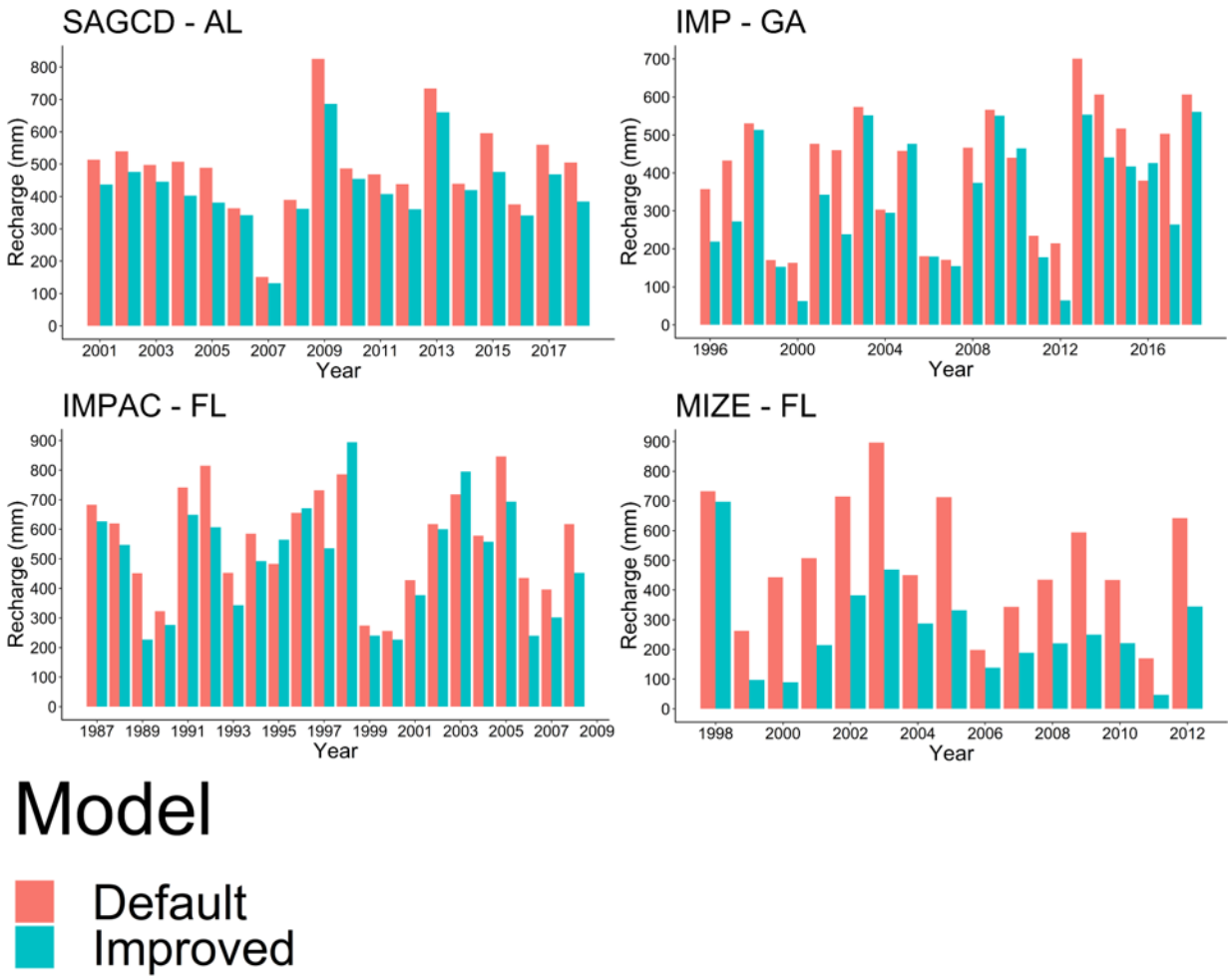

Figure 9. Effects of improved forest parameterization on groundwater recharge. Mean annual groundwater recharge is compared for the default and improved model parameterizations across all study sites over the entire simulation period.

TABLES

Table 1. Site and stand characteristics.

Site characteristic	SAGCD - AL	IMP - GA	IMPAC - FL	MIZE - FL
Latitude	33.8434° N	32.1241° N	29.7603° N	29.7548° N
Longitude	-86.2993° W	-84.6552° W	-82.2906° W	-82.1633° W
Annual average precipitation (mm)	1,500	1,282	1,300	1,256
Annual average temperature (°C)	16	18	20.5	20.5
Annual average solar radiation (MJ/m^2)	16.87	17.67	17.7	17.9
Dominant Hyrdologic Soil Group	D	C	A	B
Elevation range (m)	177-192	176-189	50-57	38-50
Average stand biomass (tons/ha)	56	82	133	73
Average LAI (m^2/m^2)	1.76	1.6	2.2	5.5
Stand age in the first year of measured data (years)	4	6	4	3
Observation period	2002-2010	1999-2010	1987-2008	2001-2012

Table 2. Description of input data and sources.

	Data	Description	Source
Model input data	Topography	National Elevation Dataset at 10 meters resolution	United States Department of Agriculture (USDA) Geospatial Data Gateway (https://datagateway.nrcs.usda.gov/)
	Land use	2008 Cropland Data Layer	United States Department of Agriculture (USDA) Geospatial Data Gateway (https://datagateway.nrcs.usda.gov/)
	Soil	Gridded Soil Survey Geographic (gSSURGO)	United States Department of Agriculture (USDA) Geospatial Data Gateway (https://datagateway.nrcs.usda.gov/)
	Climate	Daily precipitation, maximum/minimum temperature, solar radiation, wind speed	PRISM climate group (http://www.prism.oregonstate.edu/),National Land Data Assimilation Systems (NLDAS) phase 2 (https://ldas.gsfc.nasa.gov/nldas/NLDAS2model_download.php), National Solar Radiation Database (https://nsrdb.nrel.gov/)
	Atmospheric deposition	Wet and dry deposition of nitrate and ammonia	National Atmospheric Deposition Program (NADP) (http://nadp.slh.wisc.edu/)
Model calibration	Seasonal LAI	4 days composite dataset at 500 meters pixel resolution	Moderate Resolution Imaging Spectroradiometer (MODIS) (https://lpdaac.usgs.gov/products/mcd15a3hv006/)
	ET	8 days composite dataset at 500 meters pixel resolution	Moderate Resolution Imaging Spectroradiometer (MODIS) (https://lpdaac.usgs.gov/products/mod16a2v006/)
	Biomass	Field-measured annual total trees biomass	Long-term field studies conducted FMRC, FBRC, and PMRC in Georgia, Florida and Alabama, respectively
	Annual LAI	Field-measured annual LAI	Long-term field studies conducted FMRC, FBRC, and PMRC in Georgia, Florida and Alabama, respectively

Table 3. Summary and sources of data used for model parameterization.

Parameterization approach	Parameter (units)	Default value*	Parameterized value/range – loblolly pine	Parameterized value/range – slash pine	Reference
Data fitting	*FRGRW1*	0.15	–	–	–
	LAIMX1	0.7	–	–	–
	FRGRW2	0.25	–	–	–
	LAIMX2	0.99	–	–	–
	DLAI	0.99	–	–	–
	HEAT_UNITS	1,800	–	–	–
	EPCO	0.95	0.48	0.38	–
Expert knowledge	*MAT_YRS* (years)	30	3-5	3-5	–
	CURYR_MAT (years)	–	1	1	–
	ESCO	1	0.8-1	0.8-1	–
Literature review	*BIO_E* ((kg/ha)/(MJ/m2))	15	2.5-11.6	2.7-12.6	1,2,3,4
	RDMX (m)	3.5	1.5-3	1.6-3.3	5,6,7,8,9,20
	T_OPT (Celsius)	30	25	25	10,11
	T_BASE (Celsius)	0	4	5	10,11
	GSI (m/s)	0.002	0 - 0.0118	0 - 0.036	12,11,2,13,14,15,21
	VPDFR (kPa)	4	0.7 - 3.7	1 - 3.5	13,15,16,22
	EXT_COEF	0.65	0.41-0.69	0.46-0.715	1,11,17,18
	CANMX (mm, % of total rainfall)	0	0.5-1.8 mm, 14-28%	0.5-1.8 mm , 14-28%	19
	CHTMX (m)	10	7 - 18	8.5 – 19.8	5
	BIO_LEAF	0.3	0.02	0.02	23
Field observations	*BMX_TREES* (tons/ha)	1,000	185-200	113-200	–
Remote-sensing	*BLAI* ($m^2/m^{2)}$	5	2.4-4	4.7-7	–
	ALAI_MIN ($m^2/m^{2)}$	0.75	0.7-1.6	2.4-3.4	–

References: 1: (Schultz, 1997); 2: (Roth, 2010); 3: (Pell, 2015); 4: (Allen et al., 2005); 5: (Martin and Jokela, 2004); 6: (Schenk and Jackson, 2002); 7: (Torreano and Morris, 1998); 8: (Qi et al., 2018); 9: (Albaugh et al., 2006); 10: (Gonzalez-Benecke et al., 2014); 11: (Gonzalez-Benecke et al., 2016); 12: (Samuelson et al., 2012); 13: (Wightman et al., 2016); 14: (Aspinwall et al., 2011); 15: (Bartkowiak et al., 2015); 16: (Bracho et al., 2018); 17: (Sampson and Allen, 1998); 18: (White et al., 2000); 19: (Gavazzi et al., 2016); 20: (Rees and Comerford, 1986); 21: (Johnson et al., 1995); 22: (Teskey et al., 1994); 23: (Poorter et al., 2012).

*: The default parameter values refer to the forest type Evergreen Forests (FRSE) in SWAT's plant database

Table 4. Calibrated values of parameters used for LAI, biomass, and ET calibration.

		BEST VALUE			
	PARAMETER	MIZE - FL	IMP - GA	IMPAC - FL	SAGCD - AL
LAI + Biomass	v__EXT_COEF{128}.plant.dat	0.65	0.54	0.57	0.66
	v__BMX_TREES{128}.plant.dat	126.82	164.56	198.64	134.83
	v__BIO_LEAF{128}.plant.dat	0.023	0.02	0.02	0.02
	v__BIO_E{128}.plant.dat	11.37	6.02	9.76	8.57
	v__T_BASE{128}.plant.dat	5	4	4	0
	v__T_OPT{128}.plant.dat	25	25	25	24
	v__BLAI{128}.plant.dat	7.06	3.04	3	3.73
	v__ALAI_MIN{128}.plant.dat	2.10	0.81	1	1.12
	v__MAT_YRS{128}.plant.dat	3	4	2	3.30
	v__CURYR_MAT{[1],1}.mgt	1	1	1	1
	v__RDMX{128}.plant.dat	1.68	2.0	1.58	1.96
	v__VPDFR{128}.plant.dat	2.52	2.76	1.73	1.51
LAI shape	v__HEAT_UNITS{[1],1}.mgt	1771.25	4485	5518.84	5912.39
	v__DLAI{128}.plant.dat	0.99	0.91	0.95	0.89
	v__FRGRW1{128}.plant.dat	0.18	0.15	0.21	0.31
	v__FRGRW2{128}.plant.dat	0.81	0.36	0.49	0.45
	v__LAIMX1{128}.plant.dat	0.49	0.34	0.35	0.52
	v__LAIMX2{128}.plant.dat	0.61	0.71	0.69	0.69
ET	v__CANMX.hru	0.94	0.59	0.52	1.59
	v__ESCO.hru	0.82	0.81	0.86	0.84
	v__GSI{128}.plant.dat	0.009	0.011	0.006	0.01
	v__CHTMX{128}.plant.dat	18.32	16.84	7.25	7.14
	v__EPCO.hru	0.38	0.48	0.48	0.48

Table 5. Effects of improved forest parameterization on water fluxes across all sites. The percentage change refers to the difference between the default and improved model parameterizations. Positive values denote increase in the water balance component with the improved model, while negative values denote decrease with the improved model.

	% change - SAGCD - AL	% change - IMP - GA	% change - IMPAC - FL	% change - MIZE - FL
Precipitation (PRECIP)	0%	0%	0%	0%
Green water flow (ET)	18%	15%	10%	-14%
Percolation (PERC)	-15%	-18%	-13%	-48%
Surface discharge (SURQ)	-13%	-15%	-6%	-23%
Lateral discharge (LATQ)	0%	0%	-5%	-16%
Total groundwater recharge (GW_RCHG)	-15%	-18%	-13%	-47%
Deep aquifer recharge (DA_RCHG)	-15%	-16%	-13%	-47%
Shallow aquifer recharge (SA_RCHG)	-15%	-19%	-13%	-47%
Baseflow (GW_Q)	-16%	-20%	-13%	-49%
Surface blue water (LATQ + SURQ + GW_Q)	-15%	-17%	-13%	-45%
Subsurface blue water (GW_RCHG) - (GW_Q)	-9%	-7%	-8%	-26%

REFERENCES

Abbaspour, K.C., 2015. SWATCalibration and Uncertainty Programs 100.

Abbaspour, K.C., Johnson, C.A., Genuchten, M.T. van, 2004. Estimating Uncertain Flow and Transport Parameters Using a Sequential Uncertainty Fitting Procedure. Vadose Zone Journal 3, 1340–1352. https://doi.org/10.2113/3.4.1340

Albaugh, T.J., Allen, H.L., Kress, L.W., 2006. Root and stem partitioning of *Pinus taeda*. Trees, Vol. 20: 176-185.

Alemayehu, T., Griensven, A. van, Woldegiorgis, B.T., Bauwens, W., 2017. An improved SWAT vegetation growth module and its evaluation for four tropical ecosystems. Hydrology and Earth System Sciences 21, 4449–4467. https://doi.org/10.5194/hess-21-4449-2017

Allen, C.B., Will, R.E., Jacobson, M.A., 2005. Production Efficiency and Radiation Use Efficiency of Four Tree Species Receiving Irrigation and Fertilization. for sci 51, 556–569. https://doi.org/10.1093/forestscience/51.6.556

Amatya, D.M., Jha, M.K., 2011. Evaluating the SWAT model for a low-gradient forested watershed in coastal South Carolina. American Society of Agricultural and Biological Engineers (ASABE) 54(6):2151-2163 54, 2151–2163.

Amatya, D.M., Skaggs, R.W., 2001. Hydrologic Modeling of a Drained Pine Plantation on Poorly Drained Soils. for sci 47, 103–114. https://doi.org/10.1093/forestscience/47.1.103

Arnold, J.G., Srinivasan, R., Muttiah, R.S., Williams, J.R., 1998. Large Area Hydrologic Modeling and Assessment Part I: Model Development1. JAWRA Journal of the American Water Resources Association 34, 73–89. https://doi.org/10.1111/j.1752-1688.1998.tb05961.x

Arnold JG, Kiniry JR, Srinivasan R, Williams JR, Haney EB, Neitsch SL (2011) Soil and Water Assessment Tool Input/Output File Documentation-Version 2009 Texas Water Resources Institute Technical. Report 365.

Aspinwall, M.J., King, J.S., McKeand, S.E., Domec, J.-C., 2011. Leaf-level gas-exchange uniformity and photosynthetic capacity among loblolly pine (Pinus taeda L.) genotypes of contrasting inherent genetic variation. Tree Physiol 31, 78–91. https://doi.org/10.1093/treephys/tpq107

Bartkowiak, S.M., Samuelson, L.J., McGuire, M.A., Teskey, R.O., 2015. Fertilization increases sensitivity of canopy stomatal conductance and transpiration to throughfall reduction in an 8-year-old loblolly pine plantation. Forest Ecology and Management 354, 87–96. https://doi.org/10.1016/j.foreco.2015.06.033

Bracho, R., Starr, G., Gholz, H.L., Martin, T.A., Cropper, W.P., Loescher, H.W., 2012. Controls on carbon dynamics by ecosystem structure and climate for southeastern U.S. slash pine plantations. Ecological Monographs 82, 101–128. https://doi.org/10.1890/11-0587.1

Bracho, R., Vogel, J.G., Will, R.E., Noormets, A., Samuelson, L.J., Jokela, E.J., Gonzalez-Benecke, C.A., Gezan, S.A., Markewitz, D., Seiler, J.R., Strahm, B.D., Teskey, R.O., Fox, T.R., Kane, M.B., Laviner, M.A., McElligot, K.M., Yang, J., Lin, W., Meek, C.R., Cucinella, J., Akers, M.K., Martin, T.A., 2018. Carbon accumulation in loblolly pine plantations is increased by fertilization across a soil moisture availability gradient. Forest Ecology and Management 424, 39–52. https://doi.org/10.1016/j.foreco.2018.04.029

Cibin, R., Trybula, E., Chaubey, I., Brouder, S.M., Volenec, J.J., 2016. Watershed-scale impacts of bioenergy crops on hydrology and water quality using improved SWAT model. GCB Bioenergy 8, 837–848. https://doi.org/10.1111/gcbb.12307

Falkenmark M., Rockström J., 2006. The New Blue and Green Water Paradigm: Breaking New Ground for Water Resources Planning and Management. Journal of Water Resources Planning and Management 132, 129–132. https://doi.org/10.1061/(ASCE)0733-9496(2006)132:3(129)

Ford, C.R., McGuire, M.A., Mitchell, R.J., Teskey, R.O., 2004. Assessing variation in the radial profile of sap flux density in Pinus species and its effect on daily water use. Tree physiology. https://doi.org/10.1093/treephys/24.3.241

Gassman, P.W., Williams, J.R., Benson, V.W., Izaurralde, R.C., Hauck, L.M., Jones, C.A., Atwood, J.D., Kiniry, J.R., Flowers, J.D., 2004. Historical Development and Applications of the EPIC and APEX Models. https://doi.org/10.13031/2013.17074

Gavazzi, M.J., Sun, G., McNulty, S.G., Treasure, E.A., Wightman, M.G., 2016. Canopy Rainfall Interception Measured over Ten Years in a Coastal Plain Loblolly Pine (Pinus taeda L.) Plantation. Trans. ASABE 59, 601–610. https://doi.org/10.13031/trans.59.11101

Golden, H.E., Evenson, G.R., Tian, S., Amatya, D.M., Sun, G., 2016. Hydrological modelling in forested systems., in: Amatya, D.M., Williams, T.M., Bren, L., Jong, C. de (Eds.), Forest Hydrology: Processes, Management and Assessment. CABI, Wallingford, pp. 141–161. https://doi.org/10.1079/9781780646602.0141

Gonzalez-Benecke, C.A., Gezan, S.A., Albaugh, T.J., Allen, H.L., Burkhart, H.E., Fox, T.R., Jokela, E.J., Maier, C.A., Martin, T.A., Rubilar, R.A., Samuelson, L.J., 2014a. Local and general above-stump biomass functions for loblolly pine and slash pine trees. Forest Ecology and Management 334, 254–276. https://doi.org/10.1016/j.foreco.2014.09.002

Gonzalez-Benecke, C.A., Jokela, E.J., Cropper, W.P., Bracho, R., Leduc, D.J., 2014b. Parameterization of the 3-PG model for Pinus elliottii stands using alternative methods to estimate fertility rating, biomass partitioning and canopy closure. Forest Ecology and Management 327, 55–75. https://doi.org/10.1016/j.foreco.2014.04.030

Gonzalez-Benecke, C.A., Martin, T.A., Cropper, Wendell P., 2011. Whole-tree water relations of co-occurring mature Pinus palustris and Pinus elliottii var. elliottii. Can. J. For. Res. 41, 509–523. https://doi.org/10.1139/X10-230

Gonzalez-Benecke, C.A., Teskey, R.O., Martin, T.A., Jokela, E.J., Fox, T.R., Kane, M.B., Noormets, A., 2016. Regional validation and improved parameterization of the 3-PG model for Pinus taeda stands. Forest Ecology and Management 361, 237–256. https://doi.org/10.1016/j.foreco.2015.11.025

Gorelick, N., Hancher, M., Dixon, M., Ilyushchenko, S., Thau, D., Moore, R., 2017. Google Earth Engine: Planetary-scale geospatial analysis for everyone. Remote Sensing of Environment, Big Remotely Sensed Data: tools, applications and experiences 202, 18–27. https://doi.org/10.1016/j.rse.2017.06.031

Guo, T., Engel, B.A., Shao, G., Arnold, J.G., Srinivasan, R., Kiniry, J.R., 2018. Development and improvement of the simulation of woody bioenergy crops in the Soil and Water Assessment Tool (SWAT). Environmental Modelling & Software. https://doi.org/10.1016/j.envsoft.2018.08.030

Gupta, H.V., Kling, H., Yilmaz, K.K., Martinez, G.F., 2009. Decomposition of the mean squared error and NSE performance criteria: Implications for improving hydrological modelling. Journal of Hydrology 377, 80–91. https://doi.org/10.1016/j.jhydrol.2009.08.003

Hargreaves, George H, Zohrab A. Samani, 1985. Reference Crop Evapotranspiration from Temperature. Applied Engineering in Agriculture 1, 96–99. https://doi.org/10.13031/2013.26773

Iiames, J.S., Cooter, E., Schwede, D., Williams, J., 2018. A Comparison of Simulated and Field-Derived Leaf Area Index (LAI) and Canopy Height Values from Four Forest Complexes in the Southeastern USA. Forests 9, 26. https://doi.org/10.3390/f9010026

Johnson, J.D., Byres, D.P., Dean, T.J., 1995. Diurnal water relations and gas exchange of two slash pine (Pinus elliottii) families exposed to chronic ozone levels and acidic rain *. New Phytologist 131, 381–392. https://doi.org/10.1111/j.1469-8137.1995.tb03075.x

Jokela, E.J., Martin, T.A., 2000. Effects of ontogeny and soil nutrient supply on production, allocation, and leaf area efficiency in loblolly and slash pine stands. Can. J. For. Res. 30, 1511–1524. https://doi.org/10.1139/x00-082

Karki, R., Srivastava, P., Kalin, L., Lamba, J., Bosch, D.D., 2019. Multi-variable sensitivity analysis, calibration, and validation of a field-scale SWAT model: Building Stakeholder Trust in Hydrologic/Water Quality Modeling</i>, in: 2019 Boston, Massachusetts July 7- July 10, 2019. Presented at the 2019 Boston, Massachusetts July 7- July 10, 2019, American Society of Agricultural and Biological Engineers. https://doi.org/10.13031/aim.201901362

Lohrey RE, Kossuth SV (1990) Pinus elliottii Engelm. slash pine. In: Burns RM, Honkala BH (eds) Silvics of North America, vol 1. Conifers FS-USDA, Washington DC, Agric. Handb. 654, pp 338–347).

Marek, G.W., Gowda, P.H., Evett, S.R., Baumhardt, R.L., Brauer, D.A., Howell, T., Marek, T.H., Srinivasan, R., 2016. Calibration and Validation of the SWAT Model for Predicting Daily ET over Irrigated Crops in the Texas High Plains Using Lysimetric Data. https://doi.org/10.13031/trans.59.10926

Martin, T.A., 1999. Winter Season Tree Sap Flow and Stand Transpiration in an Intensively-Managed Loblolly and Slash Pine Plantation. Journal of Sustainable Forestry 10, 155–163. https://doi.org/10.1300/J091v10n01_18

Martin, T.A., Jokela, E.J., 2004. Developmental Patterns and Nutrition Impact Radiation Use Efficiency Components in Southern Pine Stands. Ecological Applications 14, 1839–1854. https://doi.org/10.1890/03-5262

McLaughlin, D.L., Kaplan, D.A., Cohen, M.J., 2013. Managing Forests for Increased Regional Water Yield in the Southeastern U.S. Coastal Plain. JAWRA Journal of the American Water Resources Association 49, 953–965. https://doi.org/10.1111/jawr.12073

Mittelstet, A.R., 2015. Using SWAT to simulate crop yields and salinity levels in the North Fork River Basin, USA. International Journal of Agricultural and Biological Engineering 8, 16.

Monteith, J.L., 1965. Evaporation and environment. Symposia of the Society for Experimental Biology 19, 205–234

Mu, Q., et al., 2013. A remotely sensed global terrestrial drought severity index. Bulletin of the American Meteorological Society, 94 (1), doi:10.1175/BAMS-D-11-00213.1.

Myneni, Y.K., 2015. MOD15A2H MODIS/Terra Leaf Area Index/FPAR 8-Day L4 Global 500m SIN Grid V006. https://doi.org/10.5067/modis/mod15a2h.006

Naderi, M., 2020. Assessment of water security under climate change for the large watershed of Dorudzan Dam in southern Iran. Hydrogeol J. https://doi.org/10.1007/s10040-020-02159-1

Nair, S.S., King, K.W., Witter, J.D., Sohngen, B.L., Fausey, N.R., 2011. Importance of Crop Yield in Calibrating Watershed Water Quality Simulation Tools1. JAWRA Journal of the American Water Resources Association 47, 1285–1297. https://doi.org/10.1111/j.1752-1688.2011.00570.x

Neitsch, S., Arnold, J.G., Kiniry, J.R., Williams, J., 2011. Soil & Water Assessment Tool Theoretical Documentation Version 2009. Texas Water Resources Institute Technical Report No. 406, College Station, TX, pp. 618.

Pell, C., 2015. The Effects of Fertilization and Four Years of Throughfall Reduction on Leaf Physiology of Loblolly Pine (Pinus taeda L.).

Poorter, H., Niklas, K.J., Reich, P.B., Oleksyn, J., Poot, P., Mommer, L., 2012. Biomass allocation to leaves, stems and roots: meta-analyses of interspecific variation and environmental control. New Phytologist 193, 30–50. https://doi.org/10.1111/j.1469-8137.2011.03952.x

Priestley, C.H.B., Taylor, R.J., 1972. On the Assessment of Surface Heat Flux and Evaporation Using Large-Scale Parameters. Mon. Wea. Rev. 100, 81–92.

https://doi.org/10.1175/1520-0493(1972)100<0081:OTAOSH>2.3.CO;2

Rees, K.C.J.V., Comerford, N.B., 1986. Vertical Root Distribution and Strontium Uptake of a Slash Pine Stand on a Florida Spodosol. Soil Science Society of America Journal 50, 1042–1046. https://doi.org/10.2136/sssaj1986.03615995005000040041x

Roth, B., 2010. Genotype x environment interactions in selected loblolly (Pinus taeda L.) and slash pine (P. elliottii Engelm. var. elliottii) plantations in the southeastern United States. https://doi.org/10.13140/rg.2.1.4418.5041

Running, Q.M., 2017. MOD16A2 MODIS/Terra Net Evapotranspiration 8-Day L4 Global 500m SIN Grid V006. https://doi.org/10.5067/modis/mod16a2.006

Russell, M.B., Amateis, R.L., Burkhart, H.E., 2010. Implementing Regional Locale and Thinning Response in the Loblolly Pine Height-Diameter Relationship. Southern Journal of Applied Forestry 34, 21–27. https://doi.org/10.1093/sjaf/34.1.21

Saleh, J. R. Williams, J. C. Wood, L. M. Hauck, W. H. Blackburn, 2004. APPLICATION OF APEX FOR FORESTRY. Transactions of the ASAE 47, 751–765. https://doi.org/10.13031/2013.16107

Sampson, D.A., Allen, H.L., 1998. Light attenuation in a 14-year-old loblolly pine stand as influenced by fertilization and irrigation. Trees 13, 80–87. https://doi.org/10.1007/s004680050190

Samuelson, L.J., Stokes, T.A., Johnsen, K.H., 2012. Ecophysiological comparison of 50-year-old longleaf pine, slash pine and loblolly pine. Forest Ecology and Management 274, 108–115. https://doi.org/10.1016/j.foreco.2012.02.017

Samuelson, L.J., Kane, M.B., Markewitz, D., Teskey, R.O., Akers, M.K., Stokes, T.A., Pell, C.J., Qi, J., 2017. Fertilization increased leaf water use efficiency and growth of Pinus taeda subjected to five years of throughfall reduction. Can. J. For. Res. 48, 227–236. https://doi.org/10.1139/cjfr-2017-0357

Samuelson, L.J., Pell, C.J., Stokes, T.A., Bartkowiak, S.M., Akers, M.K., Kane, M., Markewitz, D., McGuire, M.A., Teskey, R.O., 2014. Two-year throughfall and fertilization effects on leaf physiology and growth of loblolly pine in the Georgia Piedmont. Forest Ecology and Management 330, 29–37. https://doi.org/10.1016/j.foreco.2014.06.030

Schenk, H.J., Jackson, R.B., 2002. Rooting depths, lateral root spreads and below-ground/above-ground allometries of plants in water-limited ecosystems. Journal of Ecology 90, 480–494. https://doi.org/10.1046/j.1365-2745.2002.00682.x

Schultz, R.P., 1997. Loblolly pine: the ecology and culture of loblolly pine (<I>Pinus taeda</I> L.). Agriculture Handbook 713. Washington, D.C.: U.S. Department of Agriculture, Forest Service. 493 p.

Skaggs, R.W., 1978. A water management model for shallow water table soils [WWW Document]. Environmental Science. URL https://www.semanticscholar.org/paper/A-water-management-model-for-shallow-water-table-Skaggs/ca09421c349952eae28717d2c6ebbfcdab6654a6 (accessed 5.9.20)

Srinivasan, X. Zhang, J. Arnold, 2010. SWAT Ungauged: Hydrological Budget and Crop Yield Predictions in the Upper Mississippi River Basin. Transactions of the ASABE 53, 1533–1546. https://doi.org/10.13031/2013.34903

Strauch, M., Volk, M., 2013. SWAT plant growth modification for improved modeling of perennial vegetation in the tropics. Ecological Modelling 269, 98–112. https://doi.org/10.1016/j.ecolmodel.2013.08.013

Teskey, R.O., Gholz, H.L., Cropper, W., 1994. (15) (PDF) Influence of climate and fertilization on net photosynthesis of mature slash pine [WWW Document]. Tree Physiology. URL https://www.researchgate.net/publication/8690702_Influence_of_climate_and_fertilization_on_net_photosynthesis_of_mature_slash_pine (accessed 2.25.20).

Torreano, S.J., Morris, L.A., 1998. Loblolly Pine Root Growth and Distribution under Water Stress.

Trybula, E.M., Cibin, R., Burks, J.L., Chaubey, I., Brouder, S.M., Volenec, J.J., 2015. Perennial rhizomatous grasses as bioenergy feedstock in SWAT: parameter development and model improvement. GCB Bioenergy 7, 1185–1202. https://doi.org/10.1111/gcbb.12210

Veettil, A.V., Mishra, A.K., 2016. Water security assessment using blue and green water footprint concepts. Journal of Hydrology 542, 589–602. https://doi.org/10.1016/j.jhydrol.2016.09.032

Wang, R., Bowling, L.C., Cherkauer, K.A., 2015. Estimation of the effects of climate variability on crop yield in the Midwest USA | Elsevier Enhanced Reader [WWW Document]. Agricultural and Forest Meteorology. https://doi.org/10.1016/j.agrformet.2015.10.001

White, M.A., Thornton, P.E., Running, S.W., Nemani, R.R., 2000. Parameterization and Sensitivity Analysis of the BIOME–BGC Terrestrial Ecosystem Model: Net Primary Production Controls. Earth Interact. 4, 1–85. https://doi.org/10.1175/1087-3562(2000)004<0003:PASAOT>2.0.CO;2

Wightman, M.G., Martin, T.A., Gonzalez-Benecke, C.A., Jokela, E.J., Cropper, J., Ward, E.J. (ORCID:0000000250475464), 2016. Loblolly pine productivity and water relations in response to

throughfall reduction and fertilizer application on a poorly drained site in northern Florida. Forests 7. https://doi.org/10.3390/f7100214

Will, R.E., Fox, T., Akers, M., Domec, J.-C., González-Benecke, C., Jokela, E.J., Kane, M., Laviner, M.A., Lokuta, G., Markewitz, D., McGuire, M.A., Meek, C., Noormets, A., Samuelson, L., Seiler, J., Strahm, B., Teskey, R., Vogel, J., Ward, E., West, J., Wilson, D., Martin, T.A., 2015. A Range-Wide Experiment to Investigate Nutrient and Soil Moisture Interactions in Loblolly Pine Plantations. Forests 6, 2014–2028. https://doi.org/10.3390/f6062014

Williams, J.R., 1990. The erosion-productivity impact calculator (EPIC) model: a case history. Phil. Trans. R. Soc. Lond. B 329, 421–428. https://doi.org/10.1098/rstb.1990.0184

Williams, J.W., Izaurralde, R.C., Steglich, E.M., 2008. Theoretical Documentation 131.

Yang, Q., Almendinger, J.E., Zhang, X., Huang, M., Chen, X., Leng, G., Zhou, Y., Zhao, K., Asrar, G.R., Srinivasan, R., Li, X., 2018. Enhancing SWAT simulation of forest ecosystems for water resource assessment: A case study in the St. Croix River basin. Ecological Engineering 120, 422–431. https://doi.org/10.1016/j.ecoleng.2018.06.020

Yang, Q., Zhang, X., 2016. Improving SWAT for simulating water and carbon fluxes of forest ecosystems. Science of The Total Environment 569–570, 1478–1488. https://doi.org/10.1016/j.scitotenv.2016.06.238

Yang, Q., Zhang, X., Almendinger, J.E., Huang, M., Leng, G., Zhou, Y., Zhao, K., Asrar, G.R., Li, X., Qiu, J., 2019. Improving the SWAT forest module for enhancing water resource projections: A case study in the St. Croix River basin. Hydrological Processes 33, 864–875. https://doi.org/10.1002/hyp.13370

Zhao, D., Kane, M., Borders, B., Subedi, S., Akers, M., 2012. Effects of cultural intensity and planting density on stand-level aboveground biomass production and allocation for 12-year-old loblolly pine plantations in the Upper Coastal Plain and Piedmont of the southeastern United States. Can. J. For. Res. 42, 111–122. https://doi.org/10.1139/x11-166

CHAPTER 3: Effects of Improved Forest Dynamics for Watershed Hydrological Processes: A modeling approach in the Southeastern United States

ABSTRACT

This study aimed to explore how the characterization of forest processes affects watershed hydrological responses in hydrologic models. To that end, we applied the widely used Soil and Water Assessment Tool (SWAT) model to two forested watersheds in the Southeastern United States. Although forests can cover a large portion of watersheds, tree attributes such as leaf area index (LAI), biomass accumulation, and processes such as evapotranspiration (ET) are rarely calibrated in hydrological modeling studies. The advent of freely and readily available remote-sensing data combined with field observations from forestry studies and published literature, allowed us to develop an improved forest parameterization for SWAT. In this paper, we tested our proposed parameterization at watershed-scale in Florida and Georgia and compared simulated LAI, biomass, and ET with the default model settings. Our results showed major improvements in predicted monthly LAI and ET based on MODIS reference data (*NSE* > 0.6). Simulated forest biomass showed better agreement with USDA forest biomass gridded data. Through a series of modeling experiments, we isolated the benefits of LAI, biomass, and ET in predicting streamflow and baseflow at watershed level. The combined benefits of improved LAI, biomass, and ET predictions yielded the most optimal model configuration where terrestrial and in-stream processes were simulated reasonably well. In the next step, we performed automated model calibration using two calibration strategies. In the first calibration scheme (M_0), SWAT was calibrated for daily streamflow without adjusting LAI, biomass, and ET. In the next calibration scheme ($M_{LAI+BM+ET}$), previously calibrated parameters constraining LAI, biomass, and ET were incorporated into the model and daily streamflow was recalibrated. The $M_{LAI+BM+ET}$ model showed superior performance and reduced uncertainties in predicting daily streamflow, with *NSE* values ranging from 0.52 to 0.8. Our findings reveal the importance of accurately representing forest dynamics in hydrological models.

KEYWORDS: SWAT, Forest modeling, Watershed hydrology, LAI, ET, Biomass, MODIS

INTRODUCTION

Any ecosystem in a watershed affects the quantity and quality of the water passing through it by either improving or degrading the supply of hydrologic services (Brauman et al., 2007). For example, forested ecosystems might increase rainfall infiltration rates while decreasing the water yield. This is mainly due to the higher water infiltration capacity of forest soils compared to other land uses (Bruijnzeel, 2004). Water yield is a valuable ecosystem service (Ajaz Ahmed et al., 2017) defined as the total outflow from a drainage area during a given period (NSCS, 1985). The long-term water yield of a system can be understood as the difference between the input precipitation and the water lost through evapotranspiration (ET) (Anderson et al., 1976), and is many times the only source of supply for both surface and groundwater resources (McLaughlin et al., 2013). Globally, approximately 60% of the rainfall is lost to the atmosphere as vapor through ET (Oki and Kanae, 2006). In highly intensive pine plantations in Florida and North Carolina, for instance, ET losses as high as 90% have been reported (Gholz and Clark, 2002; Sun et al., 2010). Through the use, transport, and partitioning of water, forest ecosystems can significantly alter the volume of water reaching downstream locations and users (Brauman et al., 2007). As a consequence, alterations in terrestrial ecosystems may be reflected in aquatic ecosystems (Yang et al., 2018). Given the important economic (e.g., provision of raw materials such as timber and fiber) and ecological (e.g., provision of wildlife habitat and water supply) value provided by forests (Martin et al., 2017), it is vital to understand the forest-water relationships at the watershed-scale. This is especially true for highly forested regions such as the Southeastern U.S., where forests cover 99 million hectares and correspond to approximately one-third of the forested land in the contiguous U.S. (Bracho et al., 2018).

Field experiments like paired catchments have been used worldwide as a method for studying the relationships between forests and hydrology (Bosch and Hewlett, 1982). Likewise, field-scale experiments like litter traps, destructive sampling, and lysimeters, for example, are traditionally employed to measure key forest attributes such as leaf area index (LAI), total and aboveground biomass, and ET losses (Jonckheere et al., 2004; Teuling, 2018). These methods are usually time-consuming and do not provide large-scale insights. Alternatively, watershed-scale hydrological models have been successfully employed to investigate the interactions among forests and components of the hydrological cycle (Brown et al., 2015; Golden et al., 2016). A hydrological model capable of accounting for the spatial and temporal variability of factors affecting hydrological processes (e.g., intra-annual plant growth cycle, landscape heterogeneity) is a useful tool for understanding, predicting, and managing water resources (Khaki et al., 2019; Loizu et al., 2018; Zhang et al., 2019).

The performance of hydrological models in predicting a given target variable is critically important for an accurate representation of the simulated system (Jiang and Wang, 2019). Physically- and process-based models, which usually have numerous parameters, need to be calibrated to ensure that key hydrological processes are being reasonably replicated by the model. At larger scales, where different land uses and forest types spread across the landscape, for example, watershed-scale models are especially suitable tools. Even though forests can regulate water cycling and significantly affect water fluxes within the watershed, watershed modelers rarely pay attention to the accuracy of their models in capturing forest attributes and processes such as LAI, biomass, and ET. As a consequence, most watershed scale modeling applications primarily focus on in-stream processes and overlook terrestrial processes such as vegetation growth and forest dynamics (Yang et al., 2018). Streamflow is usually selected as the only variable to constrain

the performance of watershed models since streamflow data is relatively easy to obtain (Li Zejun et al., 2020). The information contained in gauged streamflow data may not sufficiently capture vertical fluxes and how they vary in space and time within the watershed (Rajib et al., 2018). For instance, other hydrological fluxes such as infiltration, soil evaporation, plant transpiration, and evapotranspiration evolve at different spatial and temporal scales within the watershed and affect the water balance. As a result, relying only on streamflow data lump horizontal water movement (i.e., runoff) and vertical water fluxes (e.g., evapotranspiration) together (Li Zejun et al., 2020). This may lead to erroneous conclusions if the model is used to assess the impacts of forest management practices (e.g., thinning, fertilization) or deforestation/afforestation on water resources, for example.

The Soil and Water Assessment Tool (SWAT) (Arnold et al., 1998) has been extensively applied worldwide to estimate water yield (Abou Rafee et al., 2019; Adla et al., 2019; Kaur et al., 2019), sediment loss (Wang and Kalin, 2018; Brighenti et al., 2019; Himanshu et al., 2019; Mishra et al., 2007), nutrient loading (Ramesh et al., 2020; Akhavan et al., 2010; Chu et al., 2004; Haas et al., 2016), assess the impacts of climate change (Dosdogru et al., 2020; Ahn et al., 2016; Anjum et al., 2019; Awan and Ismaeel, 2014), and land use/cover change (Wang and Kalin, 2011; Anand et al., 2018; Jodar-Abellan et al., 2018; Li et al., 2014). As of December 31, 2019, over 3,460 peer-reviewed journal papers have been published testing SWAT around the world.

SWAT has not been sufficiently tested in forested ecosystems yet (Yang et al., 2018) and had shown some limitations to accurately simulate plant growth (Zhang et al., 2020), especially when it comes to LAI development. To address these issues, some studies have been carried out to revise SWAT's plant database. For example, Strauch and Volk (2013) proposed a new plant growth approach based on changes in soil moisture for tropical regions and presented a logistic

LAI decline function. Similarly, Alemayehu et al. (2017) presented a quotient of rainfall and reference evapotranspiration to initialize the plant growth cycle in SWAT. The authors tested the methodology for a variety of land uses in Kenya and Tanzania and showed improvements in simulated LAI based on remote-sensing derived data. Yang and Zhang (2016) identified unrealistic parameter values representing evergreen forest, deciduous forests, and mixed forests in SWAT and proposed an improved model parameterization tested at ten Ameriflux sites. Yang et al. (2018) extended the previous study to the watershed-scale and showed positive effects for streamflow prediction. Watson et al. (2005) replaced the original SWAT plant growth model with the 3-PG forest growth model to better reproduce the growth of *Eucalyptus* trees in Australia. More recently, Lai et al. (2020) presented a forest growth model featuring variable density and mixed vegetation types in SWAT. Their results showed that the modified model outperformed the original model in simulating flow and nutrient load.

Although all of these studies offer valuable insights and potential contributions to the modeling community, they fall into oversimplifications (e.g., lumped forest types), insufficient representation of plant growth components (e.g., LAI + biomass + ET), an excessive amount of input data (e.g., forest growth data required by 3-PG), and lack of demonstration of the extents to which forest processes affect the watershed hydrology. To the best of the author's knowledge, no study in the literature conducted a thorough parameterization of individual forest attributes for species-specific trees in SWAT. Most of the modeling studies found in the literature lumped parameters for groups of forests and thus did not consider underlying characteristics of specific forest types, such as pines. In forested regions such as the southeastern U.S., for example, where specific pine species like loblolly pine (*Pinus taeda L.*) and slash pine (*Pinus elliottii*) dominate

the landscape, it is necessary to better test SWAT's skills and tune the model to better represent these tree species.

Considering that forests can cover large portions of watersheds and largely interfere with the hydrological cycle and that SWAT has been widely applied as a hydrological prediction and assessment tool, it is fundamental to understand and evaluate the model's skills in forested ecosystems. LAI and biomass, besides being key forest attributes representing forest growth and dynamics, play important roles in SWAT's hydrological computations. For instance, LAI affects plant transpiration, canopy rainfall storage, and evapotranspiration (if the Penman-Monteith method is used to simulate ET) in SWAT (Neitsch et al., 2011). Likewise, aboveground biomass and soil residue affect the soil evaporation rates in the model. SWAT's semi-distributed characteristic capable of discretizing the landscape into smaller units combined with the vast amount of freely-available remote-sensing data presents a great opportunity for modelers to move from the traditional modeling calibration approach (i.e., streamflow only) and incorporate additional constraints into the models. A large number of studies have reported the benefits of using remote-sensing derived data to increase the accuracy of watershed models (Gui Ziling et al., 2019; Ha et al., 2018; Herman et al., 2018; Jiang and Wang, 2019; Ma et al., 2019; Odusanya et al., 2019; Parajuli et al., 2018; Rajib et al., 2016; Tobin and Bennett, 2017; Y. Zhang et al., 2020). In a previous effort, we developed an improved SWAT parameterization for loblolly pine and slash pine, the two major pine species in the southeastern United States. Our methodology was based on remote-sensing data combined with field observations and was successfully tested at different field-scale sites across the Southeastern United States. Although our proposed parameterization outperformed the default model setting in predicting tree LAI, biomass, and ET, the hydrological implication at the watershed-scale remains unknown.

Therefore, the overreaching goal of this study is to investigate the importance of accurately capturing forest processes in watershed-scale hydrological models and assess their implications for simulated discharge and water balance computation. Our specific objectives are: (1) to assess the feasibility of transferring previously calibrated biophysical parameters to two forested watersheds; (2) to assess the effects of multi-facet model calibration (LAI + biomass + ET + streamflow) on streamflow prediction compared to traditional model calibration (streamflow only); and (3) to determine which forest attributes and processes (LAI development, biomass accumulation, or ET rates) affect streamflow and water budget the most. It is hypothesized that an enhanced representation of forest dynamics in SWAT will positively affect its performance in simulating streamflow due to a more realistic prediction of leaf area development, canopy storage, and precipitation loss as ET. The novelty of this study is demonstrating the effect of forest dynamics on hydrological processes using a ready to go improved model parameterization based on open-source remote sensing products, published literature, and shared field observations. Such level of detail and reflection of real-world interplays of natural processes (i.e., water, energy, vegetation) could never be achieved through traditional model calibration against streamflow only.

MATERIAL AND METHODS

Study sites

The Upatoi Creek and Upper Santa Fe River watersheds located in Florida and Georgia, respectively, are selected as study sites (Fig. 1). These watersheds are suitable to test our hypothesis that a better simulation of key forest processes can resonate in better streamflow prediction because both are highly forested with either loblolly or slash pine tree species and also have long-term daily streamflow records. The Upatoi Creek watershed (UCW) is in Chattahoochee County, near Columbus, Georgia, and has a drainage area of approximately 900 km^2. Upatoi Creek

is a 57 km long river running from South Columbus to the Chattahoochee River. The elevation ranges from 73 to 255 meters in the watershed and according to the Soil Survey Geographic Database (SSURGO), there are 172 different soil classes at UCW, out of which 75 are hydrological soil group (HSG) A, 47 are HSG B, and 50 are HSG C. The land use and cover at UCW is mainly dominated by loblolly pine trees (57%) and shrubs (9%), according to the National Land Cover Database (NLCD) 2016 and National Forest Type Dataset (NFTD) (Ruefenacht et al., 2008).

The Upper Santa Fe River watershed (SFRW) is part of the Santa Fe River Basin system and has a drainage area of approximately 500 km^2 and elevation ranging from 25 to 83 meters. Located predominantly in Union County, Florida, the SFRW is situated approximately 40 km north from the city of Gainesville. In terms of land use and cover, the SFRW is dominated by slash pine trees (56%) and hay-pasture (12%). Soils in the SFRW are mostly HSG's A and B with a few HSG's C.

Additional Hydrometeorological characteristics portraying both watersheds are summarized in Table 1.

The SWAT Model

The SWAT hydrological model is used in the current study to investigate the effects of forest dynamics on key hydrological processes within the study watersheds. SWAT is one of the most widely used hydrological models and a well-established tool capable of simulating various water fluxes (e.g., surface runoff, lateral flow, groundwater contribution) and plant growth. Additional model components include weather, transport of sediment, nutrients, bacteria and pesticides, and land management. SWAT is a watershed-scale, semi-distributed, continuous-time, open-source model developed by the United States Department of Agriculture (USDA) Agricultural Research Service (ARS). The model discretizes a watershed into subwatersheds,

which are further discretized into unique combinations of land use, soils, and slope called hydrological response units (HRU's) (Neitsch et al., 2011). This particular way of SWAT handling the landscape heterogeneity aids to the model's computational efficiency, since HRU's are in synthesis fractions of subwatersheds not spatially identified in model's simulations.

In SWAT, the water balance calculation for each HRU considers five storages: snow, canopy storage, the soil profile with up to ten layers, a shallow aquifer, and a deep aquifer. The water balance is calculated using the following:

$$\Delta S = \sum_{t=1}^{t}(P - Q_{total} - ET - w_{seep}) \quad (1)$$

where, ΔS is the change in water storage, P, Q_{total}, ET, and w_{seep} are the daily amount of precipitation, total water yield, evapotranspiration and the total amount of water exiting the bottom of the soil profile on a given day, respectively. The value of w_{seep} is a sum of the amount of water percolating out of the lowest soil layer and the amount of water flowing past the lowest boundary of the soil profile due to bypass flow. The total water yield (Q_{total}) represents an aggregated sum of surface runoff, lateral flow, and the base flow contribution to streamflow. In this study, surface runoff was computed using the Soil Conservation Service (SCS) Curve Number (CN) method (USDA, 1972) based on daily rainfall observations and the Penman-Monteith (Monteith, 1965) method was selected for estimating evapotranspiration.

SWAT incorporates a simplified version of the Environmental Policy Integrated Climate (EPIC) model (Williams, 1990) to simulate the growth of different types of crops and trees. The initialization of the growth cycle in SWAT is based on the Heat Unit Theory: plants require a certain amount of heat to reach maturity, which is only reached when a plant-specific total heat unit is attained. Once the plant reaches maturity, it stops transpiring and uptake of water and

nutrients. The growth cycle restarts every year based on a latitude-dependent dormancy routine or via harvest and kill operation in the model's management module. At the beginning of each growth cycle, the accumulated heat units drop to zero and the LAI is set to a plant-specific minimum value defined by the user (Neitsch et al., 2011). During the early stage of plant growth, SWAT simulates phenological development using an optimal leaf area index development curve. The plant's biomass accumulation is based on canopy light interception and the plant's efficiency in converting intercepted radiation into biomass.

Given SWAT's limitations in simulating tree growth, an improved model parameterization describing loblolly and slash pine growth and dynamics was used in this study. This improved forest parameterization was developed based on field measured forestry data, remote-sensing estimates of LAI, expert knowledge, and review of published literature. Further details about SWAT's computation of physical processes can be found in Neitsch et al. (2011).

Model setup and data acquisition

As a semi-distributed watershed-scale hydrological model, SWAT requires several geospatial inputs and weather forcing to simulate physical processes within a watershed. The ArcSWAT 2012 (version 10.4.19) interface was used in this study to delineate the watersheds and define their respective number of HRU's. First, the watershed's boundaries were delineated based on 10 meters resolution digital elevation model (DEM) from the National Elevation Dataset (NED) and hydrography network from the National Hydrography Dataset (NHD). Soil maps and soil characteristics (e.g., soil depth, soil hydraulic conductivity, available water capacity) needed to parameterize SWAT's soil database were obtained from SSURGO as gridded data (10 meters resolution) covering the watershed's drainage area. A reclassified land use map based on the publicly available 30 meters resolution NLCD 2016 was ingested in ArcSWAT.

The land use reclassification was deemed necessary to capture the spatial distribution of loblolly and slash pine across the watersheds as accurately as possible. Thus, a pre-processing step involving reclassification of NLCD 2016 was conducted using the NFTD as a background map to discretize NLCD's forest classification into species-specific and geographically-meaningful types of trees. NFTD is a publicly available geospatial dataset at 250 meters resolution developed by United States Forest Service (UFS) Forest Inventory and Analysis (FIA) program and the Geospatial Technology and Applications Center (GTAC). This dataset was created to show the extent, spatial distribution, and forest type composition of forests within the United States territory. We pre-processed this gridded dataset in ArcMap 10.4.1 to make it readable in ArcSWAT during the HRU definition phase. Initially, we isolated loblolly pine and slash pine species from the NFTD and saved them as a separate raster layers. Next, the original NLCD 2016 raster layer was overlaid with NFTD rasters. Using the erase function from the Analysis Tool toolbox and ingesting the NFTD loblolly and slash pine rasters as input (one after the other), the NLCD land use classes overlapping with loblolly and slash pine rasters were erased. The geospatial information of the previously isolated loblolly and slash pine rasters were then copied (copy function on ArcMap's main toolbar enabled through an edit session) and pasted (paste function on ArcMap's main toolbar) into the NLCD rasters that had their original classes erased in the previous step. It is worth mentioning that this sequential pre-processing was applied to the NLCD's land use classes representing forests only (e.g., forests deciduous, forests evergreen, forests mixed, and forested wetlands), exempting other land use classes such as agricultural lands and urban spaces. This decision was made to avoid misclassification, given the coarser resolution of NFTD compared to NLCD. Table 2 shows the percentage cover of each land use class with respect to the watershed's

area, before and after reclassification. Figure 2 displays the same information as spatially distributed land use maps.

As weather forcing, this study uses daily precipitation and minimum/maximum temperature from the PRISM Climate Group (http://www.prism.oregonstate.edu), hourly solar radiation and wind speed data from the North American Land Data Assimilation System (NLDAS) (https://ldas.gsfc.nasa.gov/nldas) aggregated to a daily basis, and hourly relative humidity data from the National Solar Radiation Database (NSRD) (Sengupta et al., 2018) also aggregated to daily time-step. Precipitation, temperature, and relative humidity data at 4 km resolution were extracted using the centroid of each subwatershed as a spatial reference, resulting in twenty-three virtual stations at UCW and twenty-one at SFRW. Solar radiation and wind speed estimates at 12.5 km resolution were extracted to all NLDAS grids overlapping the watershed's boundary, which resonated in eight virtual stations at both UCW and SFRW.

To assess the effects of improved SWAT forest parameterization at the watershed-scale, we compared SWAT predicted ET and LAI against MODIS derived estimates. MOD15A2H (Myneni et al., 2015) and MOD16A2 (Running et al., 2017) datasets were used to derive LAI and ET data at 4-days and 8-days intervals, respectively, at 500 meters resolution. We located areas in each watershed homogeneously covered by loblolly and slash pine and compared SWAT's outputs of LAI and ET from the largest HRU covered by loblolly and slash pine and located in the respective subwatershed against MODIS estimates. MODIS extracted data were geo-referenced and spatially aggregated to the shape of previously delineated polygons representing the located loblolly and slash pine areas using automated routines on the Google Earth Engine platform (Gorelick et al., 2017). Further details about testing SWAT's forest dynamics plausibility against remote-sensing data are described in the model calibration section. The simulated forest biomass

was compared to gridded forest biomass data from the U.S. Department of Agriculture (USDA) Forest Service Forest Biomass product, which was developed based on field measurements and statistical models (Blackard et al., 2008). We setup the initial growing conditions of slash and loblolly pine in the models by deleting all management operations assigned to the management file in ArcSWAT. Next, we assumed that trees were fully developed at the beginning of the simulation period by setting the HRU's land cover status as land cover growing from the beginning of the simulation period. Moreover, some initial physical conditions like the number of heat units (*PHU_PLT*), initial leaf area index (*LAI_INIT*), and initial biomass (*BIO_INIT*) had to be defined to configure the annual growth cycle of trees. For loblolly and slash pine, *PHU_PLT* and *LAI_INIT* were defined based on the field-scale model parameterization while *BIO_INIT* was initialized according to USDA's Forest Service forest biomass data for each watershed. For the former, the minimum biomass value reported by the USDA's Forest Service forest biomass data was assumed to be a reasonable estimate of the initial biomass.

For streamflow calibration and validation, we used daily streamflow data from the U.S. Geological Survey (USGS) gaging stations 02341800 and 02321000 at UCW and SFRW, respectively. The complete dataset used for constructing and calibrating/validating the SWAT models, as well as their sources, are summarized in Table 3. Based on the described data, SWAT2012 (revision 664) through the ArcSWAT interface with a 10%-10%-0% (land-use, soils, slope) of threshold generated 23 subbasins and 172 HRU's for UCW, whereas 21 subbasins and 138 HRU's were generated for the SFRW. The models were run from 1995 to 2018, using 3 years (1995-1997) of initialization as modeling warm up period.

Experimental design

Parameter-rich models such as SWAT can be easily calibrated for streamflow even though key intra-watershed processes such as forest dynamics are simulated poorly. This is because an observed signal (e.g., point-scale streamflow) may be reproduced in such models using thousands of different parameter sets or ranges of parameter combinations. This problem is known as equifinality (Beven and Freer, 2001), where models can give right answers for wrong reasons. One possible way of minimizing the equifinality problem is by constraining more model variables (e.g., LAI, biomass, ET) through additional observed data. Here we perform four modeling experiments prior to streamflow calibration in which we progressively constrain more variables with additional data. These experiments can help us to isolate the impacts of LAI, biomass, and ET on streamflow prediction and water budget computation without the confounding effect of streamflow-related parameters. To measure the benefits and drawbacks of each experiment we compare simulated baseflow, streamflow, watershed-average ET, and runoff coefficient against observations and remote-sensing derived estimates. Observed baseflow was estimated from observed streamflow using the Web Based Hydrograph Analysis Tool (WHAT) (Lim et al., 2005) using its standard settings for perennial streams with a porous aquifer. The experiments are as follows:

1. Default model (M_0): SWAT model is setup and run without altering plant growth related parameters.
2. ET (M_{ET}): this experiment adds ET related parameters (previously calibrated) to the default model (M_0).
3. LAI + biomass (M_{LAI+BM}): this experiment incorporates parameters controlling LAI and biomass, which are previously calibrated.

4. LAI + biomass + ET ($M_{LAI+BM+ET}$): this experiment includes calibrated parameter values representing the full coupling of vegetation, water, and energy relations in SWAT.

Comparison of M_{ET}, M_{LAI+BM}, and $M_{LAI+BM+ET}$ against M_0 tells us how much model performance has improved or deteriorated due to addition/removal of new variables. The fourth experiment ($M_{LAI+BM+ET}$) is the one we are most interested in because it fully considers the tree growth cycle in SWAT and includes the largest number of variable constraints. M_{LAI+BM} compared to M_0 tells us how much model performance has improved or deteriorated by including improved phenological development and biomass accumulation without adjusting for canopy evaporation, plant water uptake, and soil evaporation. M_{ET} shows how remote-sensed ET data can help predictions in ungauged basins or watersheds with limited streamflow records. M_0 is a baseline scenario serving as a reference to measure the advantages and disadvantages of M_{ET}, M_{LAI+BM}, and $M_{LAI+BM+ET}$.

Streamflow calibration and validation strategies

Hydrological models often cannot accurately simulate streamflow under default parameterization. Each watershed is unique, and dominant hydrological processes can vary, which default parameterization may not capture. Thus, model calibration is frequently performed to adjust selected model parameters representing the processes of interest. In this study, we employ an automated model calibration approach to enhance SWAT's accuracy in simulating streamflow at the watershed's outlet. We split the time series data into calibration (1998-2014) and validation (2015-2018) periods at both watersheds. SWAT Calibration and Uncertainty Program (SWAT-CUP) (Abbaspour, 2015), a standalone calibration software developed specifically to be used with SWAT, was used to optimize model parameters. Model calibration was carried out at daily time step using the Sequential Uncertainty Fitting algorithm (SUFI-2) option in SWAT-CUP.

In SUFI-2, global sensitivity analysis is performed by calculating the regression coefficients of the parameters generated by the Latin hypercube sampling method against the values of the defined objective function. The relative significance of each sampled parameter is measured using a t-test. Parameter sensitivities are computed by quantifying the average changes in the objective function resulting from changes in each parameter (Abbaspour, 2015). The *p-value* tests the null hypothesis that the coefficient of a parameter is equal to zero (i.e., the parameter is not sensitive). Low *p-values* (typically <0.05) indicate sensitive parameters.

In SUFI-2, uncertainty in parameters are expressed as ranges representing uncertainties associated with forcing input data (e.g., precipitation), the conceptual model, parameters, and observations (Abbaspour, 2015). Uncertainties in parameters are reflected as uncertainties in the model output variable, which are represented as the 95% probability distributions (95PPU). The 95PPU is hence the model solution in a stochastic calibration approach, considering all sources of uncertainties. SWAT-CUP provides two statistics to quantify the fit between the 95PPU and observed data*: P-factor* and *R-factor*. The *P-factor* expresses the percentage of observed data enveloped by the 95PPU, while the *R-factor* is the relative thickness of the 95PPU band and is calculated as the average of the 95PPU thickness divided by the standard deviation of the corresponding observed variable (Abbaspour et al., 2018). Ideally, most of the observations should be captured by the 95PPU (i.e., *P-factor* close to 1) in a small envelop (i.e., small *R-factor* value).

As model performance measures, this study uses the coefficient of determination (R^2), the Nash-Sutcliff-Efficiency (*NSE*), and the percentage bias (*PBIAS*). Further, *NSE* was selected as the objective function in SUFI-2 and 500 simulations were performed per iteration. The number of iterations was based on how fast the model was converging to a higher *NSE* value in the subsequent iteration. The parameters used to calibrate SWAT for streamflow in this study were

selected based on the model's structure and equations regulating discharge computation described in Neitsch et al. (2011).

We calibrated daily streamflow for the two extreme modeling experiments, M_0 (default) and $M_{LAI+BM+ET}$ (LAI + biomass + ET). Comparing these two calibration schemes can show the benefits of including all variables describing forest dynamics simulation in model calibration and how it changes the solution space (i.e., the most optimal value within the range of parameters) relative to a model constraint with gauged streamflow data only. Since $M_{LAI+BM+ET}$ considers improved LAI, biomass, and ET estimates and theoretically represents the most optimal model condition among the four experiments (i.e., a model able to predict forest attributes and streamflow reasonably well), this experiment was selected to quantify the effects of improved forest processes on automated streamflow calibration. Both calibration approaches are explained below.

Traditional model calibration (M_0)

Calibration of M_0 involved adjusting the parameters listed in Table S1 for the default model setup. This is a traditional calibration approach employed in most hydrologic modeling studies, where model parameters related to vertical fluxes (e.g., ET) and horizontal fluxes (e.g., surface runoff) are lumped together and calibrated with streamflow data only. This calibration scheme was performed to generate a base condition to which the next calibration configuration could be compared.

Multi-facet model calibration ($M_{LAI+BM+ET}$)

In this calibration scheme, we decouple horizontal (streamflow) and vertical (ET) water fluxes by constraining parameter values representing biophysical processes within a physically meaningful range. This approach does not optimize parameters controlling vertical fluxes (e.g., *CANMX*, *EPCO*, *ESCO*) when performing automated streamflow calibration, which is typically

the case in traditional calibration. Such parameters had their values derived for loblolly and slash pine trees at the field-scale level in previous chapter. At the UCW, parameters controlling the LAI development curve, water loss through ET, and tree total biomass for loblolly pine were calibrated at field-scale level using data from a loblolly pine plantation in Georgia (approximately 35 km southwest of the watershed outlet). Likewise, slash pine related parameters were calibrated using data from a slash pine plantation field in Florida located approximately 400 km southwest of the UCW outlet. For the SFRW model, loblolly and slash pine parameters were calibrated on adjacent pine plantation fields located approximately 25 km south of the watershed outlet. The multi-facet ($M_{LAI+BM+ET}$) calibration scheme transfers the most optimal parameter values representing LAI, biomass, and ET for loblolly and slash pine trees from the field-scale models to the watershed-scale models. The transferred parameter values were extended to HRU's covered by loblolly and slash pine at both watersheds. One could argue that transferring parameter values from field-scale to watershed-scale without further calibration is not adequate because of varying physical conditions (e.g., soil types, weather). Unlike reach/subbasin level parameters in SWAT, plant-specific parameters cannot vary spatially in the plant database. In other words, these parameters are species-specific and even though a given type of plant can be present in several HRU's, its parameter values cannot change from HRU to HRU. This model limitation challenges a spatially distributed calibration of biophysical parameters in SWAT-CUP. Such an effort would essentially result in a lumped calibration inconsistent with the spatially distributed characteristic of remote-sensing data. Thus, our approach is more appropriate to capture the importance of forest dynamics in hydrological models since the biophysical parameter values included in $M_{LAI+BM+ET}$ were developed based on species-specific high-quality datasets. Fig. S1 in the supplementary materials shows via boxplots the distribution of simulated LAI and ET across all HRU's covered by loblolly

and slash pine at UCW and SFRW. It is clear that minimum, median, and maximum values are similar across these HRUs, and that the variability across the watersheds is minimum.

Ecohydrological flow parameters

Biotic processes such as vegetation growth can affect the hydrologic regime within a watershed. Effects of forest hydrological processes in watershed models may not be too evident based only on simplistic analysis such as daily and seasonal streamflow, baseflow hydrographs, and mean annual water balance. In order to better understand the degree of hydrologic alteration attributable to improved forest parameterization in hydrologic models, we utilized the Indicators of Hydrologic Alterations (IHA) tool (TNC 2009). IHA was developed by the Nature Conservancy (TNC) based on Richter et al. (1996) for calculating the characteristics of natural and altered hydrologic regimes. IHA is an easy-to-use tool that summarizes long periods of daily flow data into 67 statistical parameters representing ecologically relevant conditions. These 67 statistical parameters are subdivided into two groups: the IHA parameters (33 parameters) and the Environmental Flow Component (EFC) parameters (34 parameters). In the current study, we selected 32 IHA parameters and 18 EFC parameters to compare the flow regime changes in the UCW and SFRW under M_0 and $M_{LAI+BM+ET}$ calibration schemes in relation to observed streamflow over twenty-one years (1998-2018). The description and importance of the IHA and EFC parameters used in this study are shown in Table S2 in the supplementary materials.

RESULTS

Improvements in forest dynamics

Upatoi Creek watershed (UCW)

Although SWAT was run for the 1998-2018 period, the analysis of simulated forest processes discussed here is limited to the period 2001-2018 for ET and 2003-2018 for LAI, because of MODIS data availability.

As shown in Fig. 3, both LAI and ET predictions for loblolly pine improved significantly under $M_{LAI+BM+ET}$. The default SWAT parameterization largely overestimated the annual maximum LAI in comparison to MODIS. According to MODIS estimates, the average monthly LAI from 2003 to 2018 at UCW was 1.78 m^2/m^2. In the simulation with M_0, the predicted average monthly LAI was 2.45 m^2/m^2, while $M_{LAI+BM+ET}$ simulated an average monthly LAI of 1.71 m^2/m^2. The superior model performance under $M_{LAI+BM+ET}$ is supported by the statistical measures shown in Table 4. As can be seen in Fig. 3, M_0 missed most of MODIS ET peaks, which were captured in the $M_{LAI+BM+ET}$ model configuration. The better goodness of fit between $M_{LAI+BM+ET}$ and MODIS ET is demonstrated in Table 4 by higher *NSE* and R^2 values. The model's inability to capture ET peaks with the M_0 model configuration translated into 30% underestimation of ET. On the other hand, $M_{LAI+BM+ET}$ overestimated ET by 18% during 2001-2018. Although significant, this overestimation is within the uncertainty margin of 20% associated with the MODIS ET product, as reported by Mu et al. (2013).

Simulated LAI and ET for slash pine failed to accurately match MODIS estimates (Fig. 3 and Table 4). These results are not alarming since slash pine cover less than 0.1% of the UCW, representing an area of only 70 hectares. Furthermore, this may indicate that the slash pine parameterization developed in FL is not suited for slash pine trees growing in GA. This finding

should not come as a surprise given the substantial geographic distance between the plantation field where slash pine was calibrated and the UCW. The significant model overestimation of ET with the $M_{LAI+BM+ET}$ model configuration is most probably a consequence of the LAI overestimation, given the role played by LAI in ET estimation. Another likely cause of the poor model performance of ET in $M_{LAI+BM+ET}$ is the value of maximum stomatal conductance (GSI) calibrated at the field-scale site in FL, which may be too high for slash pine trees occurring in GA.

We compared simulated forest biomass with USDA's Forest Service forest biomass product. To that end, we averaged simulated forest biomass in M_0 and $M_{LAI+BM+ET}$ for each subbasin. The subbasin level averaged biomass values were interpolated to the watershed area using Inverse Distance Weighting (IDW) interpolation method in ArcMap to allow for a more spatially discretized comparison against the gridded 250 meters resolution biomass product. The results are shown in Fig. 4. Under M_0, the average annual simulated biomass during 1998-2018 was 64 ± 4 (average ± one standard deviation) tons/ha, while $M_{LAI+BM+ET}$ predicted an average of 104 ± 13 tons/ha during the same period. USDA reported average biomass of 64 ± 15 tons/ha. Although the average biomass predicted by M_0 matched USDA's values, M_0 failed to reach biomass values larger than 70 tons/ha. In contrast, the maximum biomass predicted by $M_{LAI+BM+ET}$ reached values up to 121 tons/ha, closer to 146 tons/ha of maximum biomass from USDA forest biomass data. The spatial distribution pattern of simulated biomass is similar in M_0 and $M_{LAI+BM+ET}$, although $M_{LAI+BM+ET}$ showed better agreement with USDA biomass data in the northwestern portion of the watershed. In this area, which is heavily covered by loblolly pine (Fig. 2A), M_0 tended to underestimate biomass.

Upper Santa Fe River watershed

It is visually clear that $M_{LAI+BM+ET}$ outperformed M_0 in capturing LAI seasonality for loblolly pine (Fig. 3). The goodness of fit measured by R^2 and *NSE* and shown in Table 4 demonstrates the benefits of $M_{LAI+BM+ET}$ in comparison to M_0. The evident model overestimation in M_0 is evidenced by *PBIAS* values of 38%, which has improved to 7% in $M_{LAI+BM+ET}$. Monthly ET for loblolly pine was significantly underestimated in M_0 compared with MODIS reference time-series (Fig. 3). With the default parameterization, the average annual ET was 448 ± 58 mm during 2001-2018, which was significantly lower than MODIS estimates of 897 ± 88 mm. In the simulation with the improved model parameterization, the average annual ET increased to 740 ± mm, representing a 40% increase compared with the default model. Monthly ET simulated by $M_{LAI+BM+ET}$ was underestimated by 17.5%, which is lower than the 50% of underestimation with M_0. The good agreement between simulated monthly ET in $M_{LAI+BM+ET}$ and MODIS ET is statistically supported by the higher *NSE* and R^2 and lower *RMSE* values, as shown in Table 4.

Slash pine also had the LAI dynamics largely improved in $M_{LAI+BM+ET}$. This can be visually seen in Fig. 3, where $M_{LAI+BM+ET}$ reproduces the annual growth cycle captured by MODIS reasonably well. Moreover, the annual LAI peaks estimated by MODIS are better represented in $M_{LAI+BM+ET}$ than in M_0, although even with the $M_{LAI+BM+ET}$ model configuration SWAT could not accurately capture the bimodal LAI seasonality shown in MODIS data. This issue was also reported by Zhang et al. (2020) and is most probably attributable to SWAT's impossibility of simulating more than one growth cycle per year under the Heat Unit Theory. The average annual ET estimated by M_0 in the period 2001-2018 was 453 ± 57 mm, much lower than the average MODIS ET for the same period (999 ± 86 mm). The improved parameterization increased ET estimates by 58% compared with M_0, resulting in an annual average ET of 1,060 ± 65 mm (7%

higher than MODIS). The average annual ET simulated by the improved model was in good accordance with the ET range of 754-1168 mm/year at slash pine plantations in Florida reported by McLaughlin et al. (2013). Although the R^2 value deteriorated in $M_{LAI+BM+ET}$ compared to M_0 for slash pine, other statistical measures improved for $M_{LAI+BM+ET}$ in comparison to M_0 (Table 4).

Finally, the simulated biomass also improved in $M_{LAI+BM+ET}$ compared to M_0, based on USDA reported biomass reference data (Fig. 4). The average annual forest biomass simulated in M_0 was 92 ± 45 tons/ha, which is significantly lower than the USDA reported average of 120 ± 37 tons/ha. The $M_{LAI+BM+ET}$ model configuration increased annual average biomass estimates by 40% compared with M_0, resulting in 153 ± 50 tons/ha of biomass during 1998-2018. The improved model parameterization also ameliorated the spatial pattern of forest biomass, especially in the central portion of the watershed, where M_0 substantially underestimated biomass accumulation. Previous studies reported similar findings (Yang et al., 2018; Yang and Zhang, 2016), revealing that the default SWAT model presents some shortcomings in simulating tree biomass.

Hydrological responses to improved forest dynamics

Inclusion of forest dynamic processes in the model remarkably influenced the watershed hydrological responses. Prior to streamflow calibration, the baseline model configuration M_0 showed poor performance in simulating daily and monthly streamflow, as well as monthly baseflow, at both watersheds (Fig. 5-7). Flow duration curves of daily streamflows are shown for both watersheds in Fig. 5. As can be seen, high flows were captured reasonably well in M_0, however low flows were poorly simulated, especially at SFRW. Overall, daily streamflow was overestimated by 67% and 267% at UCW and SFRW, respectively, and *NSE* values were lower than 0.2 (Fig. 5). Similarly, monthly streamflow showed low *NSE* values and poor agreement with observed data at both watersheds (Fig. 6). M_0 overestimated most of the peaks at both study sites.

The monthly baseflow simulated by the SWAT models in M_0 show big differences compared to observations (Fig. 7). M_0 overestimated baseflow by 55% at UCW and 460% at SFRW in the period 1998-2018. Simulated mean annual baseflow was also highly overestimated at both study sites compared to observed data (Fig. S2 in the supplementary materials). The watershed-average ET simulated from 1998 to 2018 at the UCW was 614 mm/year in M_0 (Fig. S2), 25% lower than MODIS estimates (815 mm/year). Similarly, at the SFRW the simulated watershed-average ET was 546 mm/year, 57% lower than the MODIS estimated value of 1013 mm/year. Considering MODIS ET data, 24% of rainfall became runoff at SFRW, and 37% at UCW. The predicted fractions in M_0 were 59% at SFRW, and 52% at UCW, which is the direct consequence of ET underestimation.

The inclusion of calibrated ET parameters in M_{ET} dramatically improved the model's performance for streamflow and baseflow, as evidenced by increased *NSE* values (Fig. 5-7). The consistent model overestimation of streamflow and baseflow produced under M_0 was remarkably decreased at both study watershed in M_{ET}. The enhanced model performance was particularly alluring at UCW, where simulated daily streamflow was overestimated by 12% and baseflow by less than 1% in M_{ET}. By analyzing the exceedance probability curves (Fig. 5) it is possible to notice that M_{ET} increased the agreement between simulated and observed streamflow, especially for low flows (≥ 70%) at SFRW. Similarly, monthly streamflow and baseflow peak estimates improved in M_{ET} in comparison to M_0 (Fig. 6 and Fig. 7). The main effect of M_{ET} configuration on the watershed water budget was with respect to baseflow (Fig. 8). Increases in annual average ET of 25% at UCW (2% overestimation) and 33% at SFRW (20% underestimation) in M_{ET} compared to M_0 led to reductions in mean annual baseflow of 41% and 40%, respectively. Higher ET simulated in M_{ET} reduced water yields in the watersheds. Under the M_{ET} model configuration, 37% of

precipitation became discharge at UCW, which perfectly matched the 37% calculated using MODIS derived data. Also, 38% of the incoming precipitation resulted in modeled discharge at the SFRW, relatively close to the 24% estimated using observed data. Other studies have also shown the benefits of constraining ET in hydrological models based on remote-sensing data (Herman et al., 2018; Odusanya et al., 2019; Rajib et al., 2018, 2018; Strauch and Volk, 2013). The results of M_{ET} suggest that readily available remote-sensing ET data can help to improve the performance of hydrological models in predicting streamflow and baseflow in ungauged watersheds. It is worth highlighting that ET-related parameters were not re-calibrated for the study watersheds but rather transferred from the field-scale level. The former may indicate that the model performance could be further improved by carrying out a site-specific calibration at each watershed.

In the next model configuration (M_{LAI+BM}), we added calibrated parameter values regulating LAI and biomass prediction to the baseline model (but removed ET). As shown by the rating metrics and the flow temporal variability displayed in Figures 5-7, the model performance for streamflow and baseflow in M_{LAI+BM} deteriorated compared to M_{ET}. SWAT performed particularly poorly in M_{LAI+BM} at the UCW, where the performance metrics worsened even in comparison to the baseline model M_0. In contrast, M_{LAI+BM} showed superior performance compared to M_0 for all statistical measures at SFRW. This difference can be understood by considering the different tree growth and dynamics of loblolly pine and slash pine. As described in section 2.1, UCW is dominated by loblolly pine while the SFRW is mainly covered by slash pine trees. As shown in Fig. 3, the M_0 configuration considerably overestimated LAI for loblolly pine at UCW whereas underestimated it for slash pine at the SFRW. As a result of lower simulated LAI at UCW, after incorporating previously calibrated LAI parameters, compared to M_0, simulated

ET in M_{LAI+BM} has decreased 22% (Fig. S2). Consequently, the simulated baseflow increased 16% in relation to M_0 and was further overestimated (Fig. S2), which lead to the deterioration of model performance by M_{LAI+BM}. As expected, due to lower ET losses in M_{LAI+BM} the runoff coefficient increased to 0.63, deviating significantly from 0.37 calculated with observed data. The extent to which the watershed water balance was impacted by LAI and biomass (Fig. 8) highlights the importance of considering forest dynamics in hydrologic modeling studies, and the necessity of including ET in the modeling spectrum. At the SFRW, because of larger LAI values obtained after the incorporation of pre-calibrated LAI parameters (Fig. 3), the M_{LAI+BM} configuration predicted higher ET rates compared to M_0, increasing the watershed-average ET by 12%. Accordingly, the simulated streamflow and baseflow were reduced in M_{LAI+BM} (Fig. S2), which ameliorated the model's performance compared to M_0.

Results from $M_{LAI+BM+ET}$ were the most telling in terms of the impacts of forest processes on the model performance in simulating hydrological processes. Under $M_{LAI+BM+ET}$, the models were constraint with the largest number of variables among all experiments, and, besides showing the best performance in predicting streamflow and baseflow, the models also predicted forest growth and dynamics reasonably well under this parameterization. At UCW, the model performance for streamflow and baseflow simulations slightly deteriorated compared to M_{ET} but largely improved in relation to M_0 and M_{LAI+BM} (Fig. 5-7). Compared to MODIS derived data, the watershed-average ET predicted in $M_{LAI+BM+ET}$ was less than 1% higher and showed the closest agreement with MODIS estimates among all modeling experiments at the UCW (Fig. S2). The mean annual baseflow simulated in $M_{LAI+BM+ET}$ also showed good agreement with the observed data (2% overestimation) (Fig. S2). Although the inclusion of improved LAI and biomass into the model configuration led to deterioration in model performance compared to M_{ET}, it is more

coherent to include biophysical parameters values representing LAI development and biomass accumulation along with ET calibration, given the interplays between tree attributes (e.g., aboveground biomass and canopy) and the volume of water lost to the atmosphere as vapor. Additionally, enhanced model representation of tree attributes such as LAI and biomass may positively influence water quality applications. For instance, the adjusted total biomass to residue ratio *(BIO_LEAF*) from 30% to 2% reduces the amount of plant residue on the soil that is available for mineralization and nitrification. Likewise, the sediment yield simulated in SWAT through the Universal Soil Loss Equation (USLE) (Williams, 1975) is affected by the amount of residue on the soil surface. The combined positive effects of M_{ET} and M_{LAI+BM} at SFRW yielded $M_{LAI+BM+ET}$ as the best model configuration at this study site. The agreement between simulated and observed streamflow and baseflow at the watershed outlet increased under $M_{LAI+BM+ET}$ (Fig.5-7) compared to the other experimental conditions, as indicated by the highest goodness of fit measured by *NSE* and R^2. The model overestimation of horizontal fluxes were also the smallest under $M_{LAI+BM+ET}$ at SFRW. This was mainly because of the better agreement between watershed-average simulated ET and MODIS derived data (Fig. S2), which decreased the simulated water yield compared to the other modeling experiments. The runoff coefficient estimated based on simulated ET (0.34) was the closest to the observed runoff coefficient (0.24) among all scenarios. The changes produced in the water balance components, as we progressively moved from one experiment to the next, are shown in Fig. 8. There was a significant difference between M_0 and $M_{LAI+BM+ET}$, with a drastic increase in predicted ET and consequent decrease in predicted baseflow under the $M_{LAI+BM+ET}$ configuration at both watersheds. The results of $M_{LAI+BM+ET}$ indicate that the main improvement in streamflow and baseflow prediction came from the ET component. Studies such as Strauch and Volk (2013) and Alemayehu et al. (2017) also reported improvements in modeled

streamflow under enhanced LAI and ET predictions. Similarly, Yang et al. (2018) showed how enhanced biomass and ET estimates can improve the model's performance in simulating streamflow and sediment losses in a forested watershed. However, our study is the first to fully consider the effects of forest dynamics (i.e., LAI, biomass, and ET) on hydrological processes by constraining parameter values representing nationally relevant tree species.

Streamflow calibration and validation

As mentioned earlier, SWAT was calibrated for streamflow only under M_0 and $M_{LAI+BM+ET}$. Note again that M_0 represents the current practice in watershed modeling. Based on the visual comparison and statistical measures, $M_{LAI+BM+ET}$ proved to be the better model in predicting daily streamflow at both watersheds during the calibration and validation periods (Fig. 9). According to the model performance evaluation criteria proposed by Moriasi et al. (2015), the results achieved with the multi-facet calibration scheme ranged from "good" to "very good" at UCW, and "satisfactory" to "very good" at SFRW. Under the traditional calibration scheme, the model performance fell within the same range of categories at UCW, but deteriorated to unsatisfactory-satisfactory at SFRW. The enhanced model performance achieved with the multi-facet calibration scheme shows that better representation of forest dynamic processes enables SWAT to yield more accurate streamflow estimates. It also highlights the advantages of decoupling horizontal hydrological fluxes (i.e., streamflow) from vertical hydrological fluxes (i.e., ET) when calibrating watershed models. In the traditional calibration approach, ET related parameters such as CANMX, EPCO, and ESCO were calibrated simultaneously with parameters regulating the horizontal water flux. Although this led to an increased mean annual ET in M_0, the watershed-average annual ET was still lower compared to MODIS estimates. This underestimation of rainfall lost through ET resulted in a higher overestimation of simulated streamflow in M_0 compared to $M_{LAI+BM+ET}$ (Fig.

9). Moreover, in the calibration period, the obtained values of *P-factor* and *R-factor* were 0.07/0.73 at SFRW/UCW, and 0.19/0.58 at SFRW/UCW, respectively, with the traditional calibration approach. Under the multi-facet calibration scheme, *P-factor* and *R-factor* ranged from 0.09-0.72 and 0.11-0.50, respectively. While the values of *P-factor* did not change significantly in regard to the calibration approach, the *R-factor* showed considerable decrease with the multi-facet calibration scheme, suggesting reduced uncertainties due to consideration of improved forest dynamic processes in the modeling framework.

Results from the global sensitivity analysis revealed that *CN*2 is the most sensitive streamflow parameter at both watersheds under M_0 and $M_{LAI+BM+ET}$ (Fig. S3 in the Supplementary materials). However, the order of sensitive parameters changed in response to the calibration approach. Parameters such as saturated soil hydraulic conductivity (*SOL_K*), groundwater revap coefficient (*GW_REVAP*), groundwater delay time (*GW_DELAY*), and deep aquifer percolation factor (*RCHRG_DP*) became less sensitive in the multi-facet calibration scheme at the UCW. An opposite trend was observed at the SFRW, where most of the groundwater-related parameters had their sensitivity increased under the multi-facet model calibration scheme, as indicated by lower *p-values* in Fig. S3.

A similar effect can be noticed by paying closer attention to the best parameter values found with the traditional and multi-facet calibration schemes (Table S1). Parameters such as *RCHRG_DP* and *GW_DELAY*, for instance, have seen their best fitted values significantly change with the calibration approach. At both study sites, *RCHRG_DP* decreased in the multi-facet calibration scheme, which is most probably because of higher ET losses in $M_{LAI+BM+ET}$ compared to M_0. In the traditional calibration approach, because of the underestimated ET rates in M_0, the models tended to lose more water through deep aquifer percolation in order to compensate for

streamflow overestimation. Similarly, the improved forest dynamics considered in the multi-facet calibration scheme decreased the lag between the time that water exits the soil profile and recharges the shallow aquifer (*GW_DELAY*). Because of excessive water yield and percolation produced in M_0, the traditional calibration scheme slowed down the recharge to the shallow aquifer by assigning larger values to *GW_DELAY*.

Although the traditional calibration approach was able to yield a "very good" model performance in predicting streamflow, it massively failed to accurately replicate key forest dynamic processes such as LAI and biomass within the watersheds (Table 4 and Fig. 3). This "very good" model performance for streamflow was accomplished at the cost of an excessively high deep aquifer percolation and lumped values of parameters regulating plant transpiration (*EPCO*), soil evaporation (*ESCO*), and canopy storage (*CANMX*) (Table S1). Alternatively, the multi-facet calibration scheme demonstrated the feasibility of constructing realistic models that can reasonably represent forest processes without losing accuracy in predicting streamflow.

Impacts of forests on ecohydrological parameters

Fig. 10 shows the fifty ecohydrological parameters and how much their values calculated based on the M_0 and $M_{LAI+BM+ET}$ calibration deviated from their values calculated using observed streamflow data. At UCW, 36 out of 50 parameters showed increased agreement with observations under $M_{LAI+BM+ET}$ configuration. The inclusion of enhanced forest dynamic processes mitigated the model overestimation of mean monthly flows, monthly low flows, the magnitude of annual minimum flows of 30 and 90 days of duration, and the magnitude and duration of annual peak flows. Additionally, outputs from the multi-facet calibration scheme reduced the model underestimation of annual maximum flows of durations ranging from 1 day to 90 days, the duration of annual low pulses, and the frequency and duration of high pulses. These parameters may have

implications on soil moisture availability for plants, habitat availability for aquatic organisms, adequate water temperatures and dissolved oxygen rates, water table levels, water quality conditions, riparian vegetation, nutrient exchanges between rivers and floodplains, and others (Fig. S2). This indicates that the benefits of accurately representing forest processes in watershed models go beyond improving the accuracy of streamflow simulations. The multi-facet approach significantly underestimated minimum annual flows of 1 to 7-days of duration, the 7-day minimum flow, and the fall rate of high flow pulses in relation to M_0.

Improving the representation of forest growth and dynamics also optimized ecohydrological parameters at the SFRW. Overall, 42 out of the 50 included statistical parameters showed better agreement with observed data under the multi-facet calibration approach. Mean monthly flows and low flows had their overestimation reduced in $M_{LAI+BM+ET}$ compared to M_0. However, the model overestimation was still high, ranging from 8% to 81% for mean monthly flows. The same applied to monthly low flow parameters, for which the model overestimation ranged from 61% to 81% compared to the observed values. The cases in which the $M_{LAI+BM+ET}$ configuration caused deterioration of ecohydrological parameters compared to M_0 were mostly related to the underestimation of high flows. For example, the maximum flows of 1-day and 90-days of duration, as well as the Julian date of maximum flow, and duration of high flow pulses were excessively underestimated with the multi-facet scheme.

CONCLUSIONS

The improved representation of forest processes in SWAT returned better streamflow and baseflow predictions. This was demonstrated by performing four modeling experiments aiming to show the individual impacts of LAI, biomass, and ET on water fluxes. Results showed that improved ET prediction is the main reason leading to more accurate streamflow and baseflow

simulations in watershed models. The improvements in forest processes substantially altered the watershed water budget towards increased ET and decreased baseflow rates.

By calibrating streamflow-related parameters with and without the inclusion of improved LAI, biomass, and ET, we demonstrated that a physically meaningful representation of forest hydrological processes led to superior model performance in predicting streamflow. Moreover, the improved forest parameterization decreased the uncertainties associated with daily streamflow prediction. The importance of forest dynamics was further scrutinized by analyzing 50 ecohydrological parameters. Our results point to the importance of accurately accounting for forest processes in watershed models, especially in highly forested watersheds. The latter not only yields a more realistic model, but also enhances the model's performance in predicting streamflow, reduces the model uncertainties, and improves the terrestrial and aquatic connections, as demonstrated by the 50 ecohydrological parameters considered here.

Given the considerable disparity between the two extreme model configurations (i.e., M_0 and $M_{LAI+BM+ET}$) in replicating the watershed water budget, the conclusions drawn by each model would largely differ. This could generate impacts on management decisions in case the models were employed to support decision-making. Therefore, we suggest that key forest processes such as LAI, biomass, and ET should be ameliorated in hydrological models before simulating streamflow.

Although our improved forest parameterization relied on field observations from nearby pine plantation fields, we did not have field-measured data within the study watersheds. Thus, our methodological insights were validated against remotely sensed LAI and ET and gridded biomass data. As with any remote-sensing estimate, there are uncertainties associated with MODIS LAI and ET data, as well as with the USDA Forest Service forest biomass data. While it may raise

uncertainties concerning the validity of our findings, the global coverage of MODIS data facilitates the replication of our methodology worldwide. Moreover, SWAT's flexible plant database allows other researches to further refine our forest parameterization for other evergreen species.

In this study, the focus of our modeling effort was on streamflow and baseflow predictions. The impacts of improved forest growth and dynamics on modeled water quality (e.g., sediment yield, nutrient load) must be addressed in a future endeavor. As demonstrated here, increased ET losses resulting from our improved forest parameterization led to decreased surface runoff and baseflow. It can be inferred that lower surface runoff and baseflow rates will likely decrease sediment and nutrient loads transported to the main channel. Additionally, the adjusted amount of biomass converted to residue every year reduces the source of fresh residue on soil surface available for mineralization and nitrification. Consequently, the forest parameterization tested in this study may resonate in less nitrate being transported to water bodies. The sediment loss may also be impacted by the improved forest parameterization, especially because the USLE's cover and management factor is computed as a function of plant residue.

Finally, by constraining the models with readily-available remote-sensing data we were able to decouple vertical water fluxes and processes (e.g., evapotranspiration, plant water uptake, soil evaporation, and canopy storage) from horizontal water fluxes (i.e., streamflow) in model calibration. This allowed us to simultaneously capture forest dynamics and in-stream processes reasonably well. Such a level of detail and representation of plant-water-energy relations would hardly be obtained through model calibration against gauged streamflow data only. Considering that the ultimate goal of watershed modeling studies typically is to draw scenarios analysis representing different real-world conditions, a model able to accurately represent terrestrial and in-stream processes can produce positive implications for watershed modeling applications.

FIGURES

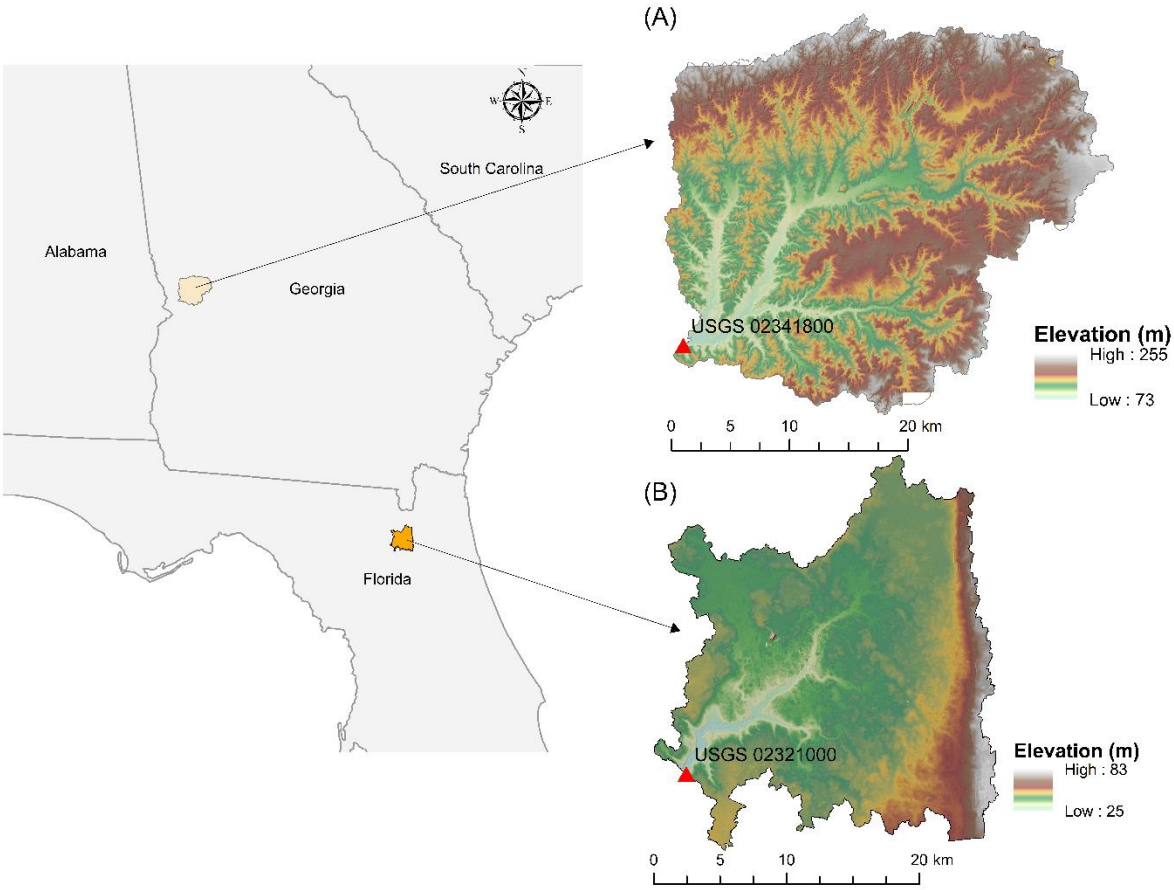

Figure 1. Location map of the selected forested watersheds. (A) Upatoi Creek watershed, dominated by loblolly pine, (B) Upper Santa Fe River watershed, dominated by slash pine.

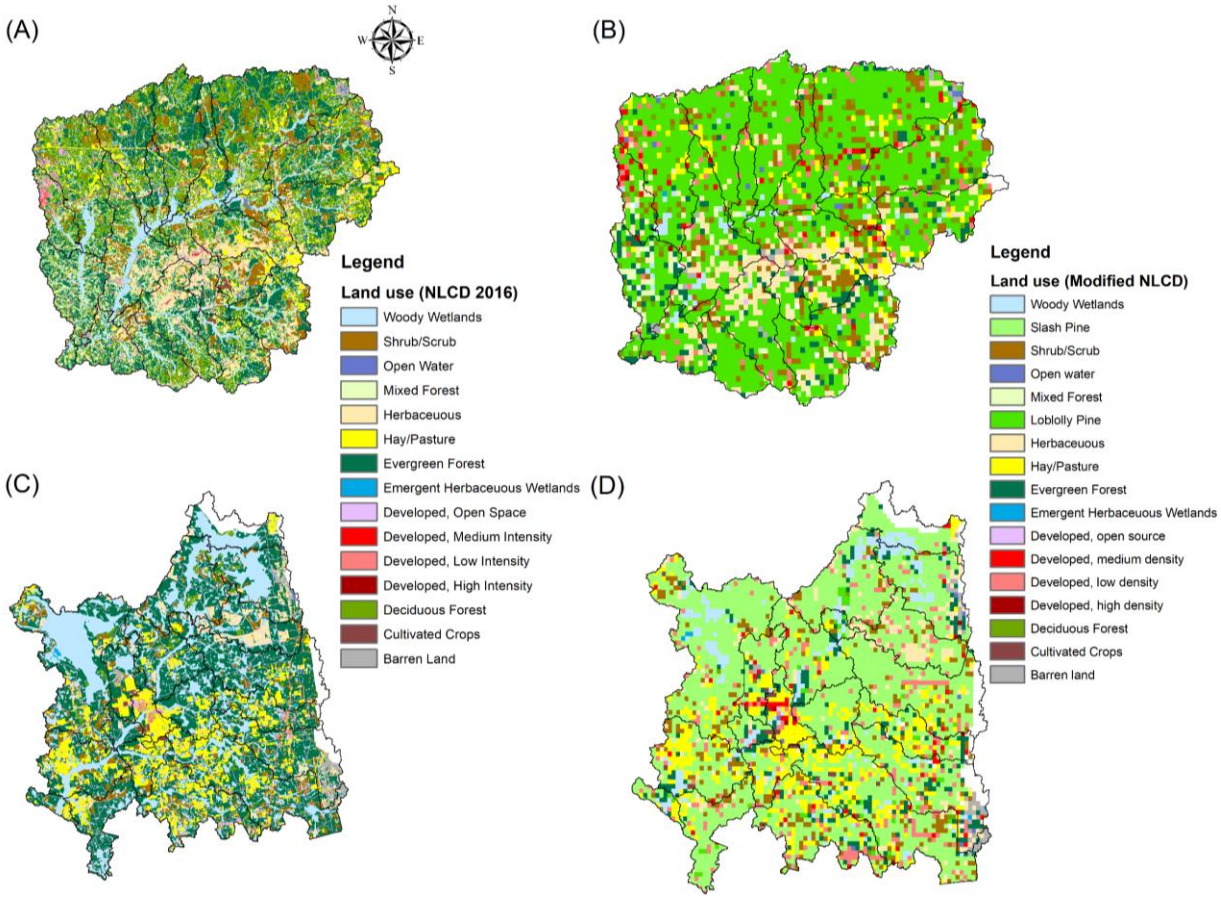

Figure 2. Spatial distribution of land cover classes before and after land use reclassification. (A) Upatoi Creek watershed before land use and cover reclassification using NLCD 2016 as land use map, (B) Upatoi Creek watershed after land use and cover reclassification using NFTD to map loblolly and slash pine areas across the watershed, (C) Upper Santa Fe River watershed before land use and cover reclassification using NLCD 2016 as land use map, (D) Upper Santa Fe River watershed after land use and cover reclassification using NFTD to map loblolly and slash pine areas across the watershed.

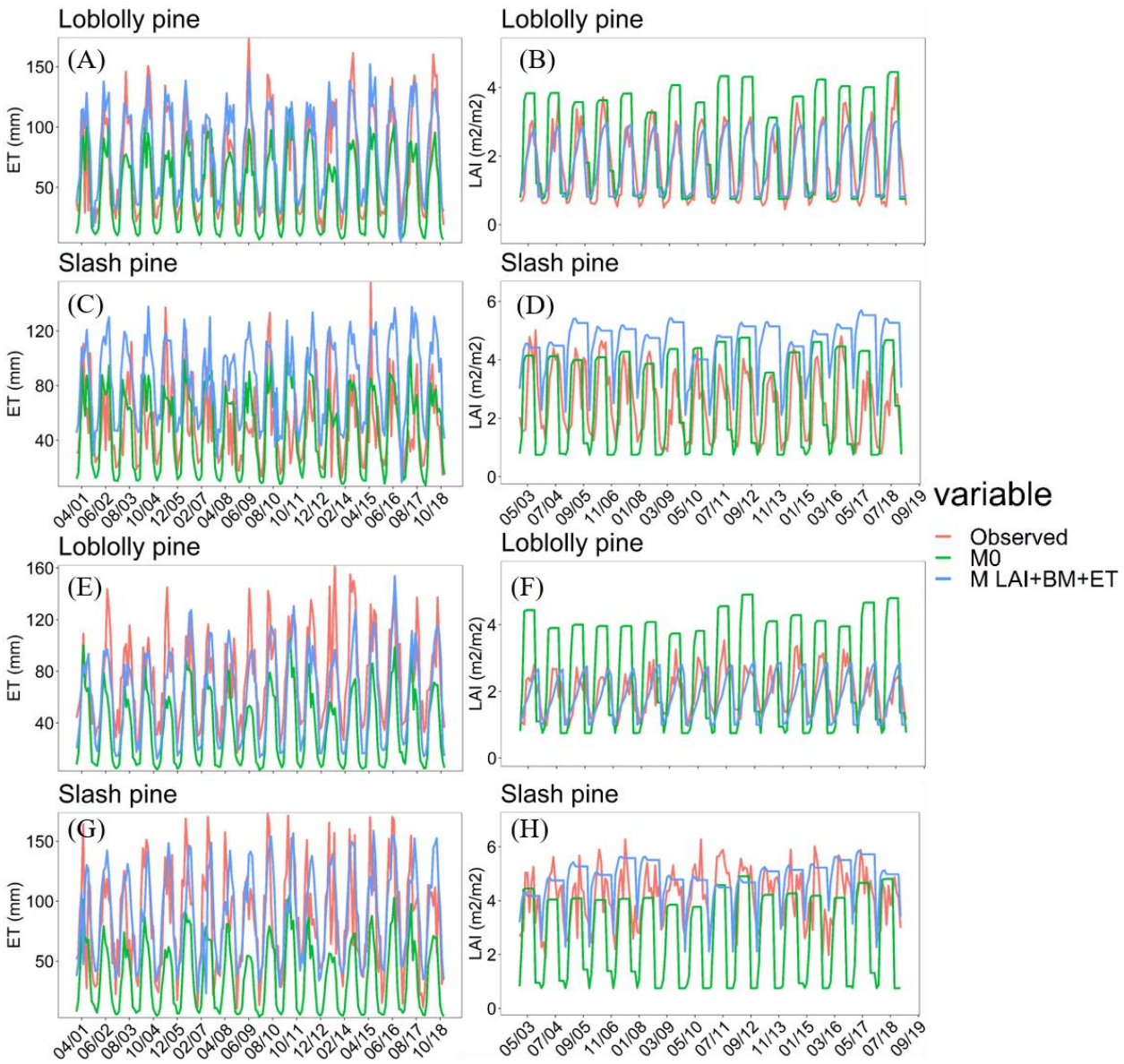

Figure 3. Simulated ET and LAI for loblolly and slash pine versus MODIS estimates at Upatoi Creek watershed (Figures A to D) and Upper Santa Fe River watershed (Figures E to H) under $M_{0 \text{ and }} M_{\text{LAI+BM+ET model}}$ configurations.

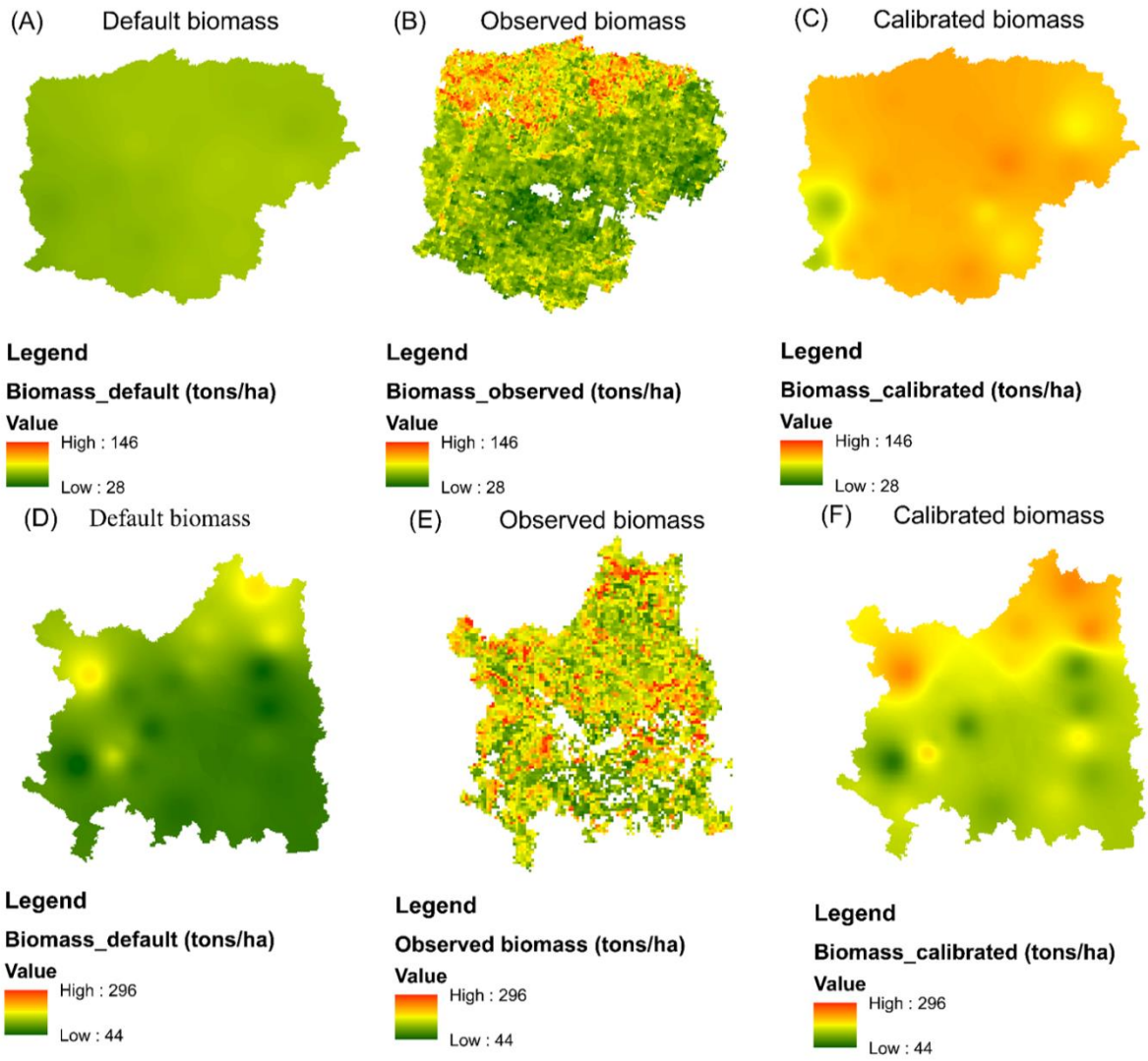

Figure 4. Simulated total forest biomass versus USDA Forest Service forest biomass product estimates at Upatoi Creek (Figures A to C) and Upper Santa Fe River watershed (Figures D to F) under $M_{0 \text{ and }} M_{LAI+BM+ET \text{ model}}$ configurations. (A-D) Biomass simulated by SWAT using default parameters in the plant database, (B-E) observed biomass for the UCW and USFRW derived from USDA Forest Service forest biomass, (C-F) biomass simulated by SWAT using previously calibrated plant-related parameters at both watersheds.

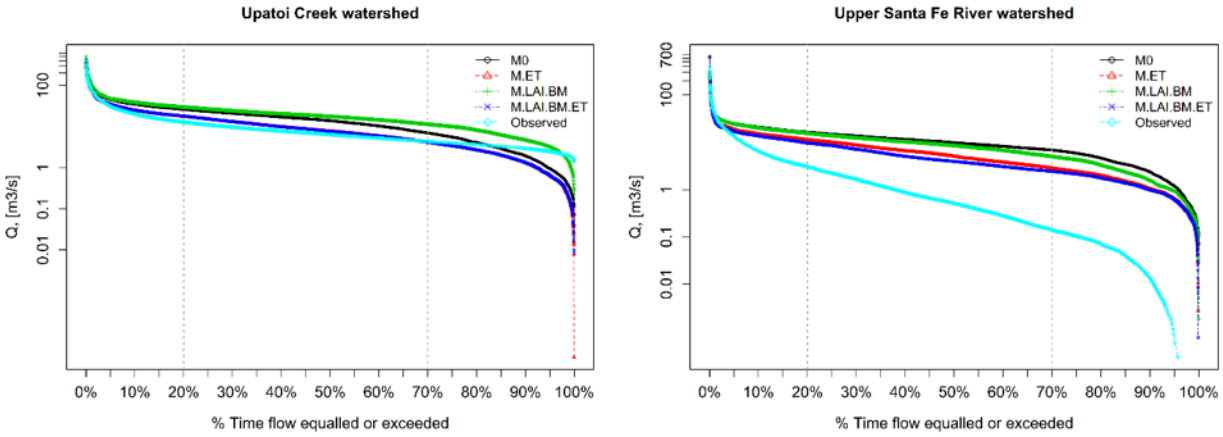

	Upatoi Creek				Upper Santa Fe			
	M_0	M_{ET}	M_{LAI+BM}	$M_{LAI+BM+ET}$	M_0	M_{ET}	M_{LAI+BM}	$M_{LAI+BM+ET}$
NSE	0.19	0.64	-0.13	0.63	-0.36	0.15	-0.23	0.24
PBIAS (%)	-67	-12	-102	-14	-268	-134	-233	-104
R2	0.63	0.69	0.60	0.69	0.41	0.44	0.42	0.45

Figure 5. Model verification under different configuration setups against USGS observed daily streamflow data for different exceedance probability of simulated streamflow at the watershed outlet from 1999 to 2019 at Upatoi Creek at Upper Santa Fe watersheds. The flow duration curve displayed here is plotted in log scale and therefore the discrepancy between simulated and observed streamflow is visually exaggerated. The statistical rating metrics displayed in the table refer to daily streamflow variability (not shown), and not to the exceedance probability curves.

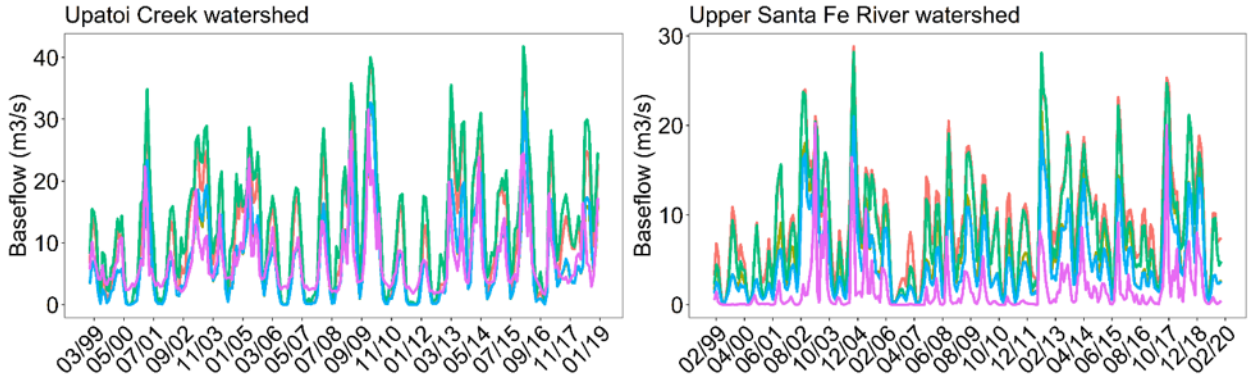

	Upatoi Creek				Upper Santa Fe			
	M_0	M_{ET}	M_{LAI+BM}	$M_{LAI+BM+ET}$	M_0	M_{ET}	M_{LAI+BM}	$M_{LAI+BM+ET}$
NSE	0.03	0.77	-0.71	0.75	-1.35	0.16	-0.93	0.39
PBIAS (%)	-67	-12	-102	-14	-268	-134	-232	-104
R2	0.77	0.81	0.73	0.80	0.60	0.65	0.61	0.68

Figure 6. Hydrograph showing monthly simulated streamflow against USGS observed data for different model configurations setups from 1999-2019.

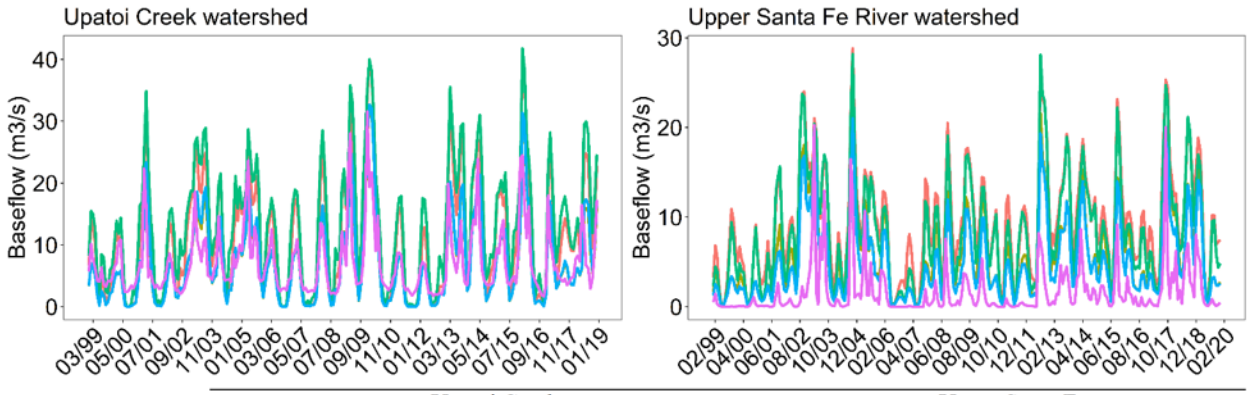

	Upatoi Creek				Upper Santa Fe			
	M_0	M_{ET}	M_{LAI+BM}	$M_{LAI+BM+ET}$	M_0	M_{ET}	M_{LAI+BM}	$M_{LAI+BM+ET}$
NSE	-0.79	0.46	-1.83	0.42	-8.26	-2.32	-6.74	-1.37
PBIAS (%)	-55	0.6	-85	-1	-461	-245	-404	-198
R2	0.65	0.67	0.60	0.66	0.40	0.46	0.41	0.48

Figure 7. Hydrograph showing monthly simulated baseflow against estimated baseflow for different model configurations setups from 1999-2019. Observed baseflow is estimated via baseflow separation program.

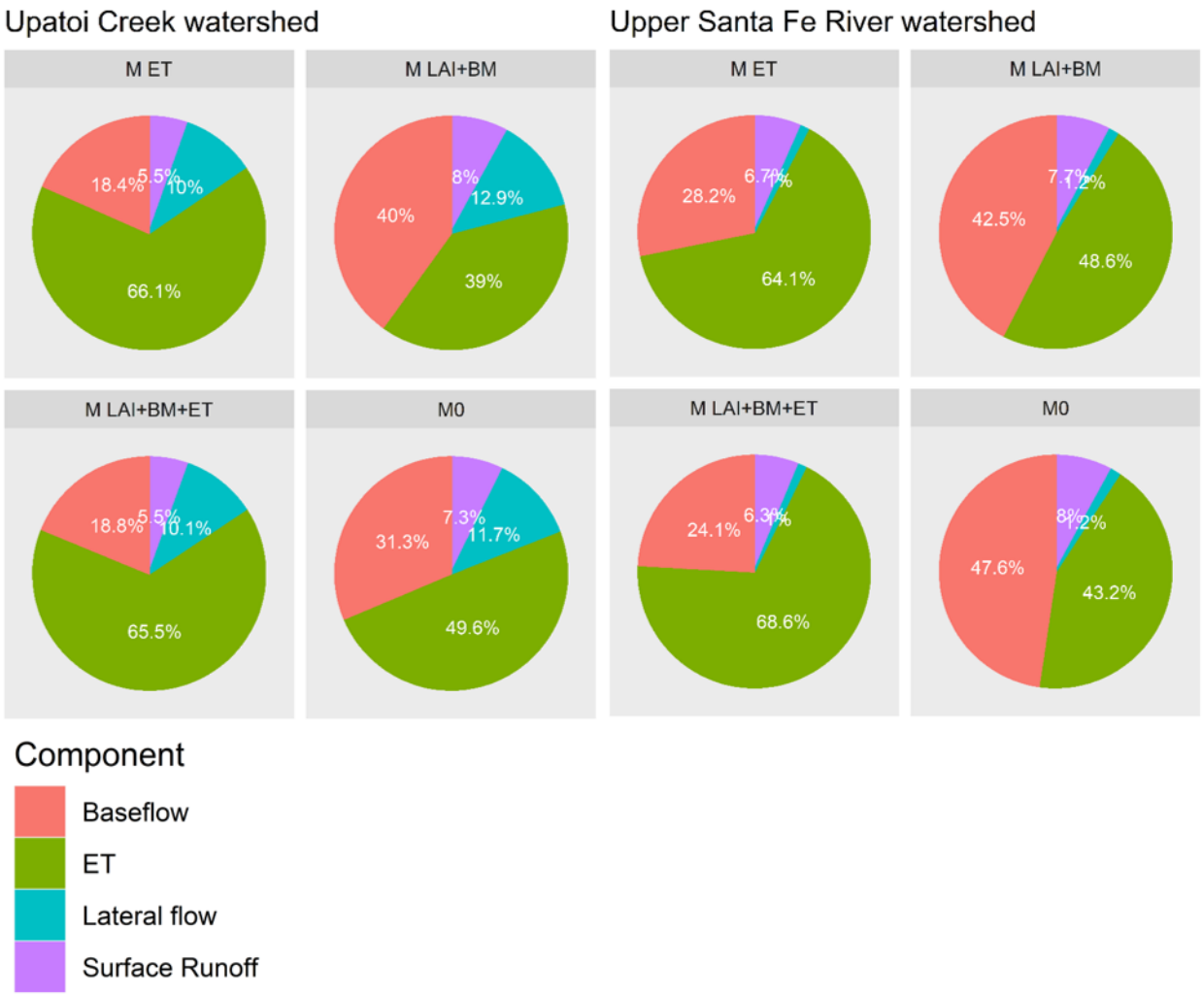

Figure 8. Change in simulated water budget under different model setup configurations from 1999 to 2019 at Upatoi Creek and Upper Santa Fe watersheds. The pie charts illustrate the mean annual water balance at each watershed during the whole simulation period.

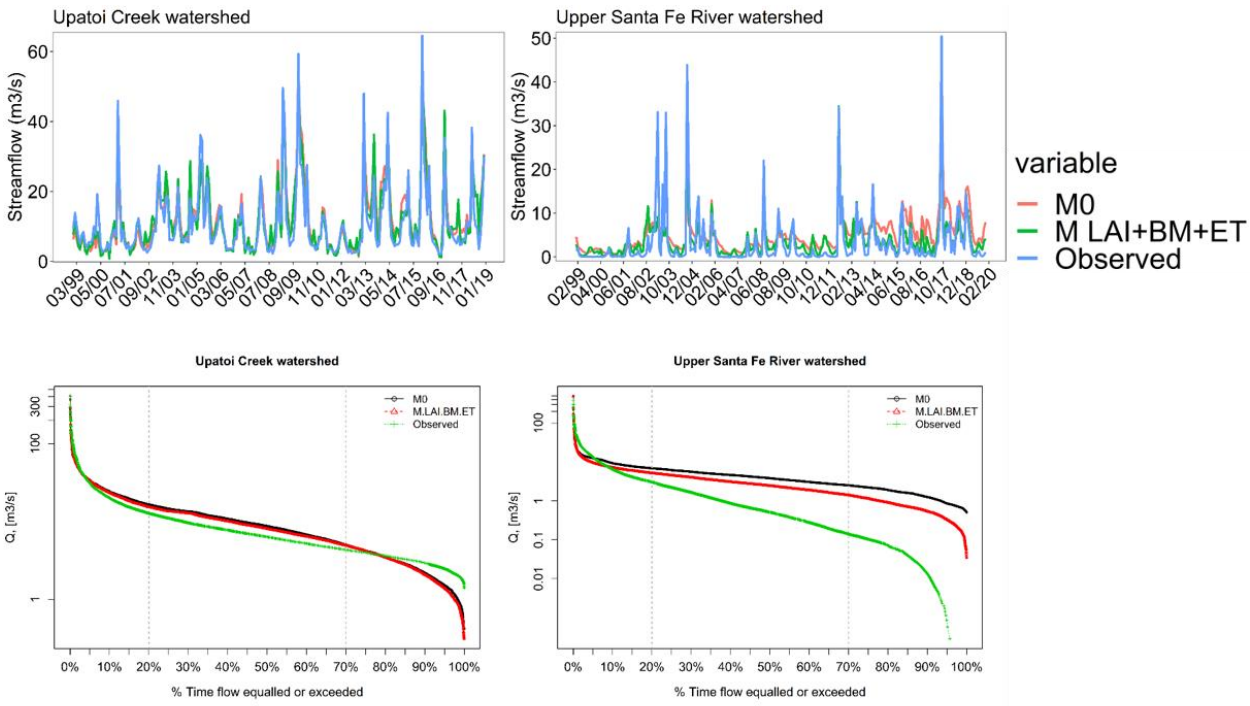

	Calibration (1999-2014)		Validation (2015-2019)		Calibration (1999-2014)		Validation (2015-2019)	
	M_0	$M_{LAI+BM+ET}$	M_0	$M_{LAI+BM+ET}$	M_0	$M_{LAI+BM+ET}$	M_0	$M_{LAI+BM+ET}$
NSE	0.72	0.76	0.78	0.80	0.41	0.52	0.57	0.73
PBIAS (%)	-10	-8	-22	-14	-43	-19	-114	-24
R2	0.73	0.76	0.79	0.80	0.42	0.52	0.68	0.74

Figure 9. Observed vs. simulated daily streamflow in calibration and validation periods under traditional and multi-facet calibration approaches. The upper hydrographs show the monthly discharge evolution in the period 1999-2019, while the bottom flow duration curves show exceedance probability of simulated streamflow at the watershed outlet from 1999 to 2019 at Upatoi Creek at Upper Santa Fe watersheds. The flow duration curve displayed here is plotted in log scale and therefore the discrepancy between simulated and observed streamflow is visually exaggerated. The statistical rating metrics displayed in the table refer to daily streamflow variability.

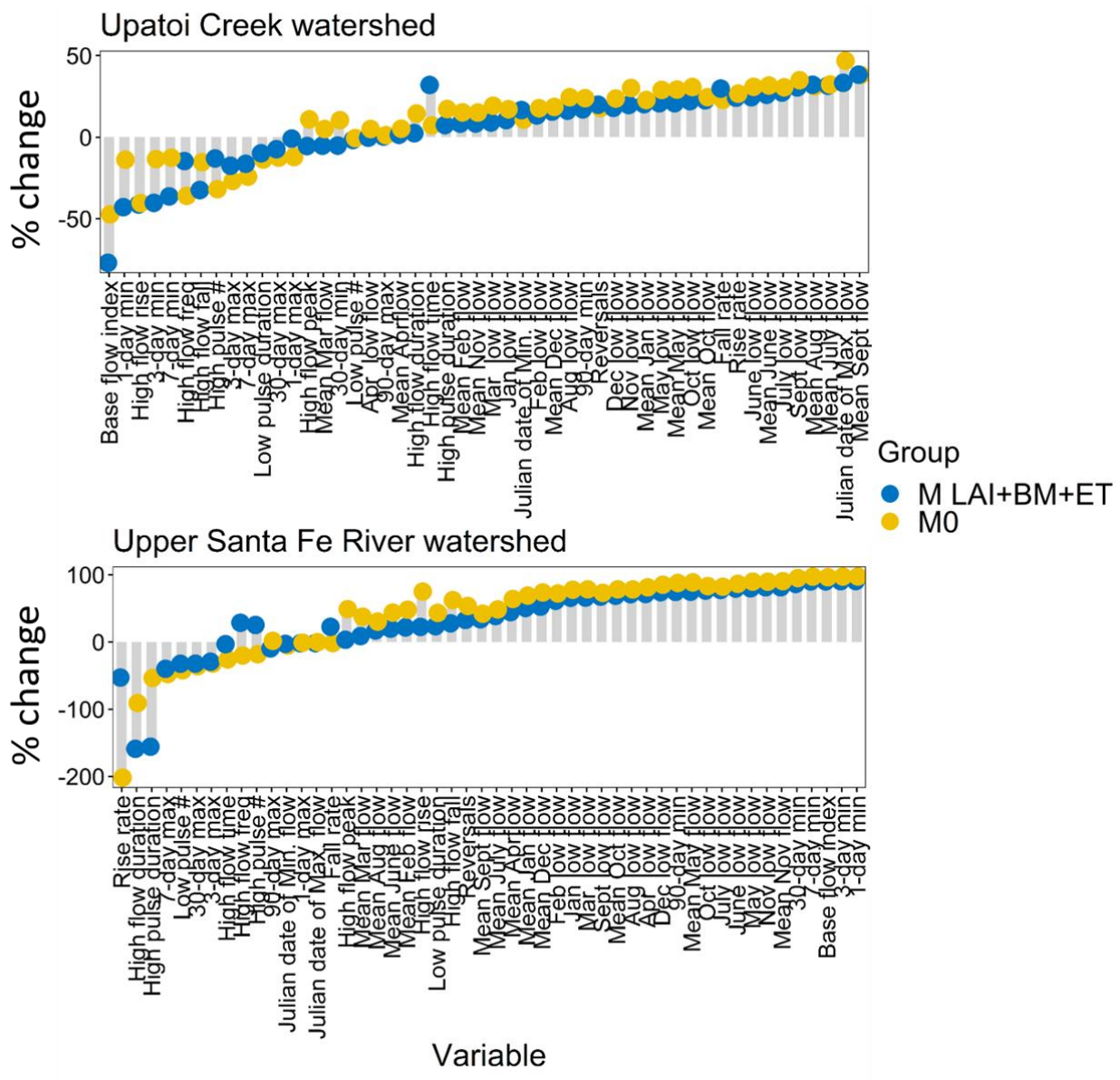

Figure 10. Percentage change of simulated statistical flow relevant parameters with traditional and multi-facet model calibration in relation to observed USGS daily streamflow data from 1999 to 2019 at Upatoi Creek and Upper Santa Fe River watersheds. Simulated streamflow time-series were fed into the IHA tool and compared against outputs of ecologically relevant parameters obtained through gauged streamflow data.

TABLES

Table 1. Watershed characteristics.

Hydrometeorological variable	Upatoi Creek	Upper Santa Fe
Latitude	32.544, 32.61 N	29.964, 30.165 N
Longitude	-84.811, -84.442 W	-82.247, -82.045 W
Area (km^2)	881.75	487.84
Average mean daily temperature (°C) (1995-2018)	18.2	20.5
Average annual precipitation (mm) (1995-2018)	1296	1326
Mean annual potential evapotranspiration (mm) (1995-2018)	1268	1215.2
Mean annual discharge (mm)* (2002-2018)	481	314
Mean daily streamflow (m^3/s) (1998-2018)	10.7	3.1

Table 2. Land use and cover change after reclassification to consider loblolly and slash pine spatial distribution across the watersheds.

	Upatoi Creek		Upper Santa Fe	
Land use class	% coverage - NLCD 2016	% coverage - Modified NLCD	% coverage - NLCD 2016	% coverage - Modified NLCD
Open Water	3%	3%	0%	0%
Developed, Open Space	4%	4%	6%	6%
Developed, Low Intensity	2%	2%	1%	1%
Developed, Medium Intensity	1%	1%	0%	0%
Developed, High Intensity	0%	0%	0%	0%
Barren Land	0%	0%	1%	1%
Deciduous Forest	14%	3%	2%	0%
Evergreen Forest	30%	4%	40%	5%
Mixed Forest	15%	3%	0%	0%
Shrub/Scrub	9%	9%	6%	6%
Herbaceuous	5%	5%	5%	5%
Hay/Pasture	4%	4%	13%	12%
Cultivated Crops	4%	4%	0%	1%
Woody Wetlands	8%	2%	25%	6%
Emergent Herbaceuous Wetlands	0%	0%	0%	0%
Slash Pine	_	0%		56%
Loblolly Pine	_	57%		1%

Table 3. Description of input data and sources.

	Data	Description	Source
Model input data	Topography	National Elevation Dataset at 10 meters resolution	United States Department of Agriculture (USDA) Geospatial Data Gateway (https://datagateway.nrcs.usda.gov/)
	Land use	2016 NLCD	United States Department of Agriculture (USDA) Geospatial Data Gateway (https://datagateway.nrcs.usda.gov/)
	Soil	Gridded Soil Survey Geographic (gSSURGO)	United States Department of Agriculture (USDA) Geospatial Data Gateway (https://datagateway.nrcs.usda.gov/)
	Climate	Daily precipitation, maximum/minimum temperature, solar radiation, wind speed	PRISM climate group (http://www.prism.oregonstate.edu/),National Land Data Assimilation Systems (NLDAS) phase 2 (https://ldas.gsfc.nasa.gov/nldas/NLDAS2model_download.php), National Solar Radiation Database (https://nsrdb.nrel.gov/)
	Atmospheric deposition	Wet and dry deposition of nitrate and ammonia	National Atmospheric Deposition Program (NADP) (http://nadp.slh.wisc.edu/)
Model calibration	Seasonal LAI	4 days composite dataset at 500 meters pixel resolution	Moderate Resolution Imaging Spectroradiometer (MODIS) (https://lpdaac.usgs.gov/products/mcd15a3hv006/)
	ET	8 days composite dataset at 500 meters pixel resolution	Moderate Resolution Imaging Spectroradiometer (MODIS) (https://lpdaac.usgs.gov/products/mod16a2v006/)
	Biomass	Field-measured annual total trees biomass	Long-term field studies conducted FMRC, FBRC, and PMRC in Georgia, Florida and Alabama, respectively
	Annual LAI	Field-measured annual LAI	Long-term field studies conducted FMRC, FBRC, and PMRC in Georgia, Florida and Alabama, respectively
	Streamflow	Daily discharge from stations USGS 02321000 (FL) and USGS 02341800 (GA)	USGS Water data (https://waterdata.usgs.gov/nwis)

Table 4. Model performance before and after the incorporation of previously calibrated parameter values regulating LAI and ET in SWAT. Values between parenthesis () represent model's performance under its default settings.

	Upper Santa Fe		Upatoi Creek	
	Loblolly pine	Slash pine	Loblolly pine	Slash pine
Monthly LAI				
R2	0.48 (0.29)	0.21 (0.25)	0.66 (0.42)	0.2 (0.27)
NSE	0.32 (-5)	-0.37 (-3)	0.65 (-0.74)	-3.1 (-0.56)
PBIAS %	7 (-38)	-16 (33)	3.9 (-38)	-82.4 (-8.2)
RMSE	0.52 (1.55)	1.15 (2)	0.58 (1.3)	2.3 (1.4)
Monthly ET				
R2	0.65 (0.57)	0.45 (0.6)	0.75 (0.68)	0.34 (0.33)
NSE	0.46 (-0.66)	0.38 (-0.60)	0.65 (0.43)	-1.5 (0)
PBIAS	17.5 (50)	-6.5 (55)	-17.8 (29.3)	-66 (3.9)
RMSE	24.9 (43.55)	31.90 (52.2)	23.36 (29.9)	42 (26.4)

REFERENCES

Abbaspour, K.C., 2015. SWATCalibration and Uncertainty Programs 100.

Abbaspour, K.C., Vaghefi, S.A., Srinivasan, R., 2018. A Guideline for Successful Calibration and Uncertainty Analysis for Soil and Water Assessment: A Review of Papers from the 2016 International SWAT Conference. Water 10, 6. https://doi.org/10.3390/w10010006

Abou Rafee, S.A., Uvo, C.B., Martins, J.A., Domingues, L.M., Rudke, A.P., Fujita, T., Freitas, E.D., 2019. Large-Scale Hydrological Modelling of the Upper Paraná River Basin. Water 11, 882. https://doi.org/10.3390/w11050882

Adla, S., Tripathi, S., Disse, M., 2019. Can We Calibrate a Daily Time-Step Hydrological Model Using Monthly Time-Step Discharge Data? Water 11, 1750. https://doi.org/10.3390/w11091750

Ahn, S.R., Jeong, J.H., Kim, S.J., 2016. Assessing drought threats to agricultural water supplies under climate change by combining the SWAT and MODSIM models for the Geum River basin, South Korea. Hydrological Sciences Journal/Journal des Sciences Hydrologiques 61, 2740–2753. https://doi.org/10.1080/02626667.2015.1112905

Ajaz Ahmed, M.A., Abd-Elrahman, A., Escobedo, F.J., Cropper, W.P., Martin, T.A., Timilsina, N., 2017. Spatially-explicit modeling of multi-scale drivers of aboveground forest biomass and water yield in watersheds of the Southeastern United States. J. Environ. Manage. 199, 158–171. https://doi.org/10.1016/j.jenvman.2017.05.013

Akhavan, S., Abedi-Koupai, J., Mousavi, S.-F., Afyuni, M., Eslamian, S.-S., Abbaspour, K.C., 2010. Application of SWAT model to investigate nitrate leaching in Hamadan–Bahar Watershed, Iran. Agriculture, Ecosystems & Environment 139, 675–688. https://doi.org/10.1016/j.agee.2010.10.015

Alemayehu, T., Griensven, A. van, Woldegiorgis, B.T., Bauwens, W., 2017. An improved SWAT vegetation growth module and its evaluation for four tropical ecosystems. Hydrology and Earth System Sciences 21, 4449–4467. https://doi.org/10.5194/hess-21-4449-2017

Anand, J., Gosain, A. k., Khosa, R., 2018. Prediction of land use changes based on Land Change Modeler and attribution of changes in the water balance of Ganga basin to land use change using the SWAT model. Science of the Total Environment 644, 503–519. https://doi.org/10.1016/j.scitotenv.2018.07.017

Anderson, H.W., Hoover, M.D., Reinhart, K.G., 1976. Forests and water: effects of forest management on floods, sedimentation, and water supply, USDA Forest Service General Technical Report PSW-18, Berkeley, California. Department of Agriculture, Forest Service, Pacific Southwest Forest and Range Experiment Station.

Anjum, M.N., Ding, Y., Shangguan, D., 2019. Simulation of the projected climate change impacts on the river flow regimes under CMIP5 RCP scenarios in the westerlies dominated belt, northern Pakistan. Atmospheric Research 227, 233–248. https://doi.org/10.1016/j.atmosres.2019.05.017

Arnold, J.G., Srinivasan, R., Muttiah, R.S., Williams, J.R., 1998. Large Area Hydrologic Modeling and Assessment Part I: Model Development1. JAWRA Journal of the American Water Resources Association 34, 73–89. https://doi.org/10.1111/j.1752-1688.1998.tb05961.x

Awan, U.K., Ismaeel, A., 2014. A new technique to map groundwater recharge in irrigated areas using a SWAT model under changing climate. Journal of Hydrology 519, 1368–1382. https://doi.org/10.1016/j.jhydrol.2014.08.049

Beven, K., Freer, J., 2001. Equifinality, data assimilation, and uncertainty estimation in mechanistic modelling of complex environmental systems using the GLUE methodology. Journal of Hydrology 249, 11–29. https://doi.org/10.1016/S0022-1694(01)00421-8

Bhatta, B., Shrestha, S., Shrestha, P.K., Talchabhadel, R., 2019. Evaluation and application of a SWAT model to assess the climate change impact on the hydrology of the Himalayan River Basin. CATENA 181, 104082–104082. https://doi.org/10.1016/j.catena.2019.104082

Blackard, J.A., Finco, M.V., Helmer, E.H., Holden, G.R., Hoppus, M.L., Jacobs, D.M., Lister, A.J., Moisen, G.G., Nelson, M.D., Riemann, R., Ruefenacht, B., Salajanu, D., Weyermann, D.L., Winterberger, K.C., Brandeis, T.J., Czaplewski, R.L., McRoberts, R.E., Patterson, P.L., Tymcio, R.P., 2008. Mapping U.S. forest biomass using nationwide forest inventory data and moderate resolution information. Remote Sensing of Environment, Remote Sensing Data Assimilation Special Issue 112, 1658–1677. https://doi.org/10.1016/j.rse.2007.08.021

Bosch, J.M., Hewlett, J.D., 1982. A review of catchment experiments to determine the effect of vegetation changes on water yield and evapotranspiration. Journal of Hydrology 55, 3–23. https://doi.org/10.1016/0022-1694(82)90117-2

Bracho, R., Starr, G., Gholz, H.L., Martin, T.A., Cropper, W.P., Loescher, H.W., 2012. Controls on carbon dynamics by ecosystem structure and climate for southeastern U.S. slash pine plantations. Ecological Monographs 82, 101–128. https://doi.org/10.1890/11-0587.1

Bracho, R., Vogel, J.G., Will, R.E., Noormets, A., Samuelson, L.J., Jokela, E.J., Gonzalez-Benecke, C.A., Gezan, S.A., Markewitz, D., Seiler, J.R., Strahm, B.D., Teskey, R.O., Fox, T.R., Kane, M.B., Laviner, M.A., McElligot, K.M., Yang, J., Lin, W., Meek, C.R., Cucinella, J., Akers, M.K., Martin, T.A., 2018. Carbon accumulation in loblolly pine plantations is increased by fertilization across a soil moisture availability gradient. Forest Ecology and Management 424, 39–52. https://doi.org/10.1016/j.foreco.2018.04.029

Brauman, K.A., Daily, G.C., Duarte, T.K., Mooney, H.A., 2007. The Nature and Value of Ecosystem Services: An Overview Highlighting Hydrologic Services. Annual Review of Environment and Resources 32, 67–98. https://doi.org/10.1146/annurev.energy.32.031306.102758

Brighenti, T.M., Bonumá, N.B., Grison, F., Mota, A. de A., Kobiyama, M., Chaffe, P.L.B., 2019. Two calibration methods for modeling streamflow and suspended sediment with the swat model. Ecological Engineering 127, 103–113. https://doi.org/10.1016/j.ecoleng.2018.11.007

Brown, S.C., Versace, V.L., Lester, R.E., Todd Walter, M., 2015. Assessing the impact of drought and forestry on streamflows in south-eastern Australia using a physically based hydrological model. Environ Earth Sci 74, 6047–6063. https://doi.org/10.1007/s12665-015-4628-8

Bruijnzeel, L.A., 2004. Hydrological functions of tropical forests: not seeing the soil for the trees? Agriculture, Ecosystems & Environment, Environmental Services and Land Use Change: Bridging the Gap between Policy and Research in Southeast Asia 104, 185–228. https://doi.org/10.1016/j.agee.2004.01.015

Chu, T.W., Shirmohammadi, A., Montas, H., Sadeghi, A., 2004. Evaluation of the Swat Model's Sediment and Nutrient Components in the Piedmont Physiographic Region of Maryland. Transactions of the ASAE 47, 1523–1538. https://doi.org/10.13031/2013.17632

Gholz, H.L., Clark, K.L., 2002. Energy exchange across a chronosequence of slash pine forests in Florida. Agricultural and Forest Meteorology 112, 87–102. https://doi.org/10.1016/S0168-1923(02)00059-X

Golden, H.E., Evenson, G.R., Tian, S., Amatya, D.M., Sun, G., 2016. Hydrological modelling in forested systems., in: Amatya, D.M., Williams, T.M., Bren, L., Jong, C. de (Eds.), Forest Hydrology: Processes, Management and Assessment. CABI, Wallingford, pp. 141–161. https://doi.org/10.1079/9781780646602.0141

Gorelick, N., Hancher, M., Dixon, M., Ilyushchenko, S., Thau, D., Moore, R., 2017. Google Earth Engine: Planetary-scale geospatial analysis for everyone. Remote Sensing of Environment, Big Remotely Sensed Data: tools, applications and experiences 202, 18–27. https://doi.org/10.1016/j.rse.2017.06.031

Gui Ziling, Liu Pan, Cheng Lei, Guo Shenglian, Wang Hao, Zhang Liping, 2019. Improving Runoff Prediction Using Remotely Sensed Actual Evapotranspiration during Rainless Periods. Journal of Hydrologic Engineering 24, 04019050. https://doi.org/10.1061/(ASCE)HE.1943-5584.0001856

Ha, L.T., Bastiaanssen, W.G.M., Van Griensven, A., Van Dijk, A.I.J.M., Senay, G.B., 2018. Calibration of Spatially Distributed Hydrological Processes and Model Parameters in SWAT Using Remote Sensing Data and an Auto-Calibration Procedure: A Case Study in a Vietnamese River Basin. Water 10, 212. https://doi.org/10.3390/w10020212

Haas, M.B., Guse, B., Pfannerstill, M., Fohrer, N., 2016. A joined multi-metric calibration of river discharge and nitrate loads with different performance measures. Journal of Hydrology 536, 534–545. https://doi.org/10.1016/j.jhydrol.2016.03.001

Herman, M.R., Nejadhashemi, A.P., Abouali, M., Hernandez-Suarez, J.S., Daneshvar, F., Zhang, Z., Anderson, M.C., Sadeghi, A.M., Hain, C.R., Sharifi, A., 2018. Evaluating the role of evapotranspiration remote sensing data in improving hydrological modeling predictability. Journal of Hydrology 556, 39–49. https://doi.org/10.1016/j.jhydrol.2017.11.009

Himanshu, S.K., Pandey, A., Yadav, B., Gupta, A., 2019. Evaluation of best management practices for sediment and nutrient loss control using SWAT model. Soil & Tillage Research 192, 42–58. https://doi.org/10.1016/j.still.2019.04.016

Ikenberry, C.D., Crumpton, W.G., Arnold, J.G., Soupir, M.L., Gassman, P.W., 2017. Evaluation of Existing and Modified Wetland Equations in the SWAT Model. Journal of the American Water Resources Association 53, 1267–1280. https://doi.org/10.1111/1752-1688.12570

Jiang, D., Wang, K., 2019. The Role of Satellite-Based Remote Sensing in Improving Simulated Streamflow: A Review. Water 11, 1615. https://doi.org/10.3390/w11081615

Jianzhong Lu, Xiaolin Cui, Xiaoling Chen, Sauvage, S., Perez, J.-M.S., 2017. Evaluation of hydrological response to extreme climate variability using SWAT model: application to the Fuhe basin of Poyang Lake watershed, China. Hydrology Research 48, 1730–1744. https://doi.org/10.2166/nh.2016.115

Jodar-Abellan, A., Valdes-Abellan, J., Pla, C., Gomariz-Castillo, F., 2018. Impact of land use changes on flash flood prediction using a sub-daily SWAT model in five Mediterranean ungauged watersheds (SE Spain) | Elsevier Enhanced Reader [WWW Document]. https://doi.org/10.1016/j.scitotenv.2018.12.034

Jonckheere, I., Fleck, S., Nackaerts, K., Muys, B., Coppin, P., Weiss, M., Baret, F, 2004. Methods for leaf area index determination. Part I: Theories, techniques and instruments. Agric. For. Meteorol. 121, 19–35

Kaur, B., Shrestha, N.K., Daggupati, P., Rudra, R.P., Goel, P.K., Shukla, R., Allataifeh, N., 2019. Water Security Assessment of the Grand River Watershed in Southwestern Ontario, Canada. Sustainability 11, 1883. https://doi.org/10.3390/su11071883

Kemanian, A.R., Julich, S., Manoranjan, V.S., Arnold, J.R., 2011. Integrating soil carbon cycling with that of nitrogen and phosphorus in the watershed model SWAT: Theory and model testing. Ecological Modelling 222, 1913–1921. https://doi.org/10.1016/j.ecolmodel.2011.03.017

Khaki, M., Hoteit, I., Kuhn, M., Forootan, E., Awange, J., 2019. Assessing data assimilation frameworks for using multi-mission satellite products in a hydrological context. Sci. Total Environ. 647, 1031–1043. https://doi.org/10.1016/j.scitotenv.2018.08.032

Kiani, F., Behtarinejad, B., Najafinejad, A., Kaboli, R., 2018. Simulation of Nitrogen and Phosphorus Losses in Loess Landforms of Northern Iran. Eurasian Soil Science 51, 176–182. https://doi.org/10.1134/S1064229318020035

Lai, G., Luo, J., Li, Q., Qiu, L., Pan, R., Zeng, X., Zhang, L., Yi, F., 2020. Modification and validation of the SWAT model based on multi-plant growth mode, a case study of the Meijiang River Basin, China. Journal of Hydrology 585, 124778. https://doi.org/10.1016/j.jhydrol.2020.124778

Li, C., Sun, F., Xu, Y., Chen, T., Liu, M., Hu, Y., 2014. Combining CLUE-S and SWAT models to forecast land use change and non-point source pollution impact at a watershed scale in Liaoning Province, China. Chinese Geographical Science 24, 540–550. https://doi.org/10.1007/s11769-014-0661-x

Li Zejun, Liu Pan, Feng Maoyuan, Cui Xueqing, He Ping, Wang Caijun, Zhang Jingwen, 2020. Evaluating the Effect of Transpiration in Hydrologic Model Simulation through Parameter Calibration. Journal of Hydrologic Engineering 25, 04020007. https://doi.org/10.1061/(ASCE)HE.1943-5584.0001895

Lim, K.J., Engel, B.A., Tang, Z., Choi, J., Kim, K.-S., Muthukrishnan, S., Tripathy, D., 2005. AUTOMATED WEB GIS BASED HYDROGRAPH ANALYSIS TOOL, WHAT. J Am Water Resources Assoc 41, 1407–1416. https://doi.org/10.1111/j.1752-1688.2005.tb03808.x

Loizu, J., Massari, C., Álvarez-Mozos, J., Tarpanelli, A., Brocca, L., Casalí, J., 2018. On the assimilation set-up of ASCAT soil moisture data for improving streamflow catchment simulation. Advances in Water Resources 111, 86–104. https://doi.org/10.1016/j.advwatres.2017.10.034

Ma, T., Duan, Z., Li, R., Song, X., 2019. Enhancing SWAT with remotely sensed LAI for improved modelling of ecohydrological process in subtropics. Journal of Hydrology 570, 802–815. https://doi.org/10.1016/j.jhydrol.2019.01.024

Martin, T.A., Adams, D.C., Cohen, M.J., Crandall, R.M., Gonzalez-Benecke, C.A., Smith, J.A., Vogel, J.G., 2017. Managing Florida's Plantation Forests in a Changing Climate. Florida's Climate: Changes, Variations, & Impacts.

McLaughlin, D.L., Kaplan, D.A., Cohen, M.J., 2013. Managing Forests for Increased Regional Water Yield in the Southeastern U.S. Coastal Plain. JAWRA Journal of the American Water Resources Association 49, 953–965. https://doi.org/10.1111/jawr.12073

Mishra, A., Froebrich, J., Gassman, P.W., 2007. Evaluation of the Swat Model for Assessing Sediment Control Structures in a Small Watershed in India. Transactions of the ASABE 50, 469–477. https://doi.org/10.13031/2013.22637

Monteith, J.L., 1965. Evaporation and environment. Symposia of the Society for Experimental Biology 19, 205–234.

Moriasi, D.N., Gitau, M.W., Pai, N., Daggupati, P., 2015. Hydrologic and Water Quality Models: Performance Measures and Evaluation Criteria.

Mu, Q., et al., 2013. A remotely sensed global terrestrial drought severity index. Bulletin of the American Meteorological Society, 94 (1), doi:10.1175/BAMS-D-11-00213.1.

Mukundan, R., Radcliffe, D.E., Risse, L.M., 2010. Spatial resolution of soil data and channel erosion effects on SWAT model predictions of flow and sediment. Journal of Soil & Water Conservation 65, 92–104. https://doi.org/10.2489/jSWC.65.2.92

Myneni, R., Knyazikhin, Y., Park, T., 2015. MOD15A2H MODIS/Terra Leaf Area Index/FPAR 8-Day L4 Global 500m SIN Grid V006 [Data set]. NASA EOSDIS Land Processes DAAC. Accessed 2020-06-08 from https://doi.org/10.5067/MODIS/MOD15A2H.006.

Neitsch, S., Arnold, J.G., Kiniry, J.R., Williams, J., 2011. Soil & Water Assessment Tool Theoretical Documentation Version 2009. Texas Water Resources Institute Technical Report No. 406, College Station, TX, pp. 618.

Odusanya, A.E., Mehdi, B., Schürz, C., Oke, A.O., Awokola, O.S., Awomeso, J.A., Adejuwon, J.O., Schulz, K., 2019. Multi-site calibration and validation of SWAT with satellite-based evapotranspiration in a data-sparse catchment in southwestern Nigeria. Hydrology and Earth System Sciences 23, 1113–1144. https://doi.org/10.5194/hess-23-1113-2019

Oki, T., Kanae, S., 2006. Global Hydrological Cycles and World Water Resources. Science 313, 1068–1072. https://doi.org/10.1126/science.1128845

Parajuli, P.B., Jayakody, P., Ouyang, Y., 2018. Evaluation of Using Remote Sensing Evapotranspiration Data in SWAT. Water Resour Manage 32, 985–996. https://doi.org/10.1007/s11269-017-1850-z

Pohlert, T., Huisman, J. a., Breuer, L., Frede, H.-G., 2007. Integration of a detailed biogeochemical model into SWAT for improved nitrogen predictions—Model development, sensitivity, and GLUE analysis. Ecological Modelling 203, 215–228. https://doi.org/10.1016/j.ecolmodel.2006.11.019

Qi, J., Wang, Q., Zhang, X., 2019. On the Use of NLDAS2 Weather Data for Hydrologic Modeling in the Upper Mississippi River Basin. Water 11, 960. https://doi.org/10.3390/w11050960

Rajib, A., Evenson, G.R., Golden, H.E., Lane, C.R., 2018. Hydrologic model predictability improves with spatially explicit calibration using remotely sensed evapotranspiration and biophysical parameters. Journal of Hydrology 567, 668–683. https://doi.org/10.1016/j.jhydrol.2018.10.024

Rajib, M.A., Merwade, V., Yu, Z., 2016. Multi-objective calibration of a hydrologic model using spatially distributed remotely sensed/in-situ soil moisture. Journal of Hydrology 536, 192–207. https://doi.org/10.1016/j.jhydrol.2016.02.037

Richter, B.D., Baumgartner, J.V., Powell, J., Braun, D.P., 1996. A Method for Assessing Hydrologic Alteration within Ecosystems. Conservation Biology 10, 1163–1174. https://doi.org/10.1046/j.1523-1739.1996.10041163.x

Risal, A., Parajuli, P.B., 2019. Quantification and simulation of nutrient sources at watershed scale in Mississippi. Science of the Total Environment 670, 633–643. https://doi.org/10.1016/j.scitotenv.2019.03.233

Romanowicz, A. a., Vanclooster, M., Rounsevell, M., La Junesse, I., 2005. Sensitivity of the SWAT model to the soil and land use data parametrisation: a case study in the Thyle catchment, Belgium. Ecological Modelling 187, 27–39. https://doi.org/10.1016/j.ecolmodel.2005.01.025

Ruefenacht, B., Finco, M.V., Nelson, M.D., Czaplewski, R., Helmer, E.H., Blackard, J.A., Holden, G.R., Lister, A.J., Salajanu, D., Weyermann, D., Winterberger, K., 2008. Conterminous U.S. and Alaska Forest Type Mapping Using Forest Inventory and Analysis Data. photogramm eng remote sensing 74, 1379–1388. https://doi.org/10.14358/PERS.74.11.1379

Running, S., Mu, Q., Zhao, M., 2017. MOD16A2 MODIS/Terra Net Evapotranspiration 8-Day L4 Global 500m SIN Grid V006 [Data set]. NASA EOSDIS Land Processes DAAC. Accessed 2020-06-08 from https://doi.org/10.5067/MODIS/MOD16A2.006.

Samuelson, L.J., Kane, M.B., Markewitz, D., Teskey, R.O., Akers, M.K., Stokes, T.A., Pell, C.J., Qi, J., 2017. Fertilization increased leaf water use efficiency and growth of Pinus taeda subjected to five years of throughfall reduction. Can. J. For. Res. 48, 227–236. https://doi.org/10.1139/cjfr-2017-0357

Sengupta, M., Xie, Y., Lopez, A., Habte, A., Maclaurin, G., Shelby, J., 2018. The National Solar Radiation Data Base (NSRDB). Renewable and Sustainable Energy Reviews 89, 51–60. https://doi.org/10.1016/j.rser.2018.03.003

Singh, A., Imtiyaz, Mohd., Isaac, R. k., Denis, D. m., 2014. Assessing the performance and uncertainty analysis of the SWAT and RBNN models for simulation of sediment yield in the Nagwa watershed, India. Hydrological Sciences Journal/Journal des Sciences Hydrologiques 59, 351–364. https://doi.org/10.1080/02626667.2013.872787

Strauch, M., Volk, M., 2013. SWAT plant growth modification for improved modeling of perennial vegetation in the tropics. Ecological Modelling 269, 98–112. https://doi.org/10.1016/j.ecolmodel.2013.08.013

Sun, G., Noormets, A., Gavazzi, M.J., McNulty, S.G., Chen, J., Domec, J.-C., King, J.S., Amatya, D.M., Skaggs, R.W., 2010. Energy and water balance of two contrasting loblolly pine plantations on the lower coastal plain of North Carolina, USA. For. Ecol. Manage. 259, 1299–1310. https://doi.org/10.1016/j.foreco.2009.09.016

Teklay, A., Dile, Y.T., Setegn, S.G., Demissie, S.S., Asfaw, D.H., 2019. Evaluation of static and dynamic land use data for watershed hydrologic process simulation: A case study in Gummara watershed, Ethiopia. CATENA 172, 65–75. https://doi.org/10.1016/j.catena.2018.08.013

Teuling, A.J., 2018. A Forest Evapotranspiration Paradox Investigated Using Lysimeter Data. Vadose Zone Journal 17, 170031. https://doi.org/10.2136/vzj2017.01.0031

The Nature Conservancy, 2009. Indicators of Hydrologic Alteration Version 7.1 User's Manual. Available at: https://www.conservationgateway.org/Documents/IHAV7.pdf (accessed on 09/01/2015).

Tobin, K.J., Bennett, M.E., 2017. Constraining SWAT Calibration with Remotely Sensed Evapotranspiration Data. JAWRA Journal of the American Water Resources Association 53, 593–604. https://doi.org/10.1111/1752-1688.12516

United States. Soil Conservation Service. (1985). National engineering handbook. Section 20, Watershed yield. Washington, D.C.:U.S. Dept. of Agriculture, Soil Conservation Service

USDA, S., 1972. National engineering handbook, section 4: Hydrology. Washington, DC.

Vigiak, O., Malagó, A., Bouraoui, F., Vanmaercke, M., Poesen, J., 2015. Adapting SWAT hillslope erosion model to predict sediment concentrations and yields in large Basins. Science of the Total Environment 538, 855–875. https://doi.org/10.1016/j.scitotenv.2015.08.095

Visakh, S., Raju, P.V., Kulkarni, S.S., Diwakar, P.G., 2019. Inter-comparison of water balance components of river basins draining into selected delta districts of Eastern India. Science of The Total Environment 654, 1258–1269. https://doi.org/10.1016/j.scitotenv.2018.11.162

Wang, Q., Liu, R., Men, C., Guo, L., Miao, Y., 2018. Effects of dynamic land use inputs on improvement of SWAT model performance and uncertainty analysis of outputs. Journal of Hydrology 563, 874–886. https://doi.org/10.1016/j.jhydrol.2018.06.063

Watson, B., Coops, N., Selvalingam, S., Ghafouri, M., 2005. Integration of 3-PG into SWAT to simulate the growth of evergreen forests. SWAT 2005 : 3rd International SWAT Conference 142–152.

Wellen, C., Arhonditsis, G.B., Long, T., Boyd, D., 2014. Quantifying the uncertainty of nonpoint source attribution in distributed water quality models: A Bayesian assessment of SWAT's sediment export predictions. Journal of Hydrology 519, 3353–3368. https://doi.org/10.1016/j.jhydrol.2014.10.007

Wightman, M.G., Martin, T.A., Gonzalez-Benecke, C.A., Jokela, E.J., Cropper, J., Ward, E.J. (ORCID:0000000250475464), 2016. Loblolly pine productivity and water relations in response to throughfall reduction and fertilizer application on a poorly drained site in northern Florida. Forests 7. https://doi.org/10.3390/f7100214

Williams, J.R. (1975) Sediment-Yield Prediction with Universal Equation Using Runoff Energy Factor. In: Present and Prospective Technology for Predicting Sediment Yield and Sources, US Department of Agriculture, Agriculture Research Service, Washington DC, 244-252.

Williams, J.R., 1990. The erosion-productivity impact calculator (EPIC) model: a case history. Phil. Trans. R. Soc. Lond. B 329, 421–428. https://doi.org/10.1098/rstb.1990.0184

Yang, Q., Almendinger, J.E., Zhang, X., Huang, M., Chen, X., Leng, G., Zhou, Y., Zhao, K., Asrar, G.R., Srinivasan, R., Li, X., 2018. Enhancing SWAT simulation of forest ecosystems for water resource assessment: A case study in the St. Croix River basin. Ecological Engineering 120, 422–431. https://doi.org/10.1016/j.ecoleng.2018.06.020

Yang, Q., Zhang, X., 2016. Improving SWAT for simulating water and carbon fluxes of forest ecosystems. Science of The Total Environment 569–570, 1478–1488. https://doi.org/10.1016/j.scitotenv.2016.06.238

Zang, C., Mao, G., 2019. A Spatial and Temporal Study of the Green and Blue Water Flow Distribution in Typical Ecosystems and its Ecosystem Services Function in an Arid Basin. Water 11, 97. https://doi.org/10.3390/w11010097

Zhang, H., Wang, B., Liu, D.L., Zhang, M., Leslie, L.M., Yu, Q., 2020. Using an improved SWAT model to simulate hydrological responses to land use change: A case study of a catchment in tropical Australia. Journal of Hydrology 585, 124822. https://doi.org/10.1016/j.jhydrol.2020.124822

Zhang, Y., Chiew, F.H.S., Liu, C., Tang, Q., Xia, J., Tian, J., Kong, D., Li, C., 2020. Can Remotely Sensed Actual Evapotranspiration Facilitate Hydrological Prediction in Ungauged Regions Without Runoff Calibration? Water Resources Research 56, e2019WR026236. https://doi.org/10.1029/2019WR026236

Zhang, Y., Sun, A., Sun, H., Gui, D., Xue, J., Liao, W., Yan, D., Zhao, N., Zeng, X., 2019. Error adjustment of TMPA satellite precipitation estimates and assessment of their hydrological utility in the middle and upper Yangtze River Basin, China. Atmospheric Research 216, 52–64. https://doi.org/10.1016/j.atmosres.2018.09.021

Zhu, Q., Zhang, X., Ma, C., Gao, C., Xu, Y.-P., 2016. Investigating the uncertainty and transferability of parameters in SWAT model under climate change. Hydrological Sciences Journal/Journal des Sciences Hydrologiques 61, 914–930. https://doi.org/10.1080/02626667.2014.1000915

CHAPTER 4: General conclusions and future directions

Although forests can cover a significant portion of a watershed and largely interfere with the water cycling, forest growth and dynamics are usually not calibrated in watershed modeling studies. One of the most widely-applied watershed models, the SWAT model, has not been sufficiently tested in forested ecosystems and the importance of forests on modeled watershed hydrological responses remains unclear. SWAT incorporates a plant growth module in which most of the plant parameters describing growth and development are based on the physiology of annual crops. Studies such as (Yang and Zhang, 2016) have reported unrealistic parameter values pertaining to evergreen forests, deciduous forests, and mixed forests in SWAT's plant database.

Considering SWAT's popularity as a hydrological assessment tool and the highly forested rate of the contiguous U.S., especially in the Southeastern regions, it is of utmost importance to understand the influence of forests in hydrological modeling studies. As part of the Floridan Aquifer Collaborative Engagement for Sustainability (FACETS) project (http://floridanwater.org), this study had access to a large dataset of field-measured data in forestry studies across the Southeastern United States. This allowed me to develop an enhanced parameterization of SWAT's plant database for evergreen forests, more specifically for loblolly pine and slash pine trees. The improved model parameterization was tested in a wide-range of field-scale sites with varying soil types, climate conditions, and management practices in Alabama, Florida, and Georgia. The widely available remote-sensing derived data allowed me to expand the field-scale model parameterization to forested watersheds located in Florida and Georgia. The latter aimed to test the plausibility and validity of the proposed new model parameterization at the watershed-scale and its respective effects on water fluxes and water balance.

In Chapter 1, the overall premise of the study and its motivation are presented. Here, I outlined three overreaching goals. These goals and their findings are summarized in the following paragraphs.

Objective 1: Construct a SWAT plant database parameterization for loblolly and slash pine based on data derived from literature, field observations and remote sensing products

This objective was addressed in Chapter 2 and consisted of the first step in improving SWAT's skills in predicting plant growth and dynamics. Plant types representing loblolly pine and slash pine were added to the model's plant database and physically-realistic parameter values were derived for each species based on field observations, published literature, and remote-sensing information. Regarding this objective, I found that:

- Most of the parameters in SWAT's plant database represent physical processes and can be obtained through field measurements (e.g., *BMX_TREES*, *BLAI*, *ALAI_MIN*, *RDMX*, *BIO_LEAF*);
- Several parameters in SWAT's plant database were out of a physically-realistic range for evergreen forests in the model's default settings (e.g., excessively high *BLAI* for loblolly pine, unrealistically high *BIO_LEAF* for trees, low *GSI* value for both loblolly and slash pine trees);
- Unrealistic values of parameters such as *BIO_E* and *BIO_LEAF* in SWAT's default parameterization were determinant for the inaccurate simulation of tree biomass accumulation;
- Unrealistic values for parameters such as *BLAI* and *ALAI_MIN* in the SWAT's default parameterization were determinant for the inaccurate simulation of LAI development;

- An excessively low value of *GSI* in the plant database was determinant for the underestimation of evapotranspiration in the model's default settings;
- Remotely-sensed LAI reference data revealed to be a useful source of information to capture the seasonality of tree growth and allowed direct derivation of values for the parameters *FRGRW1*, *LAIMX1*, *FRGRW2*, *LAIMX2*, and *DLAI*.

Objective 2: Calibrate and validate the SWAT model at the field scale basis for multiple sites across the southeastern U.S. for biomass production, LAI dynamics, and ET

This objective was addressed in Chapter 2. Given the lack of spatially-distributed field-measured data in forestry studies across large areas (e.g., watersheds), this study constructed field-scale models to represent the sites from which forest observations (e.g., LAI, total biomass, canopy height) were taken. In the current study, a simple and yet robust approach was employed to delineate physically meaningful boundaries for each pine plantation field based on Marek et al. (2016). I found that:

- SWAT has some structural limitations to simulate tree growth before maturity. This challenges the simultaneous calibration of LAI and biomass in SWAT for planted trees;
- Through model parameterization, it is possible to overcome the limitation stated above;
- Whenever possible, annual LAI and annual total biomass should be calibrated simultaneously in SWAT, instead of sequentially;
- With the default parameters, SWAT largely underestimated ET and biomass. In regards to LAI, the default parameter values led to considerable overestimation of loblolly pine LAI and underestimation of slash pine LAI;
- The improved model parameterization presented in this study can represent the growth and dynamics of loblolly pine and slash pine reasonably well in the Southeastern U.S.;

- The prediction of seasonal LAI, monthly ET, and annual total biomass improved remarkably under the new model parameterization;
- A realistic representation of forest process in hydrological models significantly affected water balance components such as surface runoff, lateral flow, baseflow, aquifer recharge;
- The improved model parameterization led to reductions in the soil water content, surface runoff rates, lateral flow, baseflow, and aquifer recharge.

Objective 3: Transfer the site-level calibrated model parameters to nearby watersheds to investigate the impact of vegetation growth calibration on watershed-scale water balance

This objective was addressed in Chapter 3 and served as a validation of the proposed improved forest parameterization presented in Chapter 2. Because of the increasing number of studies applying SWAT worldwide and the role played by key forest attributes such as LAI, and biomass in the model's hydrological computations, it is fundamental to evaluate the effects of improved LAI and biomass at the watershed-scale and the model skills in forested watersheds. Additionally, watersheds are the basic land unit used for water management and thus needed to be included as test beds to show the relevance of the improved forest parameterization on water resources. In regards to this overreaching goal, the main findings were:

- The model parameterization developed at the field-scale level is can be successfully transferred to nearby watersheds for improved simulations;
- SWAT's skills in predicting LAI, biomass, and ET at watershed-scale improved largely with the inclusion of previously calibrated biophysical parameter values;
- The improved representation of forest dynamics led to improved model performance in simulating daily and monthly streamflow and monthly baseflow;

- The main improvement in simulated streamflow and baseflow comes from enhanced ET representation in the model;
- Even without calibration of streamflow-related parameters, SWAT showed satisfactory performance in simulating daily streamflow when previously calibrated ET parameters at field-level were transferred to the watershed models;
- Multi-facet model calibration of LAI, biomass, ET, and streamflow showed superior statistical performance and reduced uncertainties compared to a traditional model calibration of streamflow only;
- The results achieved through the software IHA indicated that the enhancement of forest processes in the models yielded better agreement of ecohydrological parameters influencing soil moisture availability for plants, soil mineral availability, plant stress, nutrient exchanges between rivers and floodplains, and others, with observations.

Future directions

While this study contributes to knowledge relevant to a greater understanding of the importance of forest processes in hydrological modeling studies, there are some shortcomings, especially related to SWAT's limitations in simulating tree growth before maturity, and lack of a longer record of field-measured LAI and biomass data. Some suggestions for future studies to further learn and improve the forest-water interplays in hydrological models are outlined below:

- Gather field-measured data representing other forest types and tree species;
- Expand the forest categorization and associated parameter values in SWAT's plant database to include a broader range of forested ecosystems;
- Explore other remote-sensing products such as GLEAMS (Miralles et al., 2011), and downscaled MODIS LAI presented by Ma et al. (2019);

- Replace the fixed minimum annual LAI (ALAI_MIN) value by a fraction of the daily LAI, so that a more realistic growing pattern can be represented in the model and better capture observations;
- Include a leaf biomass algorithm in SWAT to differentiate LAI development from biomass accumulation and then allow for the simulation of tree growth prior to maturity;
- Replace the total biomass to litter ratio by a fraction of the leaf biomass over a period of time to avoid litter fall on a single day (first day of dormancy);
- Expand the applications described in Chapter 3 to water quality. Forests may affect sediment loss and nutrient cycling (especially the soil nutrient cycling) and this has to be explored in a future study.

REFERENCES

Ma, T., Duan, Z., Li, R., Song, X., 2019. Enhancing SWAT with remotely sensed LAI for improved modelling of ecohydrological process in subtropics. Journal of Hydrology 570, 802–815. https://doi.org/10.1016/j.jhydrol.2019.01.024

Marek, G.W., Gowda, P.H., Evett, S.R., Baumhardt, R.L., Brauer, D.A., Howell, T., Marek, T.H., Srinivasan, R., 2016. Calibration and Validation of the SWAT Model for Predicting Daily ET over Irrigated Crops in the Texas High Plains Using Lysimetric Data. https://doi.org/10.13031/trans.59.10926

Miralles, D.G., Holmes, T.R.H., Jeu, R.A.M.D., Gash, J.H., Meesters, A.G.C.A., Dolman, A.J., 2011. Global land-surface evaporation estimated from satellite-based observations. Hydrology and Earth System Sciences 15, 453–469. https://doi.org/10.5194/hess-15-453-2011

Yang, Q., Zhang, X., 2016. Improving SWAT for simulating water and carbon fluxes of forest ecosystems. Science of The Total Environment 569–570, 1478–1488. https://doi.org/10.1016/j.scitotenv.2016.06.238